# Title: The contribution of historical processes to contemporary extinction risk in placental mammals

**Authors:** Aryn P. Wilder<sup>1†\*</sup>, Megan A Supple<sup>2,3†\*</sup>, Ayshwarya Subramanian<sup>4</sup>, Anish Mudide<sup>5</sup>, Ross Swofford<sup>4</sup>, Aitor Serres-Armero<sup>6</sup>, Cynthia Steiner<sup>1</sup>, Klaus-Peter Koepfli<sup>7,8,9</sup>, Diane P. Genereux<sup>4</sup>, Elinor K. Karlsson<sup>4,10</sup>, Kerstin Lindblad-Toh<sup>4,11</sup>, Tomas Marques-Bonet<sup>6,12,13,14</sup>, Violeta Munoz Fuentes<sup>15</sup>, Kathleen Foley<sup>16,17</sup>, Wynn K. Meyer<sup>17</sup>, Zoonomia Consortium<sup>‡</sup>, Oliver A. Ryder<sup>1,18§\*</sup>, Beth Shapiro<sup>2,3§\*</sup>

#### **Affiliations:**

<sup>1</sup>Conservation Genetics, San Diego Zoo Wildlife Alliance; Escondido, CA 92027, USA.

<sup>2</sup>Department of Ecology and Evolutionary Biology, University of California Santa Cruz; Santa Cruz, CA 95064, USA.

<sup>3</sup>Howard Hughes Medical Institute, University of California Santa Cruz; Santa Cruz, CA 95064, USA.

<sup>4</sup>Broad Institute of MIT and Harvard; Cambridge, MA 02139, USA.

<sup>5</sup>Phillips Exeter Academy; Exeter, NH 03833, USA.

<sup>6</sup>Institute of Evolutionary Biology, Department of Experimental and Health Sciences, Universitat Pompeu Fabra; Barcelona, 08003, Spain.

<sup>7</sup>Smithsonian-Mason School of Conservation, George Mason University; Front Royal, VA 22630, USA.

<sup>8</sup>Center for Species Survival, Smithsonian Conservation Biology Institute, National Zoological Park; Washington, DC, 30008, USA.

<sup>9</sup>Computer Technologies Laboratory, ITMO University; St. Petersburg, 197101, Russia.

<sup>10</sup>Program in Bioinformatics and Integrative Biology, University of Massachusetts Medical School; Worcester, MA 01605, USA.

<sup>11</sup>Science for Life Laboratory, Department of Medical Biochemistry and Microbiology, Uppsala University; Uppsala, 751 32, Sweden.

<sup>12</sup>Catalan Institution of Research and Advanced Studies; Barcelona, 08010, Spain.

<sup>13</sup>Centre for Genomic Regulation, Barcelona Institute of Science and Technology; Barcelona, 08028, Spain.

<sup>14</sup>Institut Català de Paleontologia Miquel Crusafont, Universitat Autònoma de Barcelona; Barcelona, 08193, Spain.

<sup>15</sup>European Molecular Biology Laboratory-European Bioinformatics Institute, Wellcome Genome Campus; Hinxton, UK.

<sup>16</sup>College of Law, University of Iowa; Iowa City, IA 52242, USA.

<sup>17</sup>Lehigh University, Biological Sciences; Bethlehem, PA 18015, USA.

<sup>&</sup>lt;sup>18</sup>Department of Evolution, Behavior and Ecology, Division of Biology, University of California, San Diego; La Jolla, CA 92039 USA.

<sup>†</sup>co-lead authors

<sup>‡</sup>see list at end of manuscript

<sup>§</sup>co-senior authors

<sup>\*</sup>Corresponding authors: Email: awilder@sdzwa.org (APW), msupple@ucsc.edu (MAS), oryder@sdzwa.org (OAR), and bashapir@ucsc.edu (BS)

# **Print Page Summary:**

#### Introduction

The Anthropocene is marked by an accelerated loss of biodiversity, widespread population declines, and a global conservation crisis. Given limited resources for conservation intervention, an approach is needed to identify threatened species from among the thousands lacking adequate information for status assessment. Such prioritization for intervention could come from genome sequence data, as genomes contain information about demography, diversity, fitness, and adaptive potential. However, the relevance of genomic data for identifying at-risk species is uncertain, in part because genetic variation may better reflect past events and life histories than contemporary conservation status.

#### Rationale

The Zoonomia multispecies alignment presents an opportunity to systematically compare neutral and functional genomic diversity and their relationships to contemporary extinction risk across a large sample of diverse mammalian taxa. We surveyed 240 species spanning the Least Concern to Critically Endangered categories as published in the International Union for Conservation of Nature's Red List of Threatened Species. Using a single genome for each species, we estimated historical effective population sizes and distributions of genome-wide heterozygosity. To estimate genetic load, we identified substitutions relative to reconstructed ancestral sequences, assuming that mutations at evolutionarily conserved sites and in protein coding sequences, especially in genes essential for viability in mice, are predominantly deleterious. We examined relationships between the conservation status of species and metrics of heterozygosity, demography, and genetic load, and used these data to train and test models to distinguish threatened from non-threatened species.

#### Results

Species with smaller historical effective population sizes are more likely to be categorized as at risk of extinction, suggesting that demography, even from periods more than 10,000 years in the past, may be informative of contemporary resilience. Species with smaller historical effective population sizes also carry proportionally higher burdens of weakly and moderately deleterious alleles, consistent with theoretical expectations of the long-term accumulation and fixation of genetic load under strong genetic drift. We found weak support for a causative link between fixed drift load and extinction risk; however, other types of genetic load not captured in our data, such as rare, large-effect, deleterious alleles, may also play a role. Although ecological (e.g. physiological, life-history, and behavioral) variables were the best predictors of extinction risk, genomic variables non-randomly distinguished threatened from non-threatened species in regression and machine learning models. These results suggest that information encoded within even a single genome can provide a risk assessment in the absence of adequate ecological or population census data.

# Conclusion

Our analysis highlights the potential for genomic data to rapidly and inexpensively gauge extinction risk by leveraging relationships between contemporary conservation status and genetic variation shaped by the long-term demographic history of species. As more resequencing data and additional reference genomes become available, estimates of genetic load, recent demographic history, and accuracy of predictive models will improve. We therefore echo calls for including genomic information in assessments of the conservation status of species.

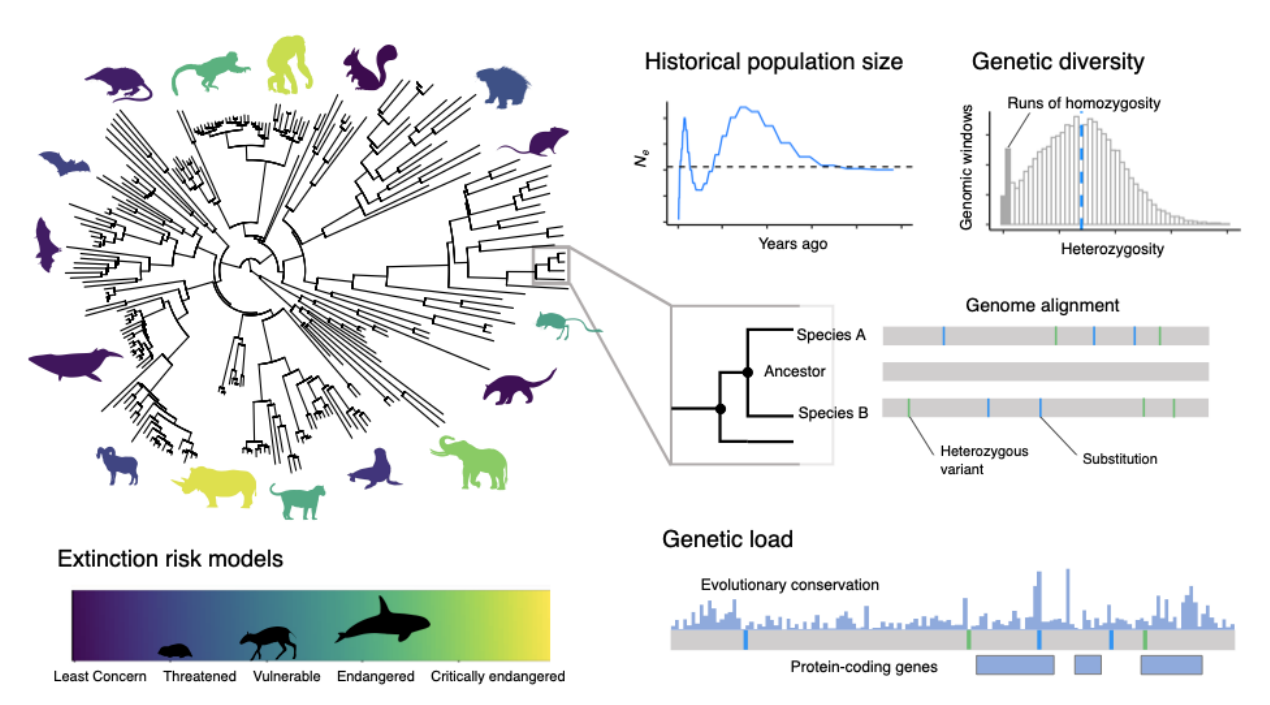


**Figure caption:** Genomic information can help predict extinction risk in diverse mammalian species. Across 240 mammals, species with smaller historical effective population sizes had lower genetic diversity, higher genetic load, and were more likely to be threatened with extinction. Genomic data were used to train models that predict whether a species is threatened, which can be valuable for assessing extinction risk in species lacking ecological or census data.

**Abstract:** Species persistence can be influenced by the amount, type, and distribution of diversity across the genome, suggesting a potential relationship between historical demography and resilience. Here, we surveyed genetic variation across single genomes of 240 mammals comprising the Zoonomia alignment to evaluate how historical effective population size ( $N_e$ ) impacts heterozygosity and deleterious genetic load and how these factors may contribute to extinction risk. We find that species with smaller historical  $N_e$  carry a proportionally larger burden of deleterious alleles due to long-term accumulation and fixation of genetic load, and have higher risk of extinction. This suggests that historical demography can inform contemporary resilience. Models that included genomic data were predictive of species' conservation status, suggesting that, in the absence of adequate census or ecological data, genomic information may provide an initial risk assessment.

**One-Sentence Summary:** Genomic data from 240 species show that information encoded within a single genome can provide a conservation risk assessment.

#### **Main Text:**

The current rate of biodiversity loss amounts to a sixth mass extinction(1) and is compounded by substantial population declines across nearly one third of vertebrate species(2). Many species need immediate conservation intervention, a process that is especially challenging for the more than 20,000 species currently listed as "Data Deficient" by the International Union for Conservation of Nature (IUCN). Fortunately, genomic data, which are increasingly available for a broad taxonomic range of species, may hold promise for helping to identify at-risk species by providing readily accessible information on demography and fitness-relevant genetic variation(3, 4). It remains poorly explored, however, to what extent genomic data on their own are sufficient to help triage endangered species for conservation intervention.

Population genetic diversity and individual heterozygosity are long recognized correlates of fitness-relevant functional variation(5, 6). Our previous analysis of 124 placental mammalian genomes showed that lower heterozygosity and stretches of homozygosity are more common in species in threatened IUCN Red List categories(7). However, functional diversity, including estimates of adaptive variation and genetic load, may also be useful correlates of population resiliency. Such measures are increasingly accessible with emerging genomic tools(8) and comparative genomics resources such as the Zoonomia alignment of placental mammalian genomes (table S1)(7). The Zoonomia alignment provides high-resolution constraint scores and reconstructed ancestral sequences that can help to identify deleterious alleles at functionally important sites(7, 9).

Here, we surveyed the distribution of neutral and functional genetic variation across 240 species in the Zoonomia alignment to determine how historical effective population sizes ( $N_e$ ) have influenced heterozygosity and deleterious genetic load (fig. S1). We test the value of genomic data to more precisely target species for conservation efforts by comparing the outcome of predictive models of conservation status that use ecological data, genomic data, or both. While we acknowledge the limitations of assuming that single genomes are representative of a species, our approach capitalizes on the unique resource provided by the Zoonomia consortium to explore whether genomic data can provide initial risk assessments that may be useful to triage data-deficient species and guide resource allocation for conservation intervention.

# Historical population size is relevant to contemporary extinction risk

Species with historically small  $N_e$  tend to be classified in threatened IUCN Red List categories (Fig. 1). Species classified as Near Threatened (NT), Vulnerable (VU), Endangered (EN) or Critically Endangered (CR) had significantly smaller harmonic mean  $N_e$  (mean<sub>threatened</sub>=18,950) compared to non-threatened species (Least Concern (LC); mean<sub>non-threatened</sub>=27,839; p<3.3e-5 when accounting for relationships across the phylogeny; Fig. 1B; figs. S2).  $N_e$  was also significantly smaller in threatened compared to non-threatened species within two of three taxonomic orders with sufficient numbers of species to test (Cetartiodactyla: mean<sub>threatened</sub>=18,336, mean<sub>non-threatened</sub>=22,648, p=0.023; and Carnivora: mean<sub>threatened</sub>=9,636, mean<sub>non-threatened</sub>=26,195, p=2.4e-5; but not Primates: mean<sub>threatened</sub>=22,508, mean<sub>non-threatened</sub>=24,373, p=0.31; fig. S3). Within these two orders in particular, large-bodied herbivores and carnivores have declined in both geographic range and population size during the Anthropocene(10, 11). Smaller populations are expected to have higher extinction risk, yet these historical  $N_e$  estimates reflect periods more than 10,000 years in the past, suggesting that long-

term characteristics of ancestral populations can be informative about population size and extinction risk today. These results support the utility of metrics of genome-wide diversity in conservation assessments, a topic that is currently debated (12, 13).

Estimates of historical  $N_e$  can also identify previously large populations that have experienced contemporary declines. Specifically, if the estimate of historical  $N_e$  is large while  $N_c$  is small, this inflates the  $N_e/N_c$  ratio. In a study of pinnipeds, for example, most species that had undergone recent declines had smaller population census sizes ( $N_c$ ) than expected based on their historical  $N_e$  (14). To test this across the taxonomic range of the Zoonomia alignment, we examined the ratio of deep historical  $N_e$  to contemporary  $N_c$  for 89 species with population census information available in PanTHERIA(15). Species in threatened IUCN categories had larger  $N_e/N_c$  ratios, i.e. smaller contemporary  $N_c$  relative to historical  $N_e$  (mean<sub>threatened</sub>=1.07e-3; mean<sub>non-threatened</sub>=4.29e-4; p=0.012; Fig. 1C). The relationship was also significant within Primates (phylolm, mean<sub>threatened</sub>=3.46e-3; mean<sub>non-threatened</sub>=1.11e-3; p=0.029), the only order with available  $N_e/N_c$  estimates and sufficient numbers of taxa in the two threat categories, indicating that the pattern holds among species with similar life-history traits. Across taxa, the largest  $N_e/N_c$  ratios included American bison ( $Bison\ bison$ ), giant panda ( $Ailuropoda\ melanoleuca$ ), and hirola ( $Beatragus\ hunteri$ ), all of which have declined due to recent human activities (16-18).

# Historically smaller populations carry proportionally larger burdens of genetic load

Historical  $N_e$  is correlated with the proportion of deleterious substitutions in mammalian genomes, reflecting the accumulation and fixation of genetic load over long evolutionary time periods. We called derived, single nucleotide substitutions for each species relative to the reconstructed sequence of the nearest ancestral phylogenetic node and called heterozygous sites from resequencing data mapped to the focal genome. We inferred the impacts of derived substitutions and heterozygous variants assuming that mutations at sites that are conserved across taxa (phyloP>2.27)(9) and nonsynonymous mutations are predominantly deleterious (fig. S1)(19). Assuming most substitutions are fixed and mutation rates are similar across the phylogeny (20)(21), the proportion of substitutions that are deleterious should be correlated with the total number of fixed deleterious mutations in the genome. Deleterious substitutions should therefore largely reflect fixed drift load that reduces the mean fitness of the population, whereas heterozygous deleterious variants reflect segregating mutational load(22).

We found that species with smaller  $N_e$  had proportionally more substitutions at evolutionarily conserved sites genome-wide (phylolm, p=9.65e-3) and proportionally more missense substitutions in genes (phylolm, p=7.76e-5; fig. S4). Phylop kurtosis, which describes the extreme phyloP outliers in the tail of the distribution across substitutions, was positively correlated with  $N_e$  (phylolm, p=0.014). This means that species with smaller  $N_e$  had smaller right tails and therefore fewer substitutions at extremely conserved sites. To further parse potential fitness impacts of mutations in protein-coding regions, we examined genes with associated viability phenotypes in single-gene knockout mouse lines classified by the International Mouse Phenotyping Consortium (IMPC), assuming that, when aggregated across many genes, viability classifications are correlated to their fitness impacts in other species(23). Species with smaller  $N_e$  had proportionally more missense mutations relative to coding mutations in nearly all categories (phylolm, p<3.00e-5; Fig. 2; figs. S5-S6). We observed proportionally fewer missense mutations in IMPC lethal genes relative to IMPC viable genes (ANOVA, p<4.42e-9; fig. S7), reflecting

stronger purifying selection in the lethal gene class, but the negative correlation was nonetheless consistent for both lethal and viable categories (Fig. 2). This relationship supports both theoretical predictions that smaller populations experiencing strong drift accumulate and fix weakly and moderately deleterious alleles (drift load)(12, 24) and empirical studies involving fewer or single taxa(25–27).

The correlations between  $N_e$  and conservation status and between  $N_e$  and drift load suggests that historical demography may influence contemporary extinction risk by shaping genome-wide diversity and genetic load. We found inconsistent relationships, however, between a species' proportional genetic load and its odds of being threatened. Species with proportionally more missense substitutions were more likely to be threatened when considering all genes (phyloglm, p=0.002; fig. S4D), as well as genes in lethal and viable IMPC categories (phyloglm, p<0.023; fig. S6), as observed in other taxa(28). Drift load estimated from evolutionary constraint across the genome, however, showed the opposite pattern: species with proportionally fewer substitutions at evolutionarily conserved sites were more likely to be threatened (phyloglm, p=1.38e-05; fig. S4C). This latter result contrasts with expectations, given that threatened species have smaller  $N_e$  on average (Fig 1) and smaller  $N_e$  is associated with proportionally more substitutions at conserved sites (phylolm, p=9.6e-3; fig. S4A). Interestingly, a previous study of 100 mammal genomes also found that threatened species had lower mean conservation scores across mutations(29). They suggested that the pattern may reflect fewer recessive deleterious alleles due to purging or the loss of these rare alleles to drift. The conflicting relationships between conservation status and metrics of drift load thus do not provide strong support for a mechanistic link between fixed drift load as measured in this study and species' resilience against extinction.

# Genomic information can help predict extinction risk

Historical  $N_e$  was the most consistent genomic predictor of conservation status across regression models, while the predictive value of genetic load metrics varied with phylogenetic context (Fig. 3, tables S2-S3). Ordinal and logistic regression models incorporating genomic variables with taxonomic order and dietary trophic level showed that the effect of  $N_e$  varied by ecological context. For example, an herbivore with a given  $N_e$  was more likely to be threatened than a carnivore or omnivore with the same  $N_e$  (Fig. 3B), supporting findings of elevated extinction risk in herbivores despite larger populations (30). Similarly, Carnivora and Primates both had increased risk with lower levels of severely deleterious genetic load. However, the specific metric of load that predicted conservation status differed among taxonomic orders, perhaps reflecting differences in natural history or ecological flexibility (figs. S8-S10). Principal components (PC) regression of demographic and genetic load variables showed that, overall, threatened species tended to have proportionally more deleterious mutations in coding regions, lower heterozygosity, and smaller  $N_e$  (PC1; p=0.0038), as well as proportionally more missense substitutions (PC3; p=5.6e-4; Fig. 3A, table S3). Although no single genomic variable unambiguously discriminated threatened from non-threatened species (fig. S2), many have predictive value, which will be particularly relevant for species lacking adequate ecological or census data.

Although ecological data were more powerful than genomic data to predict extinction risk in our predictive models, models using only information from single genomes nonetheless identified

species at risk of being threatened. We generated random forest models to predict conservation status from ecological traits(31, 32) and genomic features, using area under the receiver operating characteristic (AUROC) to evaluate performance. A model with AUROC of 0.5 has no predictive ability, whereas a model with AUROC of 1.0 has perfect predictive performance. We selected predictive variables from among 13 genome-wide summary statistics including demographic history, genetic diversity, and genetic load variables, ~57,000 window-based metrics per genome, and 39 ecological variables from PanTHERIA(15) including physiological, life-history, and behavioral variables (table S4). Models including only genomic features and no ecological variables (17 models; AUROC ranged from 0.69-0.82) performed worse than models including only ecological variables (1 model; AUROC 0.88) and similarly to models including both genomic and ecological variables (17 models; AUROC range 0.68-0.83; table S5). Models with only genomic features were, however, consistently better able to distinguish threatened from non-threatened species (tables S5-S6; fig. S11-13) compared to random chance (i.e. AUROC of 0.5). Models including only genomic variables performed similarly to other studies that predicted IUCN status from ecological or morphological data with comparable sample sizes (e.g. AUC ranging from 0.67-0.90 for n=171-430 species) (33–35).

The number of species with values for ecological, genome-wide summary statistics, and window-based metrics differed, which may affect model performance. To compare the predictive value of genomic and ecological features directly, we next tested models in a set of 210 species for which both data types were available (tables S4 and S6). Again, the model with genome-wide summary statistics alone was predictive of threatened status (AUROC 0.71), but performed more poorly than the model with ecological variables (AUROC 0.83). Combining genomic summary statistics with ecological variables led to a modest improvement in distinguishing threatened from non-threatened species (AUROC=0.85) compared to genomic variables alone, with  $N_e$  as the fourth most important predictor in the model after weaning age, age at first birth, and age of sexual maturity (fig. S14). Models including genomic window-based features never outperformed models with ecological variables alone (table S6), suggesting that complementary information provided by genomic versus ecological data may be better captured by summary or transformed variables (e.g. principal components) than by numerous weakly informative window features that may overwhelm the predictive models. Overall, our evaluation suggests that while genomic information from a single individual is not better than ecological data for predicting threatened status, these data do have predictive value, especially when ecological variables are unavailable.

As a demonstration of their utility, we applied our regression and random forest models to predict the status of three species considered "Data Deficient" by the IUCN (Fig. 3D). The models suggest the Upper Galilee Mountains blind mole rat (*Nannospalax galili*), which lacks ecological data, is least likely to be threatened (11-44% probability), whereas the killer whale (*Orcinus orca*), for which both ecological and genomic data are available, is more likely to be threatened (35-68% probability), consistent with the identification of some at-risk populations(36). Predictions for the Java lesser chevrotain (*Tragulus javanicus*) depend on model specifications, with the highest threat prediction from the within-order regression model (67% probability), and other models suggesting it is less likely to be threatened (24-49% probability). The results indicate that, among the three species, the killer whale should be prioritized for further study, and demonstrate how genomic data can provide a rapid and inexpensive initial conservation assessment.

#### **Discussion**

Our results provide empirical support for theoretical predictions that small populations accumulate and fix weakly and moderately deleterious alleles, and demonstrate a correlation between historical effective population size and contemporary extinction risk. We found little evidence, however, that species with historically small effective population sizes have higher risks of extinction because of elevated drift load. Alternatively, historically small populations may have elevated extinction risk simply because these populations are small and thus more vulnerable to other threats such as habitat loss or change, the introduction of infectious disease, competition with invasive species, and new hunting or predation pressures.

Despite the limitations of assuming that a single genome is representative of the diversity within a species, our comparative genomics approach allowed us to maximize the number of species analyzed to explore the power to detect genomic correlates of endangerment. Empirical studies suggest a single individual can represent a species for characteristics shaped by long-term evolutionary history; variation in the proportion of deleterious mutations is typically smaller within species than between (37, 29), and historical  $N_e$  estimates are consistent across conspecifics (38, 39). The analysis of multiple resequenced individuals per species, however, will increase accuracy and resolution by capturing intraspecific variation in genetic diversity, heterozygosity, and inbreeding (especially for species with strong population structure), enabling estimation of allele frequencies, improving inference of more recent demographic history, and allowing better detection of rare and segregating variants(e.g. inbreeding load; 22). The latter may be particularly important for estimating extinction risk, as segregating variants tend to be enriched for deleterious alleles (40, 41) and may disproportionately impact extinction risk from population bottlenecks(12). In the future, larger data sets comprising multiple individuals per species may shed light on long-standing questions about the relative impact on fitness of many weakly deleterious alleles versus a few strongly deleterious alleles (22, 25, 37, 42, 43).

Inferring real-world fitness from genomic data includes caveats. Evolutionary constraint may, for example, reflect past selection on loci that no longer impact fitness(44). Loci that seem functionally important in model species may be irrelevant to the species of interest, compensatory mutations may ameliorate the impact of deleterious mutations, and factors such as dominance, epistasis, pleiotropy, and purging may also complicate the relationship between genetic load and fitness. Finally, local differences in habitat may mean that the impact of deleterious mutations differs among individuals or populations(25, 45, 46). For these reasons, the impact of the observed proportionally higher load in smaller populations will be challenging to know in the absence of direct fitness data, such as reproductive success and the frequencies of genetic diseases and congenital abnormalities(26, 43, 47).

As additional genomes and population resequencing data become available (48), the power and accuracy of predictions of extinction risk from genomes will improve (8). Our analyses of the genomes of single individuals, which can be generated rapidly and inexpensively (49), demonstrate the potential for using genomic estimates of demography, diversity, and genetic load to triage species in need of immediate management intervention, and we join in the calls for including genomics into conservation status assessments (50–53).

#### **Materials and Methods**

We provide a summary of our materials and methods below; refer to the Supplemental Materials and Methods for further detail.

# Mammal genomes and metadata

We examined genomic variation in 240 species represented by 241 reference genomes in the Zoonomia multispecies alignment. The genome assemblies varied in quality, with contig N50 values ranging from 1 KB to 56 MB (table S1). Short-read sequence data, usually from the reference individual, were used to estimate metrics related to historical demography, heterozygosity, and heterozygous deleterious variants from single genomes. Homozygous deleterious genetic load was estimated relative to reconstructed ancestral sequences from the multispecies alignment (fig. S1). We tested correlations between all genomic metrics, and between genomic metrics and extinction risk, using a statistical framework that accounts for phylogenetic relationships across species. Using regression and machine learning models, we tested the potential for genomic data to predict the conservation status of species.

For all species, we compiled metadata on conservation status, diet, and generation time (table S1). We assigned a conservation status (Least Concern (LC), Near Threatened (NT), Vulnerable (VU), Endangered (EN) or Critically Endangered (CR)) to the lowest known taxonomic level of the sequenced sample, using the IUCN Red List of Threatened Species (IUCN Red List API v. 3) as a proxy for extinction risk. We classified each species as carnivore, herbivore, or omnivore based on(54), using information for the genus when species-specific information was unavailable. From available metadata, we categorized the sample used for both the reference genome and short-read data as a wild, captive, or domesticated individual.

Tests for correlations between variables were conducted with phylogenetic linear regression or phylogenetic logistic regression in the R package phylolm(55), incorporating the phylogenetic tree with branch lengths(56) to account for non-independence.

# Estimating historical effective population sizes and genome-wide heterozygosity

We called heterozygous positions in all genomes with short-read data using the GATK best practices pipeline as described previously(7). Briefly, we mapped paired-end sequencing data to the respective genome assemblies using BWA mem (version 0.7.15)(57), marked and removed optical duplicates, and called heterozygous variants using the HaplotypeCaller module of the GATK software suite (version 3.6)(58).

We inferred the history of effective population sizes ( $N_e$ ) for each species using PSMC (version 0.6.5-r67)(59). We called variants in each genome from scaffolds >50KB in length, filtered for sequence read coverage and base quality score, and used these as input for PSMC. We rescaled the PSMC output using species-specific generation times(60) and a mammalian mutation rate(21) and calculated the harmonic mean across temporal estimates from periods >10 kya. To compare contemporary population sizes to historical  $N_e$ , we obtained census population estimates ( $N_c$ ) for 89 species from the PanTHERIA database(15), estimating  $N_c$  as the product of population density and geographic area from census data(15, 61).

To identify runs of homozygosity (RoH), we used our previously described method(7). For every assembly, we calculated the ratio of heterozygous to callable positions in non-overlapping, 50-kb windows, and fit a 2-component Gaussian Mixture Model to the joint distribution, which is expected to be bimodal with a peak at the lower tail of the distribution corresponding to runs of

homozygosity (fig. S1B). Windows were then assigned as RoH or non-RoH and used to calculate the proportion of the genome in RoH (fRoH), genome-wide heterozygosity, and outbred heterozygosity (i.e. heterozygosity in non-RoH regions; figs. S2 and S15).

# Deleterious genetic load

We called heterozygous variants from single sample, short-read data mapped to the reference genome of each species. Homozygous substitutions were estimated from each reference genome relative to the closest reconstructed ancestral sequence in the phylogeny using the halBranchMutations tool in the Comparative Genomics Toolkit(62). Because new alleles become fixed or lost on the order of  $<4N_e$  generations(63), most homozygous substitutions between species are likely fixed. We assessed the potential functional impact of mutations by 1) evolutionary conservation of the site (phyloP), and 2) the estimated impact of the mutation on protein-coding genes. Mutations at evolutionarily conserved sites (phyloP>2.27;(9)), and those that cause nonsynonymous changes in protein-coding genes, were assumed to be predominantly harmful(19). Variant sites in each genome were assigned human-based phyloP scores estimated from the multispecies alignment(9). To infer functional impacts on protein-coding genes, each genome was annotated with human orthologs by lifting over human exon intervals to the target species. Synonymous, missense and loss-of-function variants were then estimated in the program SnpEff v.5.0e(64). We also examined mutations in single-copy genes with associated viability phenotypic data in knockout mice as classified by the International Mouse Phenotyping Consortium (IMPC)(23), using IMPC categories (e.g. lethal or viable) as a proxies for gene essentiality and the potential fitness impacts of mutations in these genes(23).

# Predicting threat from genomic variables

To predict whether a species is threatened (NT, VU, EN, and CR categories) or non-threatened (LC category), we modeled conservation status across species from genomic variables using both regression and machine learning models.

We took two main approaches in our regression models of conservation status across species, using 1) phylogenetic logistic regression to model threatened versus non-threatened status, which allowed us to test the significance of predictor variables, but not make predictions for species with unknown threat status, and 2) ordinal regression models of specific IUCN categories, which allowed us to test significance and make predictions for species with unknown threat status. Unlike logistic regression, ordinal regression did not inherently incorporate the phylogeny, so we included taxonomic order as a factor in the models. We tested 13 genomic variables (table S2), modeled individually and as principal components, and included taxonomic order and dietary trophic level, a previously described correlate of extinction risk(65). We estimated model error by fitting parameters on 80% of the data and testing the remaining 20% of the data across 100 runs with different data subsets.

We used random-forest based classification to estimate the likelihood that a species is threatened from 13 genome-wide summary statistics of heterozygosity, demographic history, and genetic load, and from 5 genomic metrics within homologous 50KB windows (table S4). We trained models using the two genomic data types (windows-based and genome-wide) separately and combined, and incorporated 39 ecological variables from the PanTHERIA database (table S4). We used the scikit-learn 1.0.2 package for fitting all the models (66).

We first split our dataset into a 75% training set and a 25% test set. For each model, we performed preprocessing and imputation steps using only the training data, then trained the model on the training set and evaluated it on the test set. We ran 5-fold cross validation on the training set to determine the optimal set of hyperparameters, tuning the number of decision trees, the maximum depth of the trees, and the number of features used at each decision to optimize a performance metric. We used AUROC to estimate how well a model predicts the correct output class. AUROC is designed to be more robust to class imbalance in comparison to a metric such as accuracy.

To leverage all available data, we first ran models using all species with data for a given data type (table S5). The number of species with values for ecological, genome-wide summary statistics, and window-based metrics differed however, which may impact the results. To compare the performance of ecological and genomic variables and their combination across the same set of species, we also trained and tested models in the set of species for which both data types were available (table S6).

The Zoonomia alignment included three species classified as "Data Deficient" by the IUCN, the Upper Galilee Mountains blind mole rat (*Nannospalax galili*), the Java lesser chevrotain (*Tragulus javanicus*), and the killer whale (*Orcinus orca*). The blind mole rat lacked ecological data on PanTHERIA. We used the within-order and across-order ordinal regression models and all random forest models to predict the probability that these species are threatened.

#### **References and Notes**

- 1. A. D. Barnosky, N. Matzke, S. Tomiya, G. O. U. Wogan, B. Swartz, T. B. Quental, C. Marshall, J. L. McGuire, E. L. Lindsey, K. C. Maguire, B. Mersey, E. A. Ferrer, Has the Earth's sixth mass extinction already arrived? *Nature*. **471**, 51–57 (2011).
- 2. G. Ceballos, A. H. Ehrlich, P. R. Ehrlich, *The Annihilation of Nature: Human Extinction of Birds and Mammals* (JHU Press, 2015).
- 3. M. A. Supple, B. Shapiro, Conservation of biodiversity in the genomics era. *Genome Biol.* **19**, 131 (2018).
- 4. B. Hansson, H. E. Morales, C. van Oosterhout, Comment on "Individual heterozygosity predicts translocation success in threatened desert tortoises." *Science*. **372** (2021), p. eabh1105.
- 5. B. Hansson, L. Westerberg, On the correlation between heterozygosity and fitness in natural populations. *Molecular Ecology.* **11** (2002), pp. 2467–2474.
- 6. J. A. DeWoody, A. M. Harder, S. Mathur, J. R. Willoughby, The long-standing significance of genetic diversity in conservation. *Mol. Ecol.* **30** (2021), pp. 4147–4154.
- 7. Zoonomia Consortium, A comparative genomics multitool for scientific discovery and conservation. *Nature*. **587**, 240–245 (2020).
- 8. C. van Oosterhout, Mutation load is the spectre of species conservation. *Nat Ecol Evol.* **4**, 1004–1006 (2020).
- 9. M. J. Christmas, I. M. Kaplow, Zoonomia consortium, Evolutionary constraint and innovation across hundreds of placental mammals. *Science*.

- 10. W. J. Ripple, J. A. Estes, R. L. Beschta, C. C. Wilmers, E. G. Ritchie, M. Hebblewhite, J. Berger, B. Elmhagen, M. Letnic, M. P. Nelson, O. J. Schmitz, D. W. Smith, A. D. Wallach, A. J. Wirsing, Status and Ecological Effects of the World's Largest Carnivores. *Science*. **343** (2014), , doi:10.1126/science.1241484.
- 11. W. J. Ripple, T. M. Newsome, C. Wolf, R. Dirzo, K. T. Everatt, M. Galetti, M. W. Hayward, G. I. H. Kerley, T. Levi, P. A. Lindsey, D. W. Macdonald, Y. Malhi, L. E. Painter, C. J. Sandom, J. Terborgh, B. Van Valkenburgh, Collapse of the world's largest herbivores. *Science Advances*. 1 (2015), doi:10.1126/sciadv.1400103.
- 12. M. Kardos, E. E. Armstrong, S. W. Fitzpatrick, S. Hauser, P. W. Hedrick, J. M. Miller, D. A. Tallmon, W. C. Funk, The crucial role of genome-wide genetic variation in conservation. *Proc. Natl. Acad. Sci. U. S. A.* **118** (2021), doi:10.1073/pnas.2104642118.
- 13. J. C. Teixeira, C. D. Huber, The inflated significance of neutral genetic diversity in conservation genetics. *Proc. Natl. Acad. Sci. U. S. A.* **118** (2021), doi:10.1073/pnas.2015096118.
- 14. C. R. Peart, S. Tusso, S. D. Pophaly, F. Botero-Castro, C.-C. Wu, D. Aurioles-Gamboa, A. B. Baird, J. W. Bickham, J. Forcada, F. Galimberti, N. J. Gemmell, J. I. Hoffman, K. M. Kovacs, M. Kunnasranta, C. Lydersen, T. Nyman, L. R. de Oliveira, A. J. Orr, S. Sanvito, M. Valtonen, A. B. A. Shafer, J. B. W. Wolf, Determinants of genetic variation across eco-evolutionary scales in pinnipeds. *Nat Ecol Evol.* 4, 1095–1104 (2020).
- 15. K. E. Jones, J. Bielby, M. Cardillo, S. A. Fritz, J. O'Dell, C. D. L. Orme, K. Safi, W. Sechrest, E. H. Boakes, C. Carbone, C. Connolly, M. J. Cutts, J. K. Foster, R. Grenyer, M. Habib, C. A. Plaster, S. A. Price, E. A. Rigby, J. Rist, A. Teacher, O. R. P. Bininda-Emonds, J. L. Gittleman, G. M. Mace, A. Purvis, PanTHERIA: a species-level database of life history, ecology, and geography of extant and recently extinct mammals. *Ecology*. **90** (2009), pp. 2648–2648.
- 16. IUCN SSC Antelope Specialist Group, "Beatragus hunteri: IUCN SSC Antelope Specialist Group" (2017), , doi:10.2305/IUCN.UK.2017-2.RLTS.T6234A50185297.en.
- 17. S. Zhao, P. Zheng, S. Dong, X. Zhan, Q. Wu, X. Guo, Y. Hu, W. He, S. Zhang, W. Fan, L. Zhu, D. Li, X. Zhang, Q. Chen, H. Zhang, Z. Zhang, X. Jin, J. Zhang, H. Yang, J. Wang, J. Wang, F. Wei, Whole-genome sequencing of giant pandas provides insights into demographic history and local adaptation. *Nat. Genet.* **45**, 67–71 (2013).
- 18. P. W. Hedrick, Conservation genetics and North American bison (Bison bison). *J. Hered.* **100**, 411–420 (2009).
- 19. B. M. Henn, L. R. Botigué, C. D. Bustamante, A. G. Clark, S. Gravel, Estimating the mutation load in human genomes. *Nat. Rev. Genet.* **16**, 333–343 (2015).
- 20. M. Kimura, Evolutionary Rate at the Molecular Level. *Nature*. **217** (1968), pp. 624–626.
- 21. S. Kumar, S. Subramanian, Mutation rates in mammalian genomes. *Proc. Natl. Acad. Sci. U. S. A.* **99**, 803–808 (2002).
- 22. P. W. Hedrick, A. Garcia-Dorado, Understanding Inbreeding Depression, Purging, and Genetic Rescue. *Trends Ecol. Evol.* **31**, 940–952 (2016).

- V. Muñoz-Fuentes, P. Cacheiro, T. F. Meehan, J. A. Aguilar-Pimentel, S. D. M. Brown, A. M. Flenniken, P. Flicek, A. Galli, H. H. Mashhadi, M. Hrabě de Angelis, J. K. Kim, K. C. K. Lloyd, C. McKerlie, H. Morgan, S. A. Murray, L. M. J. Nutter, P. T. Reilly, J. R. Seavitt, J. K. Seong, M. Simon, H. Wardle-Jones, A.-M. Mallon, D. Smedley, H. E. Parkinson, IMPC consortium, The International Mouse Phenotyping Consortium (IMPC): a functional catalogue of the mammalian genome that informs conservation. *Conserv. Genet.* 19, 995–1005 (2018).
- 24. M. Kimura, T. Maruyama, J. F. Crow, THE MUTATION LOAD IN SMALL POPULATIONS. *Genetics*. **48** (1963), pp. 1303–1312.
- 25. C. Grossen, F. Guillaume, L. F. Keller, D. Croll, Purging of highly deleterious mutations through severe bottlenecks in Alpine ibex. *Nat. Commun.* 11, 1–12 (2020).
- 26. J. A. Robinson, J. Räikkönen, L. M. Vucetich, J. A. Vucetich, R. O. Peterson, K. E. Lohmueller, R. K. Wayne, Genomic signatures of extensive inbreeding in Isle Royale wolves, a population on the threshold of extinction. *Sci Adv.* 5, eaau0757 (2019).
- 27. K. Yoshida, M. Ravinet, T. Makino, A. Toyoda, T. Kokita, S. Mori, J. Kitano, Accumulation of Deleterious Mutations in Landlocked Threespine Stickleback Populations. *Genome Biol. Evol.* **12**, 479–492 (2020).
- 28. J. Rolland, D. Schluter, J. Romiguier, Vulnerability to Fishing and Life History Traits Correlate with the Load of Deleterious Mutations in Teleosts. *Mol. Biol. Evol.* **37**, 2192–2196 (2020).
- 29. T. van der Valk, M. de Manuel, T. Marques-Bonet, K. Guschanski, Estimates of genetic load suggest frequent purging of deleterious alleles in small populations. *bioRxiv* (2021), doi:10.1101/696831.
- 30. T. B. Atwood, S. A. Valentine, E. Hammill, D. J. McCauley, E. M. P. Madin, K. H. Beard, W. D. Pearse, Herbivores at the highest risk of extinction among mammals, birds, and reptiles. *Science Advances*. **6** (2020), p. eabb8458.
- 31. L. M. Bland, B. Collen, C. D. L. Orme, J. Bielby, Predicting the conservation status of data-deficient species. *Conserv. Biol.* **29**, 250–259 (2015).
- 32. A. D. Davidson, M. J. Hamilton, A. G. Boyer, J. H. Brown, G. Ceballos, Multiple ecological pathways to extinction in mammals. *Proc. Natl. Acad. Sci. U. S. A.* **106**, 10702–10705 (2009).
- 33. R. H. L. Walls, N. K. Dulvy, Eliminating the dark matter of data deficiency by predicting the conservation status of Northeast Atlantic and Mediterranean Sea sharks and rays. *Biological Conservation.* **246** (2020), p. 108459.
- 34. D. B. Miles, Can Morphology Predict the Conservation Status of Iguanian Lizards? *Integr. Comp. Biol.* **60**, 535–548 (2020).
- 35. R. K. Kopf, C. Shaw, P. Humphries, Trait-based prediction of extinction risk of small-bodied freshwater fishes. *Conserv. Biol.* **31**, 581–591 (2017).
- 36. E. Jourdain, F. Ugarte, G. A. Víkingsson, F. I. P. Samarra, S. H. Ferguson, J. Lawson, D. Vongraven, G. Desportes, North Atlantic killer whale *Orcinus orca* populations: a review

- of current knowledge and threats to conservation. *Mammal Review*. **49** (2019), pp. 384–400.
- 37. J. A. Robinson, C. C. Kyriazis, S. F. Nigenda-Morales, A. C. Beichman, L. Rojas-Bracho, K. M. Robertson, M. C. Fontaine, R. K. Wayne, K. E. Lohmueller, B. L. Taylor, P. A. Morin, The critically endangered vaquita is not doomed to extinction by inbreeding depression. *Science*. **376**, 635–639 (2022).
- 38. N. F. Saremi, M. A. Supple, A. Byrne, J. A. Cahill, L. L. Coutinho, L. Dalén, H. V. Figueiró, W. E. Johnson, H. J. Milne, S. J. O'Brien, B. O'Connell, D. P. Onorato, S. P. D. Riley, J. A. Sikich, D. R. Stahler, P. M. S. Villela, C. Vollmers, R. K. Wayne, E. Eizirik, R. B. Corbett-Detig, R. E. Green, C. C. Wilmers, B. Shapiro, Puma genomes from North and South America provide insights into the genomic consequences of inbreeding. *Nat. Commun.* 10, 4769 (2019).
- 39. W. K. Meyer, A. Venkat, A. R. Kermany, B. van de Geijn, S. Zhang, M. Przeworski, Evolutionary history inferred from the de novo assembly of a nonmodel organism, the blue-eyed black lemur. *Mol. Ecol.* **24**, 4392–4405 (2015).
- 40. G. Bertorelle, F. Raffini, M. Bosse, C. Bortoluzzi, A. Iannucci, E. Trucchi, H. E. Morales, C. van Oosterhout, Genetic load: genomic estimates and applications in non-model animals. *Nat. Rev. Genet.* **23**, 492–503 (2022).
- 41. J. B. W. Wolf, A. Künstner, K. Nam, M. Jakobsson, H. Ellegren, Nonlinear dynamics of nonsynonymous (dN) and synonymous (dS) substitution rates affects inference of selection. *Genome Biol. Evol.* 1, 308–319 (2009).
- 42. A. Khan, K. Patel, H. Shukla, A. Viswanathan, T. van der Valk, U. Borthakur, P. Nigam, A. Zachariah, Y. V. Jhala, M. Kardos, U. Ramakrishnan, Genomic evidence for inbreeding depression and purging of deleterious genetic variation in Indian tigers. *Proc. Natl. Acad. Sci. U. S. A.* **118** (2021), doi:10.1073/pnas.2023018118.
- 43. L. Smeds, H. Ellegren, From high masked to high realized genetic load in inbred Scandinavian wolves. *Mol. Ecol.* (2022), doi:10.1111/mec.16802.
- 44. C. D. Huber, B. Y. Kim, K. E. Lohmueller, Population genetic models of GERP scores suggest pervasive turnover of constrained sites across mammalian evolution. *PLoS Genet.* **16**, e1008827 (2020).
- 45. J. A. Mee, S. Yeaman, Unpacking Conditional Neutrality: Genomic Signatures of Selection on Conditionally Beneficial and Conditionally Deleterious Mutations. *Am. Nat.* **194**, 529–540 (2019).
- 46. Y. Zhang, A. J. Stern, R. Nielsen, Evolution of the genetic architecture of local adaptations under genetic rescue is determined by mutational load and polygenicity, , doi:10.1101/2020.11.09.374413.
- 47. J. A. Robinson, C. Brown, B. Y. Kim, K. E. Lohmueller, R. K. Wayne, Purging of Strongly Deleterious Mutations Explains Long-Term Persistence and Absence of Inbreeding Depression in Island Foxes. *Curr. Biol.* **28**, 3487–3494.e4 (2018).

- 48. H. B. Shaffer, E. Toffelmier, California Conservation Genomics Project First Year Annual Report (2020) (available at https://escholarship.org/content/qt2sc7s29z/qt2sc7s29z.pdf).
- 49. O. Dudchenko, M. S. Shamim, S. S. Batra, N. C. Durand, N. T. Musial, R. Mostofa, M. Pham, B. G. St Hilaire, W. Yao, E. Stamenova, M. Hoeger, S. K. Nyquist, V. Korchina, K. Pletch, J. P. Flanagan, A. Tomaszewicz, D. McAloose, C. P. Estrada, B. J. Novak, A. D. Omer, E. L. Aiden, The Juicebox Assembly Tools module facilitates *de novo* assembly of mammalian genomes with chromosome-length scaffolds for under \$1000, , doi:10.1101/254797.
- 50. F. W. Allendorf, P. A. Hohenlohe, G. Luikart, Genomics and the future of conservation genetics. *Nat. Rev. Genet.* **11**, 697–709 (2010).
- 51. B. J. Mcmahon, E. C. Teeling, J. Höglund, How and why should we implement genomics into conservation? *Evol. Appl.* 7, 999–1007 (2014).
- 52. P. Brandies, E. Peel, C. J. Hogg, K. Belov, The Value of Reference Genomes in the Conservation of Threatened Species. *Genes* . **10** (2019), doi:10.3390/genes10110846.
- 53. C. van Oosterhout, S. A. Speak, T. Birley, C. Bortoluzzi, L. Percival-Alwyn, L. H. Urban, J. J. Groombridge, G. Segelbacher, H. E. Morales, Genomic erosion in the assessment of species extinction risk and recovery potential, , doi:10.1101/2022.09.13.507768.
- 54. R. M. Nowak, E. P. Walker, Walker's Mammals of the World (JHU Press, 1999).
- 55. L. si T. Ho, C. Ané, A linear-time algorithm for Gaussian and non-Gaussian trait evolution models. *Syst. Biol.* **63**, 397–408 (2014).
- 56. N. M. Foley, V. C. Mason, A. J. Harris, K. R. Bredemeyer, J. Damas, H. A. Lewin, E. Eizirik, J. Gates, Zoonomia Consortium, M. S. Springer, W. J. Murphy, A genomic timescale for placental mammal evolution. *Science*.
- 57. H. Li, Aligning sequence reads, clone sequences and assembly contigs with BWA-MEM (2013), (available at http://arxiv.org/abs/1303.3997).
- 58. A. McKenna, M. Hanna, E. Banks, A. Sivachenko, K. Cibulskis, A. Kernytsky, K. Garimella, D. Altshuler, S. Gabriel, M. Daly, M. A. DePristo, The Genome Analysis Toolkit: a MapReduce framework for analyzing next-generation DNA sequencing data. *Genome Res.* **20**, 1297–1303 (2010).
- 59. H. Li, R. Durbin, Inference of human population history from individual whole-genome sequences. *Nature*. **475**, 493–496 (2011).
- 60. M. Pacifici, L. Santini, M. D. Marco, D. Baisero, L. Francucci, G. G. Marasini, P. Visconti, C. Rondinini, Generation length for mammals. *Nature Conservation*. **5**, 89–94 (2013).
- 61. A. B. Roddy, D. Alvarez-Ponce, S. W. Roy, Mammals with Small Populations Do Not Exhibit Larger Genomes. *Molecular Biology and Evolution.* **38** (2021), pp. 3737–3741.

- 62. G. Hickey, B. Paten, D. Earl, D. Zerbino, D. Haussler, HAL: a hierarchical format for storing and analyzing multiple genome alignments. *Bioinformatics*. **29** (2013), pp. 1341–1342.
- 63. S. P. Otto, M. C. Whitlock, Fixation Probabilities and Times. *Encyclopedia of Life Sciences* (2006), doi:10.1038/npg.els.0005464.
- 64. P. Cingolani, A. Platts, L. L. Wang, M. Coon, T. Nguyen, L. Wang, S. J. Land, X. Lu, D. M. Ruden, A program for annotating and predicting the effects of single nucleotide polymorphisms, SnpEff. *Fly.* **6** (2012), pp. 80–92.
- 65. A. Purvis, J. L. Gittleman, G. Cowlishaw, G. M. Mace, Predicting extinction risk in declining species. *Proc. Biol. Sci.* **267**, 1947–1952 (2000).
- 66. A. Abraham, F. Pedregosa, M. Eickenberg, P. Gervais, A. Mueller, J. Kossaifi, A. Gramfort, B. Thirion, G. Varoquaux, Machine learning for neuroimaging with scikit-learn. *Front. Neuroinform.* **8**, 14 (2014).
- 67. M. Martin, Cutadapt removes adapter sequences from high-throughput sequencing reads. *EMBnet.journal.* **17** (2011), p. 10.
- 68. Broad Institute, Picard Toolkit (2019), (available at http://broadinstitute.github.io/picard/).
- 69. G. Gower, J. Tuke, A. B. Rohrlach, J. Soubrier, B. Llamas, N. Bean, A. Cooper, Population size history from short genomic scaffolds: how short is too short? *bioRxiv* (2018), doi:10.1101/382036.
- 70. H. Li, B. Handsaker, A. Wysoker, T. Fennell, J. Ruan, N. Homer, G. Marth, G. Abecasis, R. Durbin, 1000 Genome Project Data Processing Subgroup, The Sequence Alignment/Map format and SAMtools. *Bioinformatics*. **25**, 2078–2079 (2009).
- 71. H. Li, B. Handsaker, P. Danecek, S. McCarthy, J. Marshall, BCFtools.
- 72. H. Li, Implementation of the Pairwise Sequentially Markovian Coalescent (PSMC) model (2016), (available at https://github.com/lh3/psmc).
- 73. A. H. Freedman, I. Gronau, R. M. Schweizer, D. Ortega-Del Vecchyo, E. Han, P. M. Silva, M. Galaverni, Z. Fan, P. Marx, B. Lorente-Galdos, H. Beale, O. Ramirez, F. Hormozdiari, C. Alkan, C. Vilà, K. Squire, E. Geffen, J. Kusak, A. R. Boyko, H. G. Parker, C. Lee, V. Tadigotla, A. Wilton, A. Siepel, C. D. Bustamante, T. T. Harkins, S. F. Nelson, E. A. Ostrander, T. Marques-Bonet, R. K. Wayne, J. Novembre, Genome sequencing highlights the dynamic early history of dogs. *PLoS Genet.* 10, e1004016 (2014).
- 74. A. H. Patton, M. J. Margres, A. R. Stahlke, S. Hendricks, K. Lewallen, R. K. Hamede, M. Ruiz-Aravena, O. Ryder, H. I. McCallum, M. E. Jones, P. A. Hohenlohe, A. Storfer, Contemporary Demographic Reconstruction Methods Are Robust to Genome Assembly Quality: A Case Study in Tasmanian Devils. *Mol. Biol. Evol.* 36, 2906–2921 (2019).
- 75. M. T. R. Hawkins, R. R. Culligan, C. L. Frasier, R. B. Dikow, R. Hagenson, R. Lei, E. E. Louis Jr, Genome sequence and population declines in the critically endangered greater bamboo lemur (Prolemur simus) and implications for conservation. *BMC Genomics*. **19**, 445 (2018).

- 76. R. Frankham, Effective population size/adult population size ratios in wildlife: a review. *Genet. Res.* **89**, 491–503 (2007).
- 77. J. Schreiber, Pomegranate: fast and flexible probabilistic modeling in python. *J. Mach. Learn. Res.* **18**, 5992–5997 (2018).
- J. Armstrong, G. Hickey, M. Diekhans, I. T. Fiddes, A. M. Novak, A. Deran, Q. Fang, D. Xie, S. Feng, J. Stiller, D. Genereux, J. Johnson, V. D. Marinescu, J. Alföldi, R. S. Harris, K. Lindblad-Toh, D. Haussler, E. Karlsson, E. D. Jarvis, G. Zhang, B. Paten, Progressive Cactus is a multiple-genome aligner for the thousand-genome era. *Nature*. 587, 246–251 (2020).
- 79. A. Siepel, K. S. Pollard, D. Haussler, New Methods for Detecting Lineage-Specific Selection. *Lecture Notes in Computer Science* (2006), pp. 190–205.
- 80. K. Lindblad-Toh, M. Garber, O. Zuk, M. F. Lin, B. J. Parker, S. Washietl, P. Kheradpour, J. Ernst, G. Jordan, E. Mauceli, L. D. Ward, C. B. Lowe, A. K. Holloway, M. Clamp, S. Gnerre, J. Alföldi, K. Beal, J. Chang, H. Clawson, J. Cuff, F. Di Palma, S. Fitzgerald, P. Flicek, M. Guttman, M. J. Hubisz, D. B. Jaffe, I. Jungreis, W. J. Kent, D. Kostka, M. Lara, A. L. Martins, T. Massingham, I. Moltke, B. J. Raney, M. D. Rasmussen, J. Robinson, A. Stark, A. J. Vilella, J. Wen, X. Xie, M. C. Zody, Broad Institute Sequencing Platform and Whole Genome Assembly Team, J. Baldwin, T. Bloom, C. W. Chin, D. Heiman, R. Nicol, C. Nusbaum, S. Young, J. Wilkinson, K. C. Worley, C. L. Kovar, D. M. Muzny, R. A. Gibbs, Baylor College of Medicine Human Genome Sequencing Center Sequencing Team, A. Cree, H. H. Dihn, G. Fowler, S. Jhangiani, V. Joshi, S. Lee, L. R. Lewis, L. V. Nazareth, G. Okwuonu, J. Santibanez, W. C. Warren, E. R. Mardis, G. M. Weinstock, R. K. Wilson, Genome Institute at Washington University, K. Delehaunty, D. Dooling, C. Fronik, L. Fulton, B. Fulton, T. Graves, P. Minx, E. Sodergren, E. Birney, E. H. Margulies, J. Herrero, E. D. Green, D. Haussler, A. Siepel, N. Goldman, K. S. Pollard, J. S. Pedersen, E. S. Lander, M. Kellis, A high-resolution map of human evolutionary constraint using 29 mammals. Nature. 478, 476–482 (2011).
- 81. M. J. Christmas, I. M. Kaplow, Zoonomia consortium, Evolutionary constraint and innovation across hundreds of placental mammals. *Science*.
- 82. Exonerate, (available at https://www.ebi.ac.uk/about/vertebrate-genomics/software/exonerate-manual).
- 83. J. A. Robinson, C. C. Kyriazis, S. F. Nigenda-Morales, A. C. Beichman, L. Rojas-Bracho, K. M. Robertson, M. C. Fontaine, R. K. Wayne, K. E. Lohmueller, B. L. Taylor, P. A. Morin, The critically endangered vaquita is not doomed to extinction by inbreeding depression. *Science*. **376** (2022), pp. 635–639.
- 84. F. Sánchez-Barreiro, S. Gopalakrishnan, J. Ramos-Madrigal, M. V. Westbury, M. de Manuel, A. Margaryan, M. M. Ciucani, F. G. Vieira, Y. Patramanis, D. C. Kalthoff, Z. Timmons, T. Sicheritz-Pontén, L. Dalén, O. A. Ryder, G. Zhang, T. Marquès-Bonet, Y. Moodley, M. T. P. Gilbert, Historical population declines prompted significant genomic erosion in the northern and southern white rhinoceros (Ceratotherium simum). *Mol. Ecol.* 30, 6355–6369 (2021).
- 85. W. N. Venables, B. D. Ripley, *Modern Applied Statistics with S* (Springer, Fourth, 2002).

- 86. R Core Team, *R: A language and environment for statistical computing* (R Foundation for Statistical Computing, Vienna, Austria, 2015).
- 87. A. D. Foote, Y. Liu, G. W. C. Thomas, T. Vinař, J. Alföldi, J. Deng, S. Dugan, C. E. van Elk, M. E. Hunter, V. Joshi, Z. Khan, C. Kovar, S. L. Lee, K. Lindblad-Toh, A. Mancia, R. Nielsen, X. Qin, J. Qu, B. J. Raney, N. Vijay, J. B. W. Wolf, M. W. Hahn, D. M. Muzny, K. C. Worley, M. T. P. Gilbert, R. A. Gibbs, Convergent evolution of the genomes of marine mammals. *Nat. Genet.* 47, 272–275 (2015).

**Acknowledgments:** We thank Mark Diekhans for technical assistance; Irene Kaplow, Harris Lewin, members of the Conservation Genetics lab at San Diego Zoo Wildlife Alliance, and members of the Paleogenomics Lab at the University of California at Santa Cruz for discussions. We thank Marty Kardos and three other reviewers for insightful feedback. We gratefully acknowledge the MIT PRIMES program and the lab of Vijay Kuchroo at the Broad Institute for support of AM and AS. Animal images were from PhyloPic.org.

# **Funding:**

NIH grant R01 HG008742 (EKK)

Swedish Research Council (KLT)

Wallenberg Foundation (KLT)

European Research Council European Union's Horizon 2020 864203 (TMB)

MINECO/FEDER, UE grant BFU2017-86471-P (TMB)

Agencia Estatal de Investigación "Unidad de Excelencia María de Maeztu" CEX2018-000792-M (TMB)

Howard Hughes International Early Career (TMB)

Secretaria d'Universitats i Recerca (TMB)

CERCA Programme del Departament d'Economia i Coneixement de la Generalitat de Catalunya (TMB)

#### **Author contributions:**

Conceptualization: APW, MAS, ASA, CS, KPK, DPG, EKK, KLT, TMB, ZC, OAR, BS

Data analysis: APW, MAS, AS, AM, RS, ASA, VMF, KF, WKM

Interpretation of results: APW, MAS, AS, AM, OAR, BS, with input from all authors

Writing – original draft: APW, MAS, BS

Writing – review & editing: all authors

# **Competing interests:**

Authors declare that they have no competing interests.

# Data and materials availability:

The data presented in this paper are detailed in supplementary materials. Summary data and analysis scripts are available at https://github.com/LaMariposa/zoonomia\_biodiversity. NCBI accession numbers for sequence data used in analyses are given in table S1.

# **Supplementary Materials**

Materials and Methods Supplementary Text Figs. S1 to S15 Tables S1 to S6 References (66–87)

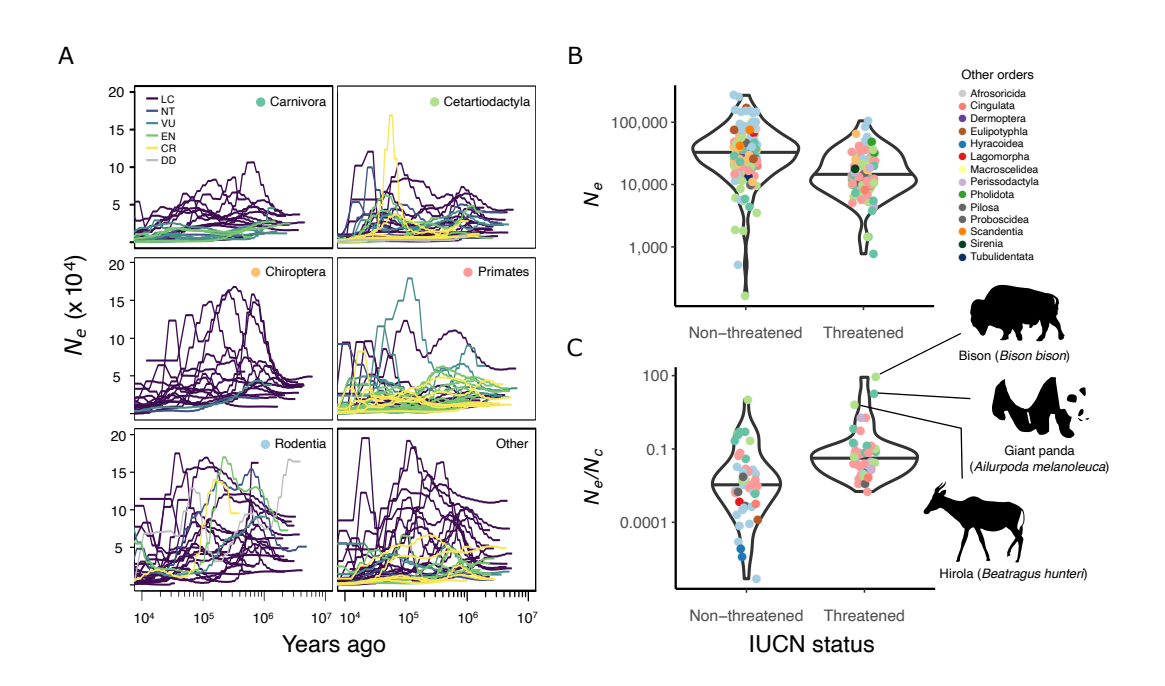
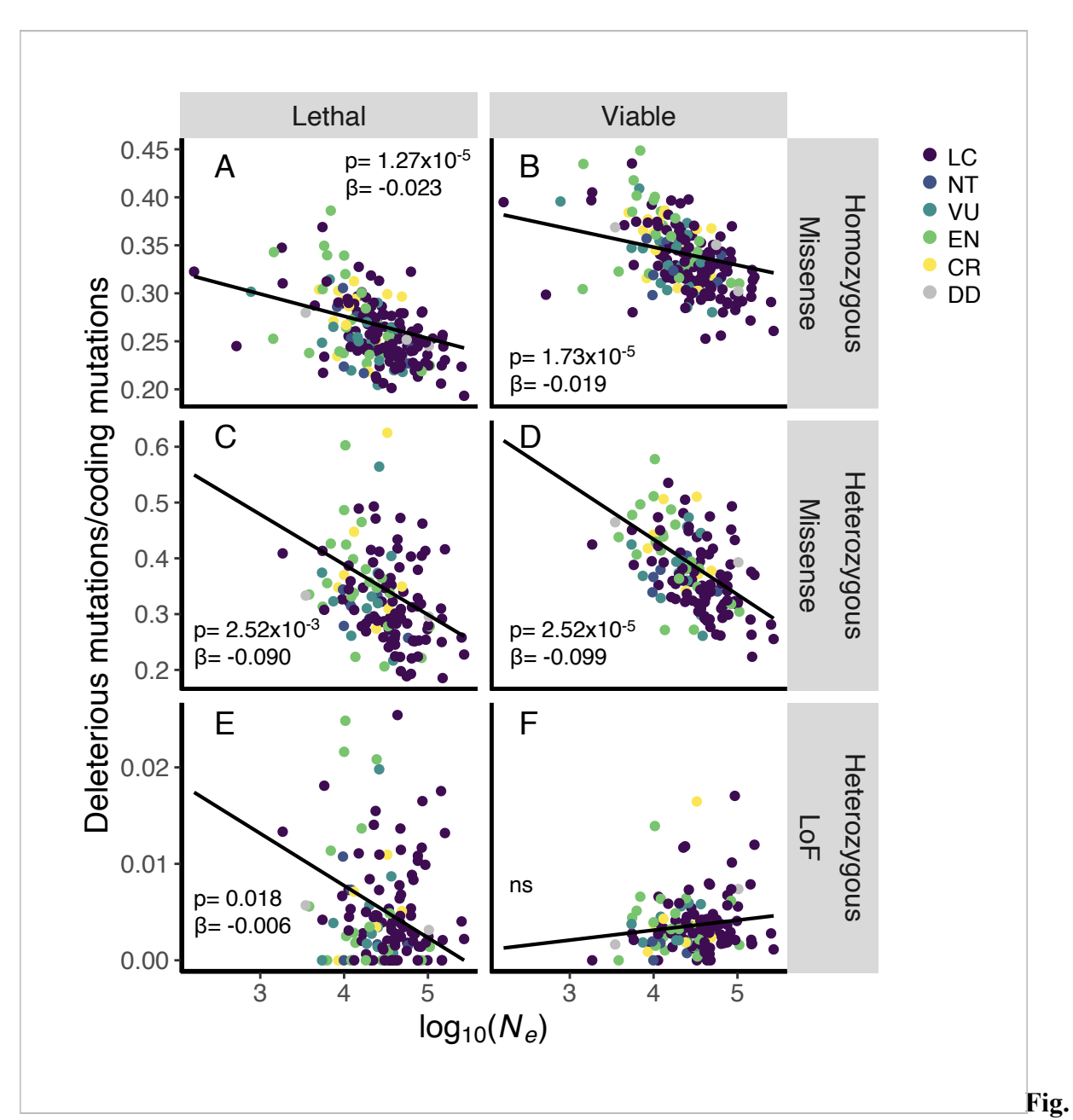


Fig. 1. Demographic history across mammalian orders and IUCN Red List categories. (A) Estimates of effective population sizes ( $N_e$ ) over time displayed by taxonomic order. Lines represent individual species, colored by IUCN status (LC= Least Concern, NT=Near Threatened, VU=Vulnerable, EN=Endangered, CR=Critically Endangered, DD=Data Deficient). Colored dots correspond to the taxonomic order of species depicted in (B) and (C). For visualization, only species with  $N_e$  estimates under 200,000 for every time point are shown. (B) Harmonic mean  $N_e$  was significantly lower in threatened IUCN categories relative to non-threatened (phylolm, p<3.3e-5). (C) The ratio of historical  $N_e$  to contemporary census population size

 $(N_e/N_c)$  can identify species with smaller  $N_c$  than expected from historical  $N_e$  (phylolm, p=0.012). Points in **(B)** and **(C)** show individual species, colored by taxonomic order.



2. Historically small populations have more deleterious genetic load in protein-coding genes. Proportion of homozygous missense substitutions (A-B), heterozygous missense variants (C-D) and heterozygous loss-of-function variants (E-F) in genes as a function of historical  $N_e$  across species. Genes were classified by associated lethal or viable phenotypes in knockout mice. Proportions of heterozygous and homozygous missense mutations were negatively correlated with  $N_e$  (all p<0.052), whereas heterozygous loss-of-function alleles were not consistently correlated with  $N_e$ . Phylogenetically corrected p-values and coefficients (phylolm) are reported.

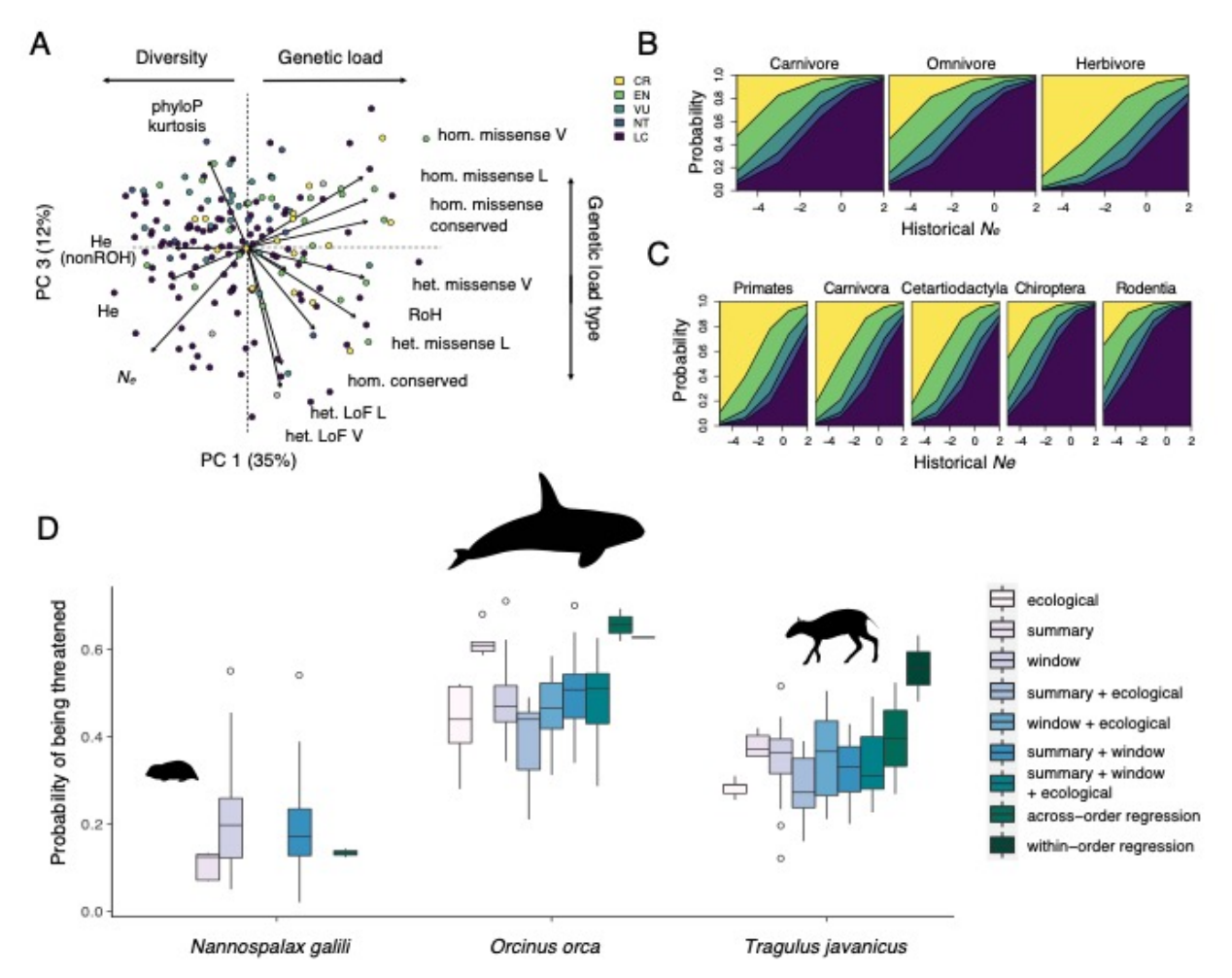


Fig. 3. Prediction of conservation status of species using genomic information. (A) Principal components (PCs) that significantly predict threatened status. PC1 describes heterozygosity,  $N_e$  and deleterious variation, and PC3 distinguishes types of deleterious variation. Loadings of genomic variables (arrows; table S3) are labeled as described in table S2 (L=IMPC lethal genes; V=IMPC viable genes). Points indicate species, colored by IUCN status as shown in (B). (B-C) Probability of assignment to IUCN categories by diet and scaled values of historical  $N_e$  (B), and by taxonomic order and historical  $N_e$  of species (C). Decreased historical  $N_e$  is consistently associated with increased risk, but the magnitude varies by diet and taxonomic order. (D) Conservation status predictions for three data deficient species using random forest models with window-based metrics (windows), ecological variables (ecological), and/or genome-wide summary variables (summary), and predictions from regression models within and across taxonomic orders. Nannospalax galili lacked ecological data and adequate within-order data, so only predictions from across-order regression and windows models are shown for this species.

#### **‡Zoonomia Consortium Members:**

Gregory Andrews<sup>1</sup>, Joel C. Armstrong<sup>2</sup>, Matteo Bianchi<sup>3</sup>, Bruce W. Birren<sup>4</sup>, Kevin R. Bredemeyer<sup>5</sup>, Ana M. Breit<sup>6</sup>, Matthew J. Christmas<sup>3</sup>, Hiram Clawson<sup>2</sup>, Joana Damas<sup>7</sup>, Federica Di Palma<sup>8,9</sup>, Mark Diekhans<sup>2</sup>, Michael X. Dong<sup>3</sup>, Eduardo Eizirik<sup>10</sup>, Kaili Fan<sup>1</sup>, Cornelia Fanter<sup>11</sup>, Nicole M. Foley<sup>5</sup>, Karin Forsberg-Nilsson<sup>12,13</sup>, Carlos J. Garcia<sup>14</sup>, John Gatesy<sup>15</sup>, Steven Gazal<sup>16</sup>, Diane P. Genereux<sup>4</sup>, Linda Goodman<sup>17</sup>, Jenna Grimshaw<sup>14</sup>, Michaela K. Halsey<sup>14</sup>, Andrew J. Harris<sup>5</sup>, Glenn Hickey<sup>18</sup>, Michael Hiller<sup>19,20,21</sup>, Allyson G. Hindle<sup>11</sup>, Robert M. Hubley<sup>22</sup>, Graham M. Hughes<sup>23</sup>, Jeremy Johnson<sup>4</sup>, David Juan<sup>24</sup>, Irene M. Kaplow<sup>25,26</sup>, Elinor K. Karlsson<sup>1,4,27</sup>, Kathleen C. Keough<sup>17,28,29</sup>, Bogdan Kirilenko<sup>19,20,21</sup>, Klaus-Peter Koepfli<sup>30,31,32</sup>. Jennifer M. Korstian<sup>14</sup>, Amanda Kowalczyk<sup>25,26</sup>, Sergey V. Kozyrev<sup>3</sup>, Alyssa J. Lawler<sup>4,26,33</sup>, Colleen Lawless<sup>23</sup>, Thomas Lehmann<sup>34</sup>, Danielle L. Levesque<sup>6</sup>, Harris A. Lewin<sup>7,35,36</sup>, Xue Li<sup>1,4,37</sup>, Abigail Lind<sup>28,29</sup>, Kerstin Lindblad-Toh<sup>3,4</sup>, Ava Mackay-Smith<sup>38</sup>, Voichita D. Marinescu<sup>3</sup>, Tomas Marques-Bonet<sup>39,40,41,42</sup>, Victor C. Mason<sup>43</sup>, Jennifer R. S. Meadows<sup>3</sup>, Wynn K. Mever<sup>44</sup>, Jill E. Moore<sup>1</sup>, Lucas R. Moreira<sup>1,4</sup>, Diana D. Moreno-Santillan<sup>14</sup>, Kathleen M. Morrill<sup>1,4,37</sup>, Gerard Muntané<sup>4</sup> William J. Murphy<sup>5</sup>, Arcadi Navarro<sup>39,41,45,46</sup>, Martin Nweeia<sup>47,48,49,50</sup>, Sylvia Ortmann<sup>51</sup>, Austin Osmanski<sup>14</sup>, Benedict Paten<sup>2</sup>, Nicole S. Paulat<sup>14</sup>, Andreas R. Pfenning<sup>25,26</sup>, BaDoi N. Phan<sup>25,26,52</sup>, Katherine S. Pollard<sup>28,29,53</sup>, Henry E. Pratt<sup>1</sup>, David A. Ray<sup>14</sup>, Steven K. Reilly<sup>38</sup>, Jeb R. Rosen<sup>22</sup>, Irina Ruf<sup>54</sup>, Louise Ryan<sup>23</sup>, Oliver A. Ryder<sup>55,56</sup>, Pardis C. Sabeti<sup>4,57,58</sup>, Daniel E. Schäfer<sup>25</sup>, Aitor Serres<sup>24</sup>, Beth Shapiro<sup>59,60</sup>, Arian F. A. Smit<sup>22</sup>, Mark Springer<sup>61</sup>, Chaitanya Srinivasan<sup>25</sup>, Cynthia Steiner<sup>55</sup>, Jessica M. Storer<sup>22</sup>, Kevin A. M. Sullivan<sup>14</sup>, Patrick F. Sullivan<sup>62,63</sup>, Elisabeth Sundströ<sup>3</sup>, Megan A. Supple<sup>59</sup>, Ross Swofford<sup>4</sup>, Joy-El Talbot<sup>64</sup>, Emma Teeling<sup>23</sup>, Jason Turner-Maier<sup>4</sup>, Alejandro Valenzuela<sup>24</sup>, Franziska Wagner<sup>65</sup>, Ola Wallerman<sup>3</sup>, Chao Wang<sup>3</sup>, Juehan Wang<sup>16</sup>, Zhiping Weng<sup>1</sup>, Aryn P. Wilder<sup>55</sup>, Morgan E. Wirthlin<sup>25,26,66</sup>, James R. Xue<sup>4,57</sup>, Xiaomeng Zhang<sup>4,25,26</sup>

#### Affiliations:

<sup>1</sup>Program in Bioinformatics and Integrative Biology, UMass Chan Medical School; Worcester, MA 01605, USA.

<sup>&</sup>lt;sup>2</sup>Genomics Institute, University of California Santa Cruz; Santa Cruz, CA 95064, USA.

<sup>&</sup>lt;sup>3</sup>Science for Life Laboratory, Department of Medical Biochemistry and Microbiology, Uppsala University; Uppsala, 751 32, Sweden.

<sup>&</sup>lt;sup>4</sup>Broad Institute of MIT and Harvard; Cambridge, MA 02139, USA.

<sup>&</sup>lt;sup>5</sup>Veterinary Integrative Biosciences, Texas A&M University; College Station, TX 77843, USA.

<sup>&</sup>lt;sup>6</sup>School of Biology and Ecology, University of Maine; Orono, ME 04469, USA.

<sup>&</sup>lt;sup>7</sup>The Genome Center, University of California Davis; Davis, CA 95616, USA.

<sup>&</sup>lt;sup>8</sup>Genome British Columbia; Vancouver, BC, Canada.

<sup>&</sup>lt;sup>9</sup>School of Biological Sciences, University of East Anglia; Norwich, UK.

- <sup>10</sup>School of Health and Life Sciences, Pontifical Catholic University of Rio Grande do Sul; Porto Alegre, 90619-900, Brazil.
- <sup>11</sup>School of Life Sciences, University of Nevada Las Vegas; Las Vegas, NV 89154, USA.
- <sup>12</sup>Biodiscovery Institute, University of Nottingham; Nottingham, UK.
- <sup>13</sup>Department of Immunology, Genetics and Pathology, Science for Life Laboratory, Uppsala University; Uppsala, 751 85, Sweden.
- <sup>14</sup>Department of Biological Sciences, Texas Tech University; Lubbock, TX 79409, USA.
- <sup>15</sup>Division of Vertebrate Zoology, American Museum of Natural History; New York, NY 10024, USA.
- <sup>16</sup>Keck School of Medicine, University of Southern California; Los Angeles, CA 90033, USA.
- <sup>17</sup>Fauna Bio Incorporated; Emeryville, CA 94608, USA.
- <sup>18</sup>Baskin School of Engineering, University of California Santa Cruz; Santa Cruz, CA 95064, USA.
- <sup>19</sup>Faculty of Biosciences, Goethe-University; 60438 Frankfurt, Germany.
- <sup>20</sup>LOEWE Centre for Translational Biodiversity Genomics; 60325 Frankfurt, Germany.
- <sup>21</sup>Senckenberg Research Institute; 60325 Frankfurt, Germany.
- <sup>22</sup>Institute for Systems Biology; Seattle, WA 98109, USA.
- <sup>23</sup>School of Biology and Environmental Science, University College Dublin; Belfield, Dublin 4, Ireland.
- <sup>24</sup>Department of Experimental and Health Sciences, Institute of Evolutionary Biology (UPF-CSIC), Universitat Pompeu Fabra; Barcelona, 08003, Spain.
- <sup>25</sup>Department of Computational Biology, School of Computer Science, Carnegie Mellon University; Pittsburgh, PA 15213, USA.
- <sup>26</sup>Neuroscience Institute, Carnegie Mellon University; Pittsburgh, PA 15213, USA.
- <sup>27</sup>Program in Molecular Medicine, UMass Chan Medical School; Worcester, MA 01605, USA.
- <sup>28</sup>Department of Epidemiology & Biostatistics, University of California San Francisco; San Francisco, CA 94158, USA.
- <sup>29</sup>Gladstone Institutes; San Francisco, CA 94158, USA.
- <sup>30</sup>Center for Species Survival, Smithsonian's National Zoo and Conservation Biology Institute; Washington, DC 20008, USA.
- <sup>31</sup>Computer Technologies Laboratory, ITMO University; St. Petersburg 197101, Russia.

- <sup>32</sup>Smithsonian-Mason School of Conservation, George Mason University; Front Royal, VA 22630, USA.
- <sup>33</sup>Department of Biological Sciences, Mellon College of Science, Carnegie Mellon University; Pittsburgh, PA 15213, USA.
- <sup>34</sup>Senckenberg Research Institute and Natural History Museum Frankfurt; 60325 Frankfurt am Main, Germany.
- <sup>35</sup>Department of Evolution and Ecology, University of California Davis; Davis, CA 95616, USA.
- <sup>36</sup>John Muir Institute for the Environment, University of California Davis; Davis, CA 95616, USA.
- <sup>37</sup>Morningside Graduate School of Biomedical Sciences, UMass Chan Medical School; Worcester, MA 01605, USA.
- <sup>38</sup>Department of Genetics, Yale School of Medicine; New Haven, CT 06510, USA.
- <sup>39</sup>Catalan Institution of Research and Advanced Studies (ICREA); Barcelona, 08010, Spain.
- <sup>40</sup>CNAG-CRG, Centre for Genomic Regulation, Barcelona Institute of Science and Technology (BIST); Barcelona, 08036, Spain.
- <sup>41</sup>Department of Medicine and LIfe Sciences, Institute of Evolutionary Biology (UPF-CSIC), Universitat Pompeu Fabra; Barcelona, 08003, Spain.
- <sup>42</sup>Institut Catalàde Paleontologia Miquel Crusafont, Universitat Autòoma de Barcelona; 08193, Cerdanyola del Vallè, Barcelona, Spain.
- <sup>43</sup>Institute of Cell Biology, University of Bern; 3012, Bern, Switzerland.
- <sup>44</sup>Department of Biological Sciences, Lehigh University; Bethlehem, PA 18015, USA.
- <sup>45</sup>BarcelonaBeta Brain Research Center, Pasqual Maragall Foundation; Barcelona, 08005, Spain.
- <sup>46</sup>CRG, Centre for Genomic Regulation, Barcelona Institute of Science and Technology (BIST); Barcelona, 08003, Spain.
- <sup>47</sup>Department of Comprehensive Care, School of Dental Medicine, Case Western Reserve University; Cleveland, OH 44106, USA.
- <sup>48</sup>Department of Vertebrate Zoology, Canadian Museum of Nature; Ottawa, Ontario K2P 2R1, Canada.
- <sup>49</sup>Department of Vertebrate Zoology, Smithsonian Institution; Washington, DC 20002, USA.
- <sup>50</sup>Narwhal Genome Initiative, Department of Restorative Dentistry and Biomaterials Sciences, Harvard School of Dental Medicine; Boston, MA 02115, USA.
- <sup>51</sup>Department of Evolutionary Ecology, Leibniz Institute for Zoo and Wildlife Research; 10315 Berlin, Germany.

- <sup>52</sup>Medical Scientist Training Program, University of Pittsburgh School of Medicine; Pittsburgh, PA 15261, USA.
- <sup>53</sup>Chan Zuckerberg Biohub; San Francisco, CA 94158, USA.
- <sup>54</sup>Division of Messel Research and Mammalogy, Senckenberg Research Institute and Natural History Museum Frankfurt; 60325 Frankfurt am Main, Germany.
- <sup>55</sup>Conservation Genetics, San Diego Zoo Wildlife Alliance; Escondido, CA 92027, USA.
- <sup>56</sup>Department of Evolution, Behavior and Ecology, School of Biological Sciences, University of California San Diego; La Jolla, CA 92039, USA.
- <sup>57</sup>Department of Organismic and Evolutionary Biology, Harvard University; Cambridge, MA 02138, USA.
- <sup>58</sup>Howard Hughes Medical Institute; Chevy Chase, MD, USA.
- <sup>59</sup>Department of Ecology and Evolutionary Biology, University of California Santa Cruz; Santa Cruz, CA 95064, USA.
- <sup>60</sup>Howard Hughes Medical Institute, University of California Santa Cruz; Santa Cruz, CA 95064, USA.
- <sup>61</sup>Department of Evolution, Ecology and Organismal Biology, University of California Riverside; Riverside, CA 92521, USA.
- <sup>62</sup>Department of Genetics, University of North Carolina Medical School; Chapel Hill, NC 27599, USA.
- <sup>63</sup>Department of Medical Epidemiology and Biostatistics, Karolinska Institutet; Stockholm, Sweden.
- <sup>64</sup>Iris Data Solutions, LLC; Orono, ME 04473, USA.
- <sup>65</sup>Museum of Zoology, Senckenberg Natural History Collections Dresden; 01109 Dresden, Germany.
- <sup>66</sup>Allen Institute for Brain Science: Seattle, WA 98109, USA



# Supplementary Materials for

# The contribution of historical processes to contemporary extinction risk in placental mammals

Aryn P. Wilder<sup>1†\*</sup>, Megan A Supple<sup>2,3†\*</sup>, Ayshwarya Subramanian<sup>4</sup>, Anish Mudide<sup>5</sup>, Ross Swofford<sup>4</sup>, Aitor Serres-Armero<sup>6</sup>, Cynthia Steiner<sup>1</sup>, Klaus-Peter Koepfli<sup>7,8,9</sup>, Diane P. Genereux<sup>4</sup>, Elinor K. Karlsson<sup>4,10</sup>, Kerstin Lindblad-Toh<sup>4,11</sup>, Tomas Marques-Bonet<sup>6,12,13,14</sup>, Violeta Munoz Fuentes<sup>15</sup>, Kathleen Foley<sup>16,17</sup>, Wynn K. Meyer<sup>17</sup>, Zoonomia Consortium<sup>‡</sup>, Oliver A. Ryder<sup>1,18§\*</sup>, Beth Shapiro<sup>2,3§\*</sup>

Correspondence to: awilder@sdzwa.org (APW), msupple@ucsc.edu (MAS), bashapir@ucsc.edu (BS), and oryder@sdzwa.org (OAR)

#### This PDF file includes:

Materials and Methods Figs. S1 to S15 Tables S1 to S6

#### **Materials and Methods**

We examined variation in 241 reference genomes from 240 species. Each species was represented by a single genome, with the exception of *Canis lupus*, which was represented by two genomes—one domestic breed and one village dog. The reference genomes varied in quality, with contig N50 values ranging from 1,039 to 56,413,054, with a median of 45,189 (table S1). For some of these species, no short-read sequencing data were available from NCBI to map to the reference genome (n=8), variant calling failed (n=11), or downstream pipelines failed (heterozygosity-related metrics, n=13, PSMC, n=12). The reference genomes were used to estimate homozygous deleterious genetic load; while the short-read sequence data (usually from the reference individual) were used to estimate metrics related to historical demography, heterozygosity, and heterozygous deleterious variants (fig. S1). We examined correlations between these metrics using statistical methods that account for relationships across the phylogeny, and examined genomic features of extinction risk to predict the conservation status of species.

# **Metadata**

We compiled metadata on conservation status, diet, and generation time for the 240 placental mammal species in the Zoonomia alignment (table S1). We determined the conservation status (Least Concern (LC), Near Threatened (NT), Vulnerable (VU), Endangered (EN) or Critically Endangered (CR)) and population trends (declining, stable or increasing) using the IUCN Red List category (IUCN Red List API v. 3) based on the scientific name of the species. We use IUCN category as a proxy for extinction risk, however we recognize that because the assessments are often done at the species level, the categorization of a species may miss important variation between populations. Where we were able to determine a specific subspecies or population for the sequenced sample, we used the IUCN category for the lower taxonomic level. For the diet category, we classified each species as either carnivore, herbivore, or omnivore based on (54). In cases where species-specific diet information was unavailable, we used data reported at the genus level. We categorized as carnivores all species for which other animals made up a majority of their diets, including terrestrial vertebrate-eaters, insectivores, piscivores, and planktivores; we also considered the vampire bat, a hematophage, to be a carnivore. Any animal with a diet composed of both plant products and animal products was considered an omnivore. Species for which the diet was all or nearly all plant products were considered herbivores; some of these species consumed insects occasionally or as a minor part of their diets. For generation time, we used a published database of mammalian generation lengths (60). If a species was not in the database, we used the value from the next closest species. We determined species specific mutation rates per generation by multiplying an average mammal mutation rate of 2.2e-9 basepairs per year (21) by the species-specific generation time in years.

We compiled additional metadata associated with provenance of the specific sample that was sequenced for the genome of each species. For 39 samples used for reference genome assembly, there were no publicly available short-read Illumina sequencing data, which were necessary for analyses based on heterozygous sites (i.e. heterozygosity, segments of homozygosity, heterozygous deleterious variants, and PSMC). For 31 of these we identified an alternate sample with resequencing data, choosing a sample as similar to the reference individual as possible (e.g. from the same population). For each sample (including both reference genome samples and, if different, short-read data samples), we determined subspecies or population

information and whether the sample was a wild (including captive offspring of wild-born parents), captive, or domesticated individual. We obtained sample information from the NCBI records and published papers that used the sample, such as the genome announcement papers. In some instances, insufficient metadata were available, but informal project summaries provided details. For 16 samples, no additional data were available and the sample metadata were marked as unknown.

# Alignment and variant calling of short-read sequencing data

We interrogated the assemblies included in the Zoonomia alignment for heterozygous positions using the GATK best practices pipeline as described previously (7). We removed adapters with Cutadapt (version 1.10)(67). This step was not done for the alignments used for PSMC analysis for the original Zoonomia genomes (7), but this difference should not affect our results since the alignment algorithm soft clips reads (57). We mapped the paired-end sequencing data corresponding to each assembly against their respective assemblies using BWA mem (version 0.7.15)(57). We marked and removed optical duplicates using the PICARD MarkDuplicates tool (version 2.5.0)(68). Finally, we called heterozygous variants using the Haplotypecaller module of the GATK software suite (version 3.6)(58).

#### Phylogenetic regression

All regressions of variables across species were conducted with phylogenetic linear regression or phylogenetic logistic regression in the R package *phylolm* (55), incorporating the phylogenetic tree with branch lengths (56) to account for non-independence. Where we report means for groups compared in phylogenetic regressions, we report the phylogenetically-adjusted means.

#### Dynamics of historical effective population sizes

We inferred the history of effective population sizes ( $N_e$ ) for each species using PSMC (version 0.6.5-r67)(59). We used the short-read alignments generated for variant calling of scaffolds greater than 50 kb (69). For each alignment, we used samtools depth (version 1.11-3-g7028dd4)(70) to determine the average depth of coverage. To prepare for PSMC, we generated a pileup file with samtools mpileup (version 1.7)(70) from the 50-kb alignment files, retaining anomalous read pairs (-A) and downgrading mapping quality for reads with excessive mismatches (-C50). We then called variants on the pileup file using beftools call (version 1.8)(71), using the consensus caller (-c). From the variant file we generated a consensus fastq file using vefutils vef2fq (version 2014)(70), with a minimum coverage of one-third the sample's average coverage and a maximum coverage of two times the sample's average coverage. We then generated a PSMC input fasta file using the PSMC's fq2psmcfa with a minimum base quality score of 20 (-q20). Finally, we ran PSMC with default parameters, except we altered the parameter intervals to -p "4+25\*2+4+6", as suggested for humans (72). We rescaled the output of PSMC using the species-specific generation times and mutation rates (see *Metadata* section).

To estimate historical  $N_e$ , we calculated the harmonic mean from the PSMC estimates of effective population size through time, excluding time intervals less than 10 kya. While our samples varied in level of inbreeding, we do not expect this to have a substantial impact on our estimates of historical  $N_e$ . Previous work examining inbred samples showed similar PSMC curves regardless of whether runs of homozygosity were included or excluded in the analysis (38, 73). Additionally, our genomic data varied in other important aspects, including genome

quality and coverage, and PSMC has been shown to be robust to variation in these characteristics (39, 74, 75).

# <u>Inferring recent population declines from N<sub>e</sub>/N<sub>c</sub> ratios</u>

To compare contemporary population sizes to historical  $N_e$ , we obtained census population estimates  $(N_c)$  for 89 species from the PanTHERIA database (15), estimating  $N_c$  as the product of population density and geographic area from census data (15, 61). Although not a true population census, it provides an overall gauge of the potential number of individuals within a species' current distribution. N<sub>c</sub> estimates ranged widely across species, from 2,909 (Bison bison) to 65,971,017,419 (Procavia capensis). Although the values are not meant to be interpreted as real census population sizes, they provide a gauge of relative census population sizes across species. As expected,  $N_c$  was strongly correlated with IUCN status (phylolm, mean<sub>threatened</sub>=16,619,347; mean<sub>non-threatened</sub>=90,341,802; p=6.1e-7), as it is a criterion for IUCN status assessments, but examining  $N_e/N_c$  ratios can nonetheless provide additional information on recent declines not reflected in the genome. Species with larger  $N_e/N_c$  ratios were slightly more likely to have "declining" population trends classified by the IUCN Redlist than "stable" or "increasing" (phyloglm,  $\beta$ = 0.59, p=0.026, where each 10-fold increase in  $N_e/N_c$  increases odds of being categorized as declining by 59%), suggesting that  $N_e/N_c$  may be useful for identifying recent declines.  $N_e/N_c$  ratios are influenced by life-history traits, including mating strategy, range size, trophic level, generation time, population structure and population fluctuations (14, 76), but we nonetheless found a comparable relationship between  $N_e/N_c$  and conservation status within Primates (phylolm, mean<sub>threatened</sub>=3.46e-3; mean<sub>non-threatened</sub>=1.11e-3; p=0.029), the only group with enough  $N_e/N_c$  estimates in both threat categories, suggesting that it is not driven by lifehistory traits alone. Because  $N_e/N_c$  ratios require population census information, and thus it is not useful for informing conservation status of species that lack this information,  $N_c/N_c$  may nonetheless be valuable for identifying species with historically large populations that have recently declined.

# Estimating runs of homozygosity (RoH) and heterozygosity

We used an identical strategy to the Zoonomia data release paper to identify runs of homozygosity (RoH) (7). Briefly, for every assembly, we calculated the ratio of heterozygous positions per callable base pair in non-overlapping, 50-kb windows. Then, we used the pomegranate python environment (77) to fit a 2-component Gaussian Mixture Model (with a third component to capture outliers and low confidence windows, such as windows with large amounts of missing data) to the joint distribution of all heterozygosity windows in the assembly. These joint distributions are expected to be bimodal, with a sharp peak at the lower tail of the distribution corresponding to low heterozygosity regions, such as runs of homozygosity. Finally, each window was assigned to its most likely component (RoH or non-RoH) based on the model's posterior probabilities. We note that this method is unable to distinguish between true segments of homozygosity and other genomic regions with very low heterozygosity. However, given the large window size, we expect that only a small proportion of the genome would be miscalled due to low heterozygosity. Additionally, all species are likely to be impacted by this minor bias, so we do not expect it to substantially affect relative estimates of metrics using RoH.

For each species, from the windows assigned as either heterozygous or homozygous we calculated the proportion of the genome in RoH (fRoH) (fig. S15), genome-wide heterozygosity, and outbred heterozygosity. To estimate fRoH we calculated the length of the genome in RoH

and divided it by the total length of the genome assigned as either RoH or non-RoH. We next calculated genome-wide heterozygosity as the mean of the heterozygosity estimates from the 50-kb windows, weighted by the length of the segment to account for the shorter segments at the ends of scaffolds. Lastly, we estimated heterozygosity in non-RoH regions (i.e. outbred heterozygosity) using the mode of the distribution of 50-kb window heterozygosity estimates with regions identified as RoH excluded. To ensure the accuracy of the estimation of the mode of the non-RoH distributions, we manually inspected both the full distribution and the non-RoH distribution. In 25 instances, we needed to correct the automated call. One scenario where this occurred was when the full distribution was not bimodal due to low overall heterozygosity and the mode of the distribution was zero. For these, we examined the full distribution and set heterozygosity to the peak when most windows were non-RoH. The second scenario where automated calls needed to be corrected was when the distribution of the non-RoH segments was bimodal due to miscalled RoH. In these instances, we were able to visually identify a clear non-RoH peak in the distribution.

Adding neutral diversity statistics for 79 additional species relative to our previous analysis (7), we substantiate the result that species with threatened IUCN status had, on average, significantly lower genome-wide heterozygosity (phylolm, meanthreatened=0.0024, meannon-threatened=0.0029, p=0.017; fig. S2). However, unlike the previous results, we found that the proportion of the genome in RoH (fRoH) was highly variable across the expanded dataset (fig. S15), and the mean was actually lower for threatened species compared to non-threatened species (phylolm, meanthreatened=0.21, meannon-threatened=0.27, p=0.015). This contrasting result is likely due to the skewed distribution of RoH (fig. S15). Furthermore, intraspecific variation in heterozygosity and fRoH, which is not captured in our data because we used a single individual from each species, may add variability that makes any correlation with endangerment status more difficult to detect.

#### Estimating deleterious genetic load

We estimated homozygous substitutions from the reference genome sequences, calling derived substitutions relative to the most recent ancestral sequence in the multispecies alignment. Reconstructed ancestral sequences are included in the multispecies alignment HAL file (https://cglgenomics.ucsc.edu/data/cactus/) that was previously generated using the program Progressive Cactus (7), which implements ancestral reconstruction for all nodes in the multiple alignment procedure by incorporating multiple ingroup and outgroup sequences (78). We used the halBranchMutations tool in the Comparative Genomics Toolkit (62), which annotates the locations of single nucleotide substitutions on a branch-by-branch basis relative to the closest ancestral node, thus calling derived substitutions arising along the branch for each species in the alignment. We assume that most of these substitutions are likely to be fixed because typically enough time has elapsed since the ancestral node for the derived alleles to have become fixed or lost (on the order of  $<4N_e$  generations)(63). We found that genomic windows that aligned to multiple regions of the genome tended to have many substitutions. Because querying the multispecies alignment HAL file to directly identify regions with duplicate alignments is very computationally expensive, we filtered regions with more substitutions than expected from a poisson distribution, though this step likely excludes true hypervariable regions from our analysis. Therefore, we filtered potentially spurious calls by fitting the number of substitutions in all 1KB windows across the genome to a poisson distribution, and removing windows identified as outliers at alpha=0.1 using the function aout.pois in the R package alphaOutlier

(https://CRAN.R-project.org/package=alphaOutlier). Heterozygous variants (which have, by definition, one derived and one ancestral allele) were identified from single sample, short-read data mapped to the reference genome of each species as described above. We included in our analysis only single nucleotide polymorphisms, heterozygous sites with genotype quality (GQ; the Phred-scaled confidence that the genotype assignment is correct)>80, and read depth (DP) < three standard deviations from the mean DP across variant sites for a given sample.

To assess the functional impact of each derived mutation, we used 1) evolutionary conservation at the site, and 2) the estimated impact of the mutation on protein-coding genes. First, for evolutionary conservation we assigned human-based conservation -log<sub>10</sub> p-values (phyloP scores) estimated by the Zoonomia consortium (9). Briefly, the PHAST v1.5 package: https://github.com/CshlSiepelLab/phast (79) was used to estimate phyloP scores under a null hypothesis of neutral evolution, performing a likelihood ratio test at each alignment column (-method LRT) of the human-referenced, 241-way, duplicate-filtered alignment. To assign these phyloP scores to derived mutations identified in each genome, we lifted over all derived mutations to the human genome using halLiftover and the 241-way mammalian alignment, ignoring paralogous alignments using the --noDupes option (62). We were specifically interested in evolutionarily conserved sites which have a positive phyloP score, and thus to minimize the influence of negative phyloP scores that reflect accelerated evolution (80), we set all negative phyloP values to 0. We noted differences in genome-wide phyloP scores across taxonomic orders. To determine whether the differences could stem from using human-based phyloP scores, we also assigned phyloP scores derived from mouse and dog genomes to heterozygous sites for a subset of 115 genomes from across the phylogeny. Mean phyloP scores from human, mouse and dog were highly correlated (r<sup>2</sup>>0.99), indicating no substantial bias stemming from the genome used as the basis for phyloP scores. Furthermore, in tests that account for phylogenetic relationships (phylolm), mean phyloP scores did not significantly differ across taxonomic orders, suggesting that phylogenetic regressions adequately account for variation across orders. Specifically, taxonomic order did not explain mean phylop across substitutions better than intercept-only phylogenetic regression models (run with the phylostep function of phylolm), suggesting that the significant relationships between phyloP and other variables identified using these methods were not driven by the phylogeny.

Second, we inferred functional impacts from genome-specific gene annotations. Genes were estimated by lifting over human annotated transcripts through genomes in the alignment via halLiftover (81). Briefly, the human exon intervals were lifted over to the target species, and for each exon the resulting range was consolidated into a single range per contig with 500 bp added to both ends. The target sequence within the resulting interval was then aligned to the human protein sequence using exonerate (82), keeping only the best alignment. The alignment was checked to make sure that it resulted in a contiguous reading frame, that the predicted protein started with methionine, and that the predicted protein was within 90-110% of the length of the human reference protein. Using these gene annotations for each genome, we estimated synonymous, missense and loss-of-function (LoF) variants using the program SnpEff v.5.0e with default settings (64). SnpEff defines LoF variants as those causing complete loss of function of the affected transcripts: stop codon-introducing (nonsense) or splice site-disrupting single nucleotide variants predicted to disrupt a transcript's reading frame, affecting more than 50% of the protein-coding sequence. For homozygous sites, the effect of the ancestral allele was predicted relative to the focal genome, and thus homozygous LoF substitutions could not be reliably called, and we instead focused only on missense substitutions for homozygous sites. We

assumed that mutations at sites that are more conserved, that cause missense and LoF changes in protein-coding genes, especially those that show lethality as a result of LoF, are more likely to be harmful and to contribute to genome-wide deleterious genetic load (19).

Given these assumptions, we measured homozygous genetic load as the distribution of phyloP scores across all homozygous substitutions (mean and Pearson's kurtosis estimated from the moments package in R), the proportion of homozygous substitutions in protein-coding genes that are missense, and the proportion of homozygous substitutions that are at an evolutionarily conserved site (phyloP>2.27; (81)). Because homozygous substitutions were estimated for each species relative to the closest ancestral node in the phylogeny, the number of substitutions depended on the distance to the nearest species in the dataset, and ranged from 145,602 for Cavia tschudii (montane guinea pig) to 53,919,964 substitutions for Hystrix cristata (crested porcupine). There was a negative correlation between the proportion of putatively deleterious substitutions and the distance between a species and its closest ancestor (e.g. log-log linear regression r<sup>2</sup>=0.415 for missense substitutions at conserved sites). Comparisons between closely related species are typically enriched for nonsynonymous substitutions relative to more distant species (41). To adjust for this bias, we performed log-log linear regressions of homozygous genetic load variables against the total number of substitutions, and for variables that were significantly correlated (proportion of missense substitutions, proportion of conserved substitutions, proportion of missense substitutions at conserved sites, and kurtosis of phyloP), we used the residuals for subsequent statistical tests of the relationship between genetic load and demographic variables. We reported p-values for the branch-length adjusted variables, and presented the non-adjusted values and their coefficients in figures for readability and interpretability. For phylogenetically corrected logistic regression tests (phyloglm), we present coefficients ( $\beta$ ) converted to the change in odds of being threatened using  $e^{\beta}$ -1.

To further parse the potential fitness consequences of mutations, we estimated the proportion of homozygous missense, heterozygous missense and heterozygous LoF single nucleotide mutations in genes that differ in their essentiality (i.e. the requirement of a gene for an organism's survival). We limited the analysis to single-copy genes with associated viability phenotypic data in knockout mice as classified by the International Mouse Phenotyping Consortium (IMPC) (23). From all genes (annotated with human orthologs as described above), we selected single-copy genes using the BUSCO mammalia odb10 dataset, searching pub og id names against the OrthoDB v.10 database, and retaining hits identified as single-copy in >90% of the mammalian species set. The IMPC set of genes with a viability phenotype (Data Release 15.0) is provided for one-to-one mouse-human orthologs, which achieve an agreement support score of at least 5 out of 12 of the inference methods implemented by HGNC Comparison of Orthology Predictions (HCOP; i.e., support>=5, one-to-one in both directions, human to mouse and mouse to human). Single-gene knockout mouse lines are assigned a lethal, subviable or viable phenotype category based on the observed number of viable homozygote pups at preweaning stage. These categories can be used as a proxy for gene essentiality and, consequently, for the potential fitness impacts of mutations in these genes (23). The number of genes in each category varied across species depending on the completeness of the annotation for that genome. The IMPC lethal category had on average 263 genes annotated in each genome (range 19-782), and the IMPC viable category had on average 530 genes (range 40-1564). Because there were relatively few genes in the IMPC subviable category, and the results from the subviable category were qualitatively similar to the lethal category, we presented results from only the viable and lethal gene categories in the main text. To minimize noise associated with estimation of

heterozygous variants from low sequencing depths, we restricted the analysis to 131 genomes with mean read depth >= 20x and mean genotype quality (GQ; the Phred-scaled confidence that the genotype assignment (GT) is correct) >= 80 across heterozygous sites. For homozygous substitutions, we restricted the analysis to 220 genomes with >=10,000 substitutions in coding regions. We evaluated both missense and LoF variants at heterozygous sites, and missense substitutions for homozygous sites. From the genome of a single individual, we are likely to capture many thousands of mildly and moderately deleterious alleles that are at high frequency or fixed (drift load), but only a few highly deleterious/lethal alleles (which are typically rare in the population and across the genome, and comprise mainly inbreeding load); thus we likely do not have high power to detect differences in highly deleterious alleles between species.

Correlations between demography, genetic diversity, genetic load and conservation status

Species with smaller historical effective population sizes tend to have higher proportions of mildly to moderately deleterious mutations in their genomes. The proportion of homozygous substitutions at conserved sites was negatively correlated with species  $N_e$  (phylolm, p=9.65e-3,  $\beta$ = -1.14e-3, where each 10-fold increase in  $N_e$  corresponds to a 1.14e-3 decrease in the proportion, fig. S4A), and the proportion of homozygous missense substitutions was negatively correlated with species  $N_e$  (phylolm,  $\beta$ = -0.020, p=7.76e-5; fig. S4B). Phylop kurtosis (which describes the extremity of phyloP outliers in the tail of the distribution across substitutions) was positively correlated with  $N_e$  (phylolm,  $\beta$ =0.851, p=0.014), i.e. species with smaller  $N_e$  had smaller right tails, suggesting fewer extreme conservation scores. In contrast to historical  $N_e$ , neither genome-wide heterozygosity nor the proportion of the genome in RoH (metrics that are influenced by more recent population history) were significantly correlated with the proportion of deleterious variation in the genome (phylolm, all p>0.098).

We then parsed the potential fitness impacts of mutations by examining genes classified as having lethal, subviable and viable phenotypes in knockout mice (figs. S5-S6). As expected for genes under strong purifying selection, there were proportionally fewer missense variants in subviable and lethal gene categories compared to genes in the viable category across species (ANOVA, all p<2e-16, fig. S7), validating the relative impacts of mutations in genes inferred from IMPC categories. The historical  $N_e$  of species was negatively correlated with the proportion of heterozygous missense variants for all IMPC categories (phylolm, all p< 2.53e-3; fig. S5), and with homozygous missense substitutions in the viable and lethal categories and in all gene categories combined (phylolm, all p< 1.72e-5; fig. S5). By contrast, heterozygous LoF variants were not significantly associated with  $N_e$ , except for a negative correlation for LoF alleles in IMPC lethal genes (phylolm, p=0.019; fig. S5), and the proportion of LoF alleles did not significantly differ between threatened and non-threatened species (fig. S6). Because of the rarity of LoF alleles in the genome, we had little power to test for differences in LoF alleles across species. To assess whether differences in annotation impacted our LoF results, we reran the regression with  $N_e$  using LoF estimates only for species with at least 200 genes in the IMPC lethal and viable categories and found that the results did not qualitatively change. Populations with smaller  $N_e$  had larger variability in the proportion of LoF alleles, especially in genes in the IMPC lethal category (fig. S5); however, the overall number of heterozygous sites is lower in these species, which adds additional stochasticity to the estimates.

While we do find that species with small  $N_e$  have proportionally higher genetic load, species with large  $N_e$  are expected to have more deleterious alleles segregating at low frequency by count

(12, 22). We examined heterozygous deleterious variants, normalized by the number of genes annotated in each genome, and found that that species with larger  $N_e$  have more heterozygous missense variants in IMPC viable genes (log-log phylolm,  $\beta$ =0.222, p=0.002) and IMPC lethal genes (log-log phylolm,  $\beta$ =0.167, p=0.03), as expected from theory.

Deleterious genetic load in threatened compared to non-threatened species was often, but not always, consistent with expectations for small compared to large populations, respectively. Phylop kurtosis was lower on average in threatened than non-threatened species (phylolm, mean<sub>threatened</sub>=22.03, mean<sub>non-threatened</sub>=22.75, p=0.001), a trend largely driven by Carnivora (phylolm, mean<sub>threatened</sub>=24.39, mean<sub>non-threatened</sub>=25.95, p=0.047) and Primates (phylolm, mean<sub>threatened</sub>=23.96, mean<sub>non-threatened</sub>=25.32, p=7.9e-4)(fig. S8). There was no significant difference in phylogenetically corrected means of proportional genetic load between threatened and non-threatened species, including the proportion of missense substitutions (phylolm, p=0.31), the proportion of substitutions at conserved sites (phylolm, p=0.46), and the proportion of missense substitutions at conserved sites (phylolm, p=0.53)).

There were significant relationships between fixed genetic load and the odds of being threatened, however, the relationship was different for protein-coding genes compared to evolutionarily conserved sites genome-wide. Species that had proportionally fewer homozygous substitutions at evolutionarily conserved sites across the genome were more likely to be threatened in logistic regression tests (phyloglm,  $\beta$ = -0.52, where each 1% increase in these substitutions is associated with a 52% decrease in odds of being threatened; p=1.38e-05; fig. S4C), even though species with smaller  $N_e$  tended to have proportionally more homozygous substitutions at conserved sites (phylolm, p=9.6e-3; fig. S4A). Species with lower kurtosis of the phyloP distribution across substitutions (i.e. fewer extremely conserved outliers) were also more likely to be threatened (phyloglm,  $\beta$ = -0.17, p=0.018, fig. S8). In protein coding regions, by contrast, species with proportionally more missense substitutions were more likely to be threatened (phyloglm,  $\beta$ =0.23, where each 1% increase in these substitutions is associated with a 23% increase in odds of being threatened; p=0.002; fig. S4D). Genomes with proportionally more missense substitutions in IMPC categorized genes were also more likely to be those of threatened species for nearly all gene categories (phyloglm, all p<0.053; fig. S6).

### <u>Impact of variation in annotation performance across species</u>

The number of genes annotated in each genome across species varied widely (range=1760-8465, mean=5992, std. dev.=1311), with Primate genomes having the most genes annotated. However, because we estimated genetic load as the proportion of deleterious mutations relative to total coding mutations (and not by counts of deleterious mutations), there was not a strong effect of different numbers of annotated genes used in the analysis. To determine whether differences in annotation performance may have impacted our results, we estimated the proportion of missense substitutions using only the subset of genes that were annotated in at least 200 species. The results were very similar and qualitatively identical. The estimated proportion of missense substitutions for species using the restricted and full sets of single-copy BUSCO genes were highly correlated ( $r^2$ =0.94). The significance of the relationships between the proportion of homozygous missense substitutions and threatened status (phyloglm,  $\beta$ = 0.20, p=0.013), and between the proportion of homozygous missense substitutions and  $N_e$  (phylolm,  $\beta$ = -0.019, p=1.72e-5) were also qualitatively identical with the more restricted set of genes relative to the full set.

Additional lines of evidence suggest that overall our estimates of genetic load are robust. 1) The observation of proportionally fewer deleterious mutations with increasing  $N_e$  fits theoretical expectations that purifying selection is more effective at removing/reducing deleterious alleles in large populations, and confirms that our classification of deleterious mutations is correlated with the true deleterious fitness impacts across mutations. 2) Mutations and derived alleles were estimated using distinct methods for homozygous versus heterozygous sites. (Homozygous derived substitutions were called relative to ancestral reconstructions from the multispecies alignment, and their impact inferred from evolutionary conservation and/or changes to protein coding sequences, whereas heterozygous variants were called from short-read data mapped to reference genomes, and a single derived allele was assumed.) Yet there are negative correlations between  $N_e$  and proportional genetic load for both mutation types (Fig. 2), which further supports our classification of deleterious alleles.

### Using single genomes to represent genetic load of a species

While a single genome can never encompass intraspecific variation, by using a single genome per species we were able to include species that had minimal genomic resources and increase the number of species analyzed. The proportions of deleterious mutations are driven by the effects of purifying selection to remove these variants and the effects of genetic drift over time, and thus we expect that individuals within a species should have similar proportions of genetic load, and these proportions would not rapidly change with, for example, recent changes in demography. For example, under population contraction, all variants (deleterious and non-deleterious) are expected to become increasingly homozygous, but the proportion of deleterious and non-deleterious homozygous mutations would not change much in the short term.

Empirical studies suggest that most individuals within a species have similar levels of proportional genetic load. For example, van der Valk, et al. (29) evaluated load based on evolutionary conservation scores (GERP) across mammals, including resequencing data from multiple individuals, and found that intraspecific variability in genetic load is typically small (+/-SD 1.3%), and is smaller than interspecific variability. In a study of the vaquita (*Phocoena sinus*), intraspecific variation in the proportion of deleterious variants was also small relative to interspecies variability (83). Other studies also suggest that proportional drift load is not sensitive to recent demographic history (84). Although intraspecific variability can not be captured by sampling a single individual, these studies suggest that it will often provide a reasonable estimate of drift load that has accumulated over long evolutionary time periods in a given species.

The only two conspecific genomes in the dataset, the domestic dog and the village dog, have shared evolutionary histories until very recently, when lineages began to diverge in the Victorian Era. As expected, the domestic dog has slightly lower historical  $N_e$  ( $N_e$ =2,131) than the village dog ( $N_e$ =2,356), and the domestic dog had a slightly higher proportion of homozygous missense substitutions (0.3603) than the village dog (0.3591). These differences are very small compared to all of the species in the dataset, which ranged from 0.224-0.434 across 239 genomes, and the two dog genomes were 202nd and 206th when species were ranked by this metric. These measures of genetic load reflect older, shared evolutionary histories that have changed little with recent population divergence and different selective conditions. Other studies also suggest that proportional drift load is not sensitive to recent demographic history. In southern white rhinos, individuals sampled before a population bottleneck and after the bottleneck showed no difference in the proportions of homozygous missense mutations relative to homozygous synonymous mutations (84). In both of these examples, however, the populations

have diverged very recently (≤200 years). With increasing time since divergence between populations, samples from different populations are expected to become increasingly dissimilar.

### Estimating heterozygosity and genetic load across homologous windows

We used the genomic distribution of heterozygosity and genetic load across mammalian taxa to train machine learning models for predicting conservation status (see below for machine learning methods). To generate matrices of heterozygosity and genetic load across homologous windows, we lifted over 50KB windows of 174 species to windows of the human genome using *halLiftover*, assigning the estimates of RoH, heterozygosity, mean phyloP across substitutions, and number of missense substitutions, from windows of each species to the window of the human genome. We averaged heterozygosity and the amount of RoH in each human-based window, and removed windows with fewer than 5KB that lifted over.

### Statistical regression models of threatened status using genomic variables

We took three approaches to model conservation status across species using regression models. First, we used a phylogenetic logistic regression model, which accounts for evolutionary relationships across species. This model allowed us to test the significance of predictor variables, but does not readily make predictions for species with unknown threat status. Second, we used ordinal regression models, which estimate parameters based on specific IUCN categories. We included taxonomic order as a factor to account for phylogenetic relationships. These models allowed us to test the significance of predictor variables and make predictions for species with unknown threat status. Third, we used principal components (PCs) to summarize genomic variables, and tested the significance of PCs as predictors of threatened status using logistic regression. We also tested the ordinal regression and PC models within taxonomic orders to explore how the predictors of conservation status vary with taxonomy.

We incorporated genomic variables with taxonomic order and dietary trophic level, a known correlate of extinction risk (65), into these regression models. We subsetted the full dataset of 240 species to remove 16 domesticated species. We identified 13 possible predictor variables related to genomic heterozygosity and genetic load (table S2). We examined these numeric variables for normality by visualizing Q-Q plots, transforming as necessary to improve normality and rescaling all variables to a Z-score. We then removed the three species with an IUCN status of "Data Deficient".

We estimated model error by running the ordinal regression and PC regression models on 80% of the data and using the predict function from the R stats package to predict the threatened status of the remaining 20% of the data. Our estimate of model error was the mean of 100 runs with different data subsets.

We used a phylogenetic logistic regression model to determine which genomic features were most predictive of conservation status and to calculate the odds of a classification of "threatened" (IUCN NT, VU, EN, CR categories), as compared to non-threatened (IUCN LC category). We combined all four non-LC categories to increase the power of our analyses and balance sample sizes between threatened and non-threatened groups. Visual inspection of genomic variables suggested that the four threatened categories were more similar to one another than to the LC category (fig. S2). To select variables for inclusion into the final model, we used phyloglm from the R phylolm package (version 2.6.3)(55) with the phylogenetic tree generated from the X chromosome for the 240 species (56). We tested each of the 13 heterozygosity and load variables and two categorical covariates (diet category and wild versus captive status)

individually against threatened status, dropping variables that were not significant at a p=0.10 threshold. For the remaining numeric variables, we examined pairwise correlations and for pairs with a correlation greater than 0.7, we removed the variable of the pair with the higher p-value in the individual models predicting conservation status. We ran phyloglm for the final phylogenetic logistic regression model with the variables that remained after filtering for significance and correlation. We retained both categorical covariates (the diet category of the species and wild versus captive status of the short-read data sample) in the final model because they were significant (p<0.10) when considered individually, and to account for their possible influence on heterozygosity and fRoH estimates. We dropped four numeric variables that were not significant individually (p>0.10), and dropped three other numeric variables that were highly correlated with, but less significant than, another variable. The final model included the phylogenetic tree, two categorical covariates, three variables related to genome heterozygosity and fRoH, and three variables related to genetic load. In this final model, both diet category and wild versus captive status significantly predicted threatened status (p<0.05); and two numeric variables significantly predicted threatened status (p<0.05): harmonic mean of the historical effective population size and proportion of the genome in RoH. As expected, lower historical effective population sizes increase the odds of being classified as threatened. Contrary to expectations, a lower proportion of the genome in RoH increases the odds of being classified as threatened, likely due to the skewed distributions of RoH and the captive samples included in the analysis. None of the genetic load metrics were significant in this model.

We used an ordinal regression model to determine which genomic features were most predictive of IUCN category, to estimate the probability of each IUCN category, and to examine how these probabilities covary with taxonomic order, diet category, and wild versus captive status. Due to the sparsity of species in a number of taxonomic orders, for this model we used only five orders that had a sufficient number of species (Carnivora, Cetartiodactyla, Chiroptera, Primates, and Rodentia). To select variables for inclusion into the final model, we used polr from the R MASS package (version 7.3.51.4)(85). We tested each of the 13 heterozygosity and load variables and three categorical covariates individually against IUCN category, dropping variables that were not significant at a p=0.10 threshold. For the remaining numeric variables, we examined pairwise correlations and for pairs with a correlation greater than 0.7, we remove the variable of the pair with the higher p-value in the individual models. We dropped six numeric variables because they were not significant individually (p>0.10); we dropped three other variables due to high correlation with and lower significance than another variable. We ran polr for the final ordinal regression model with the variables that remained after significance and correlation filtering. The final model included all three covariates, one variable related to heterozygosity, and three variables related to genetic load, and had a cross validation (CV) error of 31% for classification of threatened versus non-threatened. In the final model, taxonomic order, diet category, and harmonic mean of the historical effective population size significantly (p<0.05) predicted IUCN status. As with the previous model, lower historical  $N_e$  indicated an increased probability of being classified as threatened. The impact of a lower historical  $N_e$  was greater on species with a diet classification of herbivores, as compared to omnivores and carnivores (Fig. 3B). We then modeled extinction risk within the three taxonomic orders with sufficient samples in threatened and non-threatened categories (Carnivora, Cetartiodactyla, and Primates), using the same process as above (excluding the taxonomic order variable) to select variables in order-specific ordinal regression models. When examining taxonomic order, the impact of historical  $N_e$  was reduced in Chiroptera and Rodentia (Fig. 3C).

To retain the information from all predictor variables and account for the correlation between them, we used principal component (PC) regression. Using the same 13 predictor variables, we removed species with missing data and ran a PC analysis using promp from the R stats package (version 3.6.1)(86). We ran a linear model to predict threatened status using lm from the R stats package, including the fewest PCs that cumulatively accounted for at least 80% of the variance in the data (table S3). For the three taxonomic orders with sufficient sample sizes, we used lm from the R stats package and the same set of PCs to run order-specific PC regression models. We tested the significance of the first five PCs, which accounted for greater than 80% of the cumulative variation in the predictor variables, in predicting threatened status. Two PCs were significant: PC1 (p=0.0038; explaining 35% of the total variance) and PC3 (p=5.6e-4; explaining 13% of the total variance). PC1 broadly represents heterozygosity and genetic load metrics and PC3 separates the mildly and severely deleterious mutations (table S3).

Given the importance of taxonomic order in all the models we examined, we tested the ordinal regression and PC models within the three taxonomic orders that had enough individuals in both non-threatened and threatened categories. Carnivora showed a complex relationship between threatened status and genomic variables. While a number of variables were significant when considered individually, none significantly impacted threatened status when considered together in the ordinal regression model. When PC regression was used to incorporate all the genomic variables while reducing dimensionality and correlation, the two most significant PCs were PC1 (p=0.07) and PC4 (p=0.04) that have major contributions from historical  $N_e$  and genetic load due to viable heterozygous loss of function (fig. S9). For Carnivora, the ordinal regression model had a CV error of 28% and the PC regression model had a CV error of 38%. Within Cetartiodactyla, there were no significant (p<0.05) predictors of threatened status in either the ordinal or PC regression models, however a few predictors were significant at a p=0.10 threshold, suggesting either a weak relationship and/or a lack of power due to small sample sizes. Additionally, Cetartiodactyla contains two groups with distinct ecological niches, one terrestrial and one aquatic, which may influence the genomic predictors of extinction risk in the two groups. The ordinal regression model had a CV error of 39% and the PC regression model had a CV error of 47%. Primates had a single variable that was significantly predictive of threatened status—the kurtosis of phylop, which is a measure of the tailedness of the distribution of phylop scores across substitutions. Primate species that are threatened tend to have fewer variants in the tail of the phylop distribution (phylolm, p=0.003), suggesting that purging of deleterious variants may be common in Primates (fig. S8). For Primates, the ordinal regression model had a CV error of 39% and the PC regression model had a CV error of 44%.

To make predictions for species classified as "Data Deficient", we used the predict function from the R stats package with the ordinal regression models and the PC regression models (excluding the phylogenetic PC regression model because there is no predict function available in the phylolm package).

### Machine learning (ML) methods for categorizing IUCN status using genomic features

We next used random-forest based classification to identify the genomic features that predict "threatened" versus "non-threatened" status of species. We used two different genomic data types: 1) summary statistics of heterozygosity, RoH, and metrics of genetic load within homologous 50KB windows, and 2) genome-wide summary statistics related to heterozygosity, demographic history, and genetic load (table S4). For window-based summary statistics, we lifted over each genome to common coordinates of the human genome as described above (see

Estimating diversity across homologous windows). We generated five genomic feature matrices by estimating the following within windows of each genome: heterozygosity, RoH, mean phyloP of substitutions, number of missense substitutions, and number of missense substitutions at evolutionarily conserved sites. We ran the two genomic data types separately and combined, and additionally incorporated 39 numeric ecological features from the PanTHERIA database (table S4) to assess predictive performance of genomic features in comparison with ecological variables, considered a "gold standard" for prediction (31, 32).

We started with five genomic feature window matrices in 57,509 homologous 50KB windows for at least 197 and up to 236 species depending on the statistic (table S5). Because we observed little impact of removing domesticated species in the regression models, we included them in the random forest models. We normalized counts of missense substitutions and counts of conserved missense substitutions by dividing by the total number of protein-coding variants for a given species. For each of the five genomic feature window matrices, we removed species that had missing values in more than 30,000 windows (which varied based on the statistic).

We included 13 genome-wide summary statistics describing demographic history, diversity, and genetic load (table S4). Of a total of 39 possible ecological features, the number of features included in each model depended on the number of species that had complete data for each model included in the training set, and this varied depending on which genomic feature dataset was used (window matrices, genome-wide summary statistics, or the two types combined).

We first split our dataset into a 75% train set and a 25% test set, and removed three data-deficient species (*Orcinus orca*, *Tragulus javanicus* and *Nannospalax galili*) lacking an IUCN status. This split was defined by a reproducible seed (ranging from 1 to 5), and repeated to test for robustness. Then, to prevent data leakage, we performed preprocessing and imputation steps using only the training data. We removed window-based metrics that had (1) missing values in more than 75% of the species, or (2) features with the mode value occuring in more than 75% of non-missing values. (All genome-wide summary statistics and ecological features passed these criteria.) Missing values were imputed within a feature vector using two methods (1) computing the median across all other species, or (2) by leveraging taxonomic order as follows: first, we compute the median of the species within the same genus; if there are no non-missing values, then we move up to compute the median value within the same family; then order. Missing values within the test set were imputed analogously using only the values within the training set.

We grouped the IUCN conservation status into two classes, threatened (NT/VU/EN/CR) and non-threatened (LC), with the goal of distinguishing between threatened and non-threatened species. Our models take as input the filtered window-based statistics, genome-wide summary statistics, and ecological variables. The output is a probability of the species being threatened.

Similar to previous work (31, 32), we used random forest classifiers to assess the relationship between features and IUCN status. Random forests is an ensemble learning approach, making predictions by combining the outputs of hundreds of decision trees. We ran 5-fold cross validation on the training set to determine the optimal set of hyperparameters, which define the structure and learning process of the internal decision trees. Specifically, we tuned the number of decision trees, the maximum depth of the trees, and the number of features used at each decision to optimize a performance metric. For all models (except for the model trained on solely the 13 genomic summary variables), we added an additional hyperparameter governing the number of features selected during feature selection. During cross-validation, our median-based imputation was computed within each fold, whereas our phylogenetic imputation was computed on the entire training set. We used the area under the receiver operating characteristic

(AUROC) curve to evaluate performance. AUROC is a performance metric that estimates how well a model assigns (predicts) the correct output class, and is designed to be more robust to class imbalance in comparison to a metric such as accuracy. A model with AUROC of 0.5 has no predictive ability, whereas a model with AUROC of 1.0 has perfect predictive performance. Using the selected features and hyperparameters, we re-trained a model on the training set, evaluated it on the held-out test set, and reported the performance metric used during optimization. For all models, we ranked the features based on the model feature importance, a measure of the predictive power of the feature relative to other features in the model. Feature selection was performed in all cases except for genome summary, which had only 13 features. We used the scikit-learn 1.0.2 package for fitting all the models (66).

The number of species with values for ecological, genome-wide summary statistics, and window-based metrics varied, and so we ran two types of models: "individual" and "composite" models using 5-fold cross-validation for model selection. First we ran "individual" models including all species available for each dataset (table S5). The individual models help us evaluate the utility (i.e. predictive performance) of genomic variables as predictors of conservation status while leveraging all the data available for each metric. The method of imputation had an impact on predictive power, with imputation based on phylogeny showing superior performance over imputation based on median across all species regardless of taxonomic order (table S5). The model including only ecological variables across all available species had the best predictive AUROC (median across 5 training-test replicates was 0.88), while the models with genomic features had lower, but still good predictive power. Genomic window-based metrics varied in their predictive power, with AUROC ranging from 0.69-0.82 (table S5). The median AUROC values across five training-test replicates were 0.69 for the model with the proportion of missense substitutions, 0.70 for the proportion of conserved missense substitutions, 0.78 for RoH, 0.79 for heterozygosity, 0.74 for all window-based metrics combined, and 0.82 for the model with three window-based features combined (RoH, heterozygosity, and mean phyloP). The results suggest that windows of mean phyloP across substitutions, RoH, and heterozygosity were relatively more predictive than the other window-based features. Genome-wide summary variables were also somewhat predictive of threatened status, with a median AUROC of 0.68. There was little variance in model performance across the five training-test replicates for each individual model (mean coefficient of variation across models = 0.07, range=0.01-0.22; fig. S11).

To compare the effect of combining ecological and genomic variables on classification, we ran "composite" models, testing genomic (genome-wide summary and window-based) features and ecological features in the set of species for which both data were available (tables S4 and S6). We used the best performing window-based features derived from feature selection among the window-based features alone, and imputed missing data by phylogeny, which showed superior performance in the "individual" models. There was little variance in model performance across the five training-test replicates for each composite model (mean coefficient of variation across models = 0.08, range=0.03-0.21; fig. S12-S13). Models for 210 species with ecological variables and genomic summary statistics combined (median AUROC=0.85) modestly outperformed those with ecological variables alone (median AUROC=0.83). Among all 52 variables included in these models, there were three genomic variables that consistently appeared among the top 20 predictive features across replicates, 1) historical  $N_e$  (five replicates), 2) proportion of heterozygous missense variants in IMPC lethal genes (four replicates), and 3)

proportion of substitutions at conserved sites (three replicates) (fig. S14). Models including window-based features never outperformed models with ecological variables alone (table S6).

Our evaluation suggests that genomic variables provide reasonable predictive performance, demonstrating the utility of using genomic variables when ecological variables are unavailable. We note caveats to our models: the species included in the model affect the results, as AUROC differs between independent and composite models (tables S5 and S6); our sample size is small and including additional observations and species will likely improve predictions and decrease this stochasticity. Our study is a pilot that demonstrates the potential usefulness of genomic data for triaging data deficient species, and motivates further studies exploring larger datasets and with feature transformation (e.g. using principal components) for improved predictive performance.

### Predicting conservation status of Data Deficient species

For the three species that are IUCN classified as "Data Deficient", we used both the regression and the random forest models to predict their probability of having a threatened status (Fig. 3D). The ordinal regression models generate predictions for each specific IUCN category; however, given the reduced power to distinguish between IUCN threatened categories due to small sample sizes in each, we focused on the broader classification of threatened versus non-threatened. From the regression models overall, the Upper Galilee Mountains blind mole rat (*Nannospalax galili*) is least likely to be a threatened species, with probabilities estimated at 12% and 14%. (Note there were not enough Rodentia species classified as threatened to do an order specific model). The Java lesser chevrotain (*Tragulus javanicus*) is also predicted to be a threatened species; however, probability estimates ranged from 27-63%. The higher risk prediction is from the within-order models. A killer whale (*Orcinus orca*) from the Norwegian herring-eating population (87), is likely to be in a threatened category, with probability estimates ranging from 62-68%.

Random forest model predictions for Data Deficient species differed somewhat from the regression-based predictions, but the relative likelihoods of threat for the three species were nonetheless consistent to the regression model predictions (Fig. 3D). All genomic feature-only models consistently predicted *Nannospalax galili* as the least likely to be threatened (median probability: 0.18, range: 0.11-0.44). *Tragulus javanicus* had a higher probability of being threatened, but was more likely to be classified as not threatened (median probability: 0.32, range: 0.24-0.49). *Orcinus orca* was the most likely to be threatened (median probability: 0.48, range: 0.35-0.61).

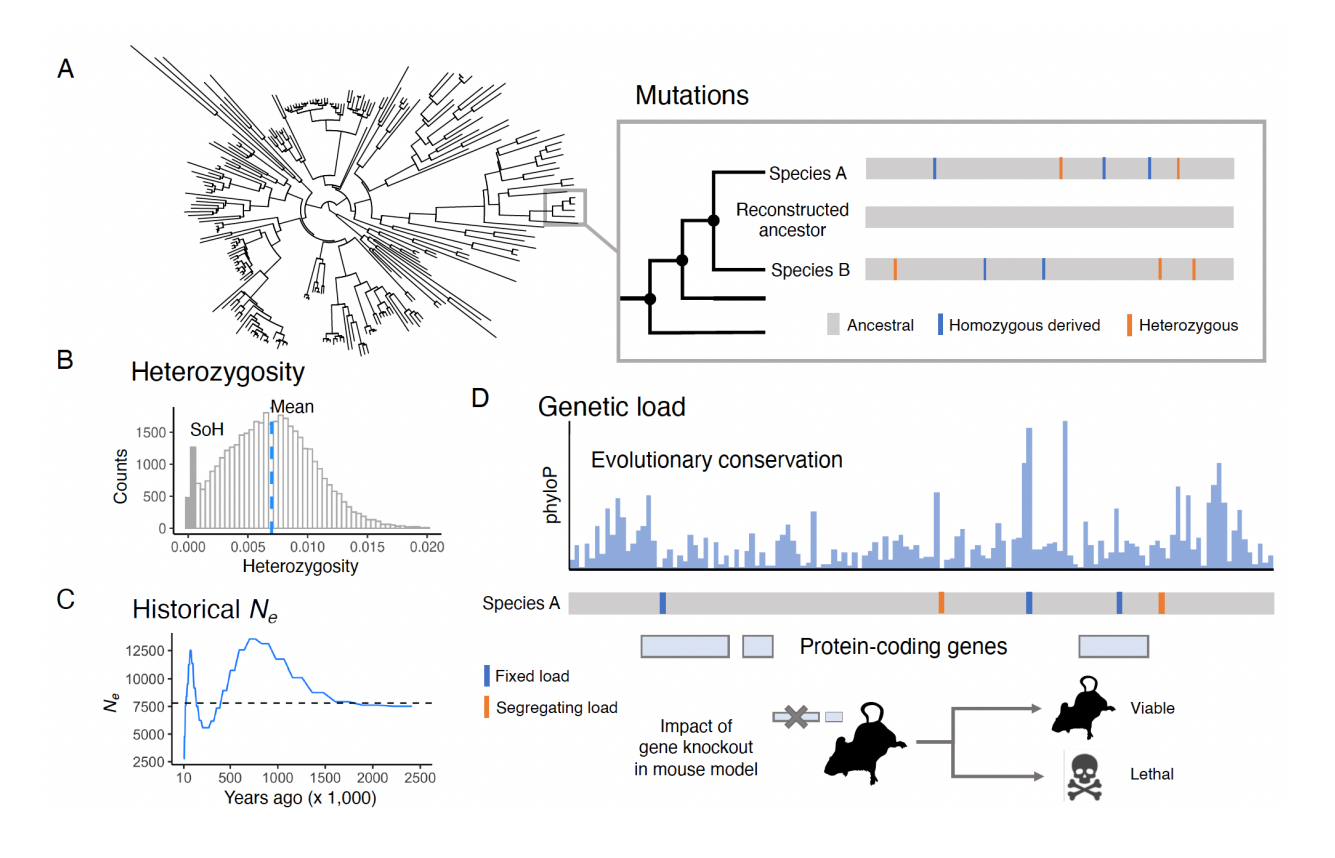


**Figure S1.**Overview of methods for estimating heterozygosity, historical  $N_e$ , and genetic load across individual mammalian genomes. (A) For each species in the Zoonomia alignment, homozygous derived substitutions were estimated relative to the reconstructed sequence of the closest ancestral node in the phylogeny. Heterozygous variants were estimated from the short-read data mapped to the reference genome. (B) Mean heterozygosity and proportion of the genome in runs of homozygosity (fRoH) were estimated from the distribution of 50-kb genomic windows. (C) Historical effective population size ( $N_e$ ) was estimated over time and summarized by the harmonic mean (dashed line). (D) Genetic load was inferred from the evolutionary conservation (measured by phyloP) of mutated positions, assuming that mutations at sites conserved across placental mammals are likely deleterious, and from the predicted impact of mutations in protein-coding genes, including single-copy genes with associated phenotypes in knockout mouse lines. Genetic load was estimated from the proportion of homozygous derived substitutions that were deleterious (fixed drift load), and the proportion of heterozygous variants that were deleterious (segregating mutational load), relative to total mutations of each type.

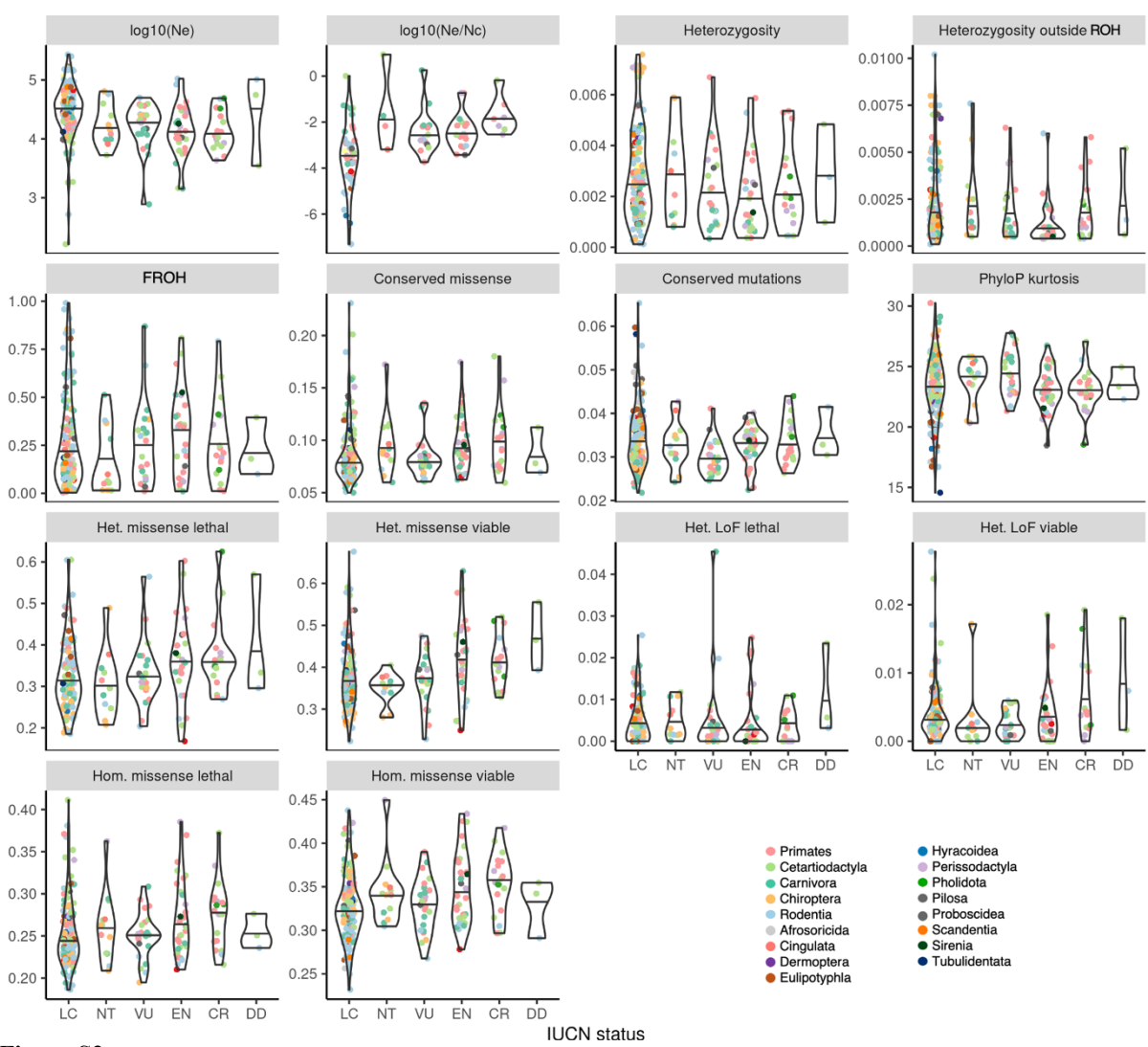


Figure S2. Distribution of genomic variables of demography, diversity and genetic load in species across IUCN threat categories. All variables (except  $N_e/N_c$ ) were used in regression and machine learning models to predict threatened and non-threatened IUCN status (see tables S2 and S4).

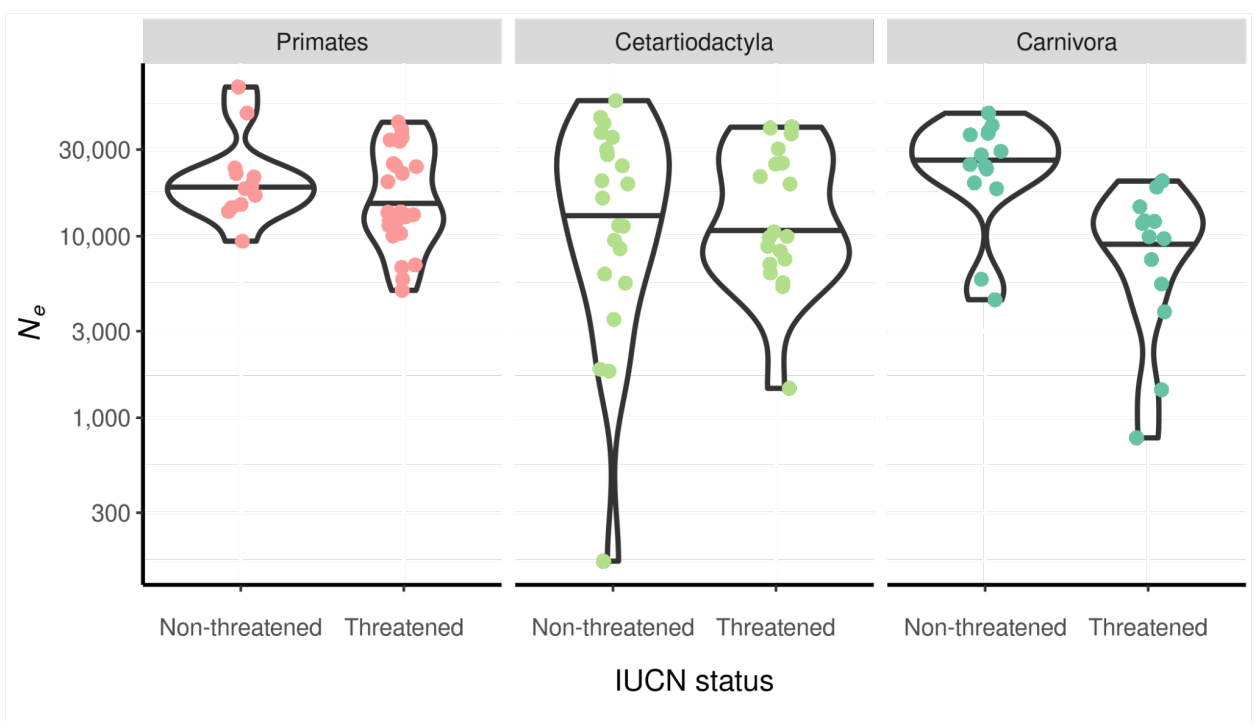
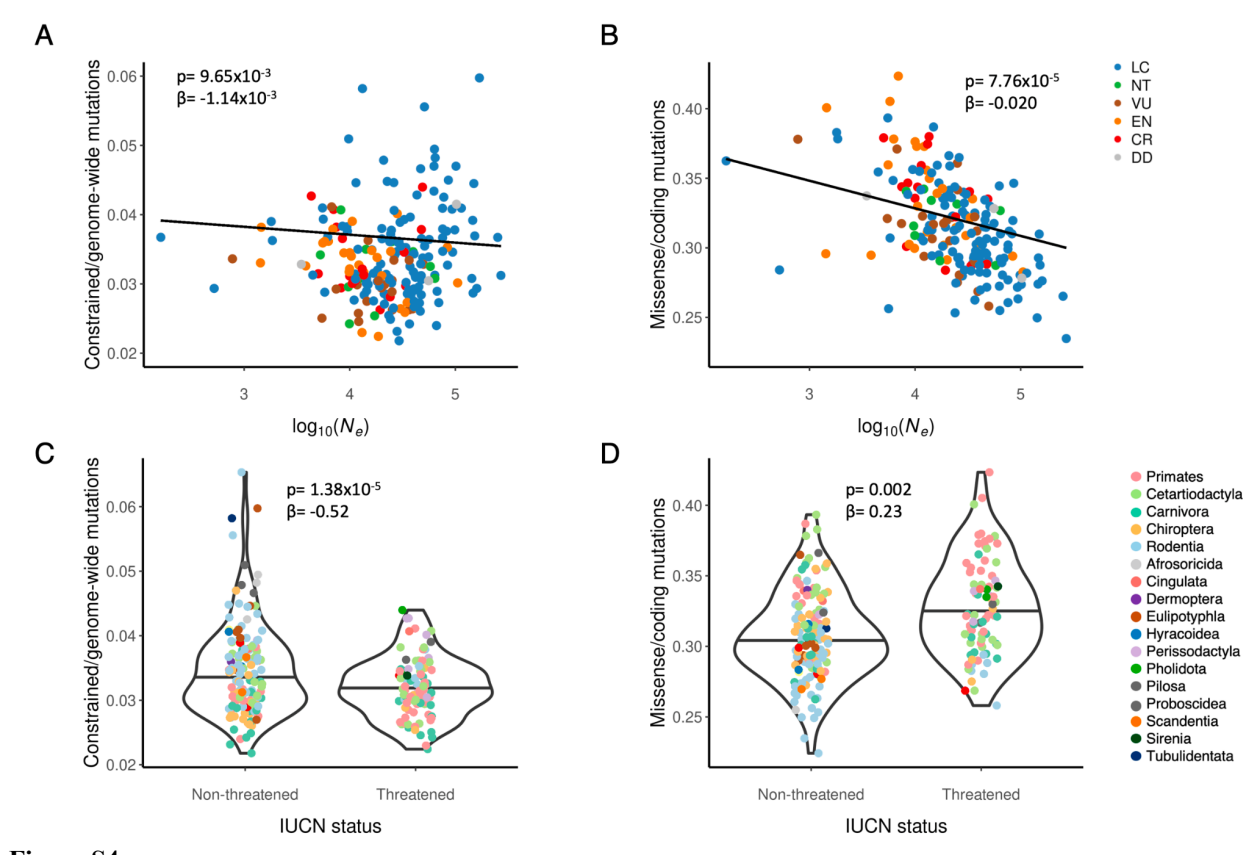


Figure S3. Effective population sizes ( $N_e$ ) were significantly smaller in threatened compared to non-threatened species within two of three taxonomic orders with enough samples in both threat categories to test: Cetartiodactyla (phylolm, p=0.023) and Carnivora (p=2.4e-5), but not Primates (phylolm, p=0.31).



**Figure S4.**Contrasting patterns of drift load based on conserved sites across the genome and missense substitutions in genes. A)  $N_e$  was negatively correlated with the proportion of homozygous substitutions that were at evolutionarily conserved sites (phylolm, p=9.6e-3, β=-0.0011, where a 10-fold increase in  $N_e$  corresponds to a decrease in proportion of 0.0011). B)  $N_e$  was negatively correlated with the proportion of homozygous missense substitutions that were at evolutionarily conserved sites (phylolm, p=7.76e-5, β= -0.020, where a 10-fold increase in  $N_e$  corresponds to a decrease in proportion of 0.020). Lines show coefficients estimated with phylogenetic correction using phylolm. C) Species that had proportionally fewer homozygous substitutions at evolutionarily conserved sites across the genome were more likely to be threatened (phyloglm; p=1.38e-05; β= -0.52). D) Species that had proportionally more homozygous missense substitutions in protein-coding genes were more likely to be threatened (phyloglm; p=0.002; β= 0.23).

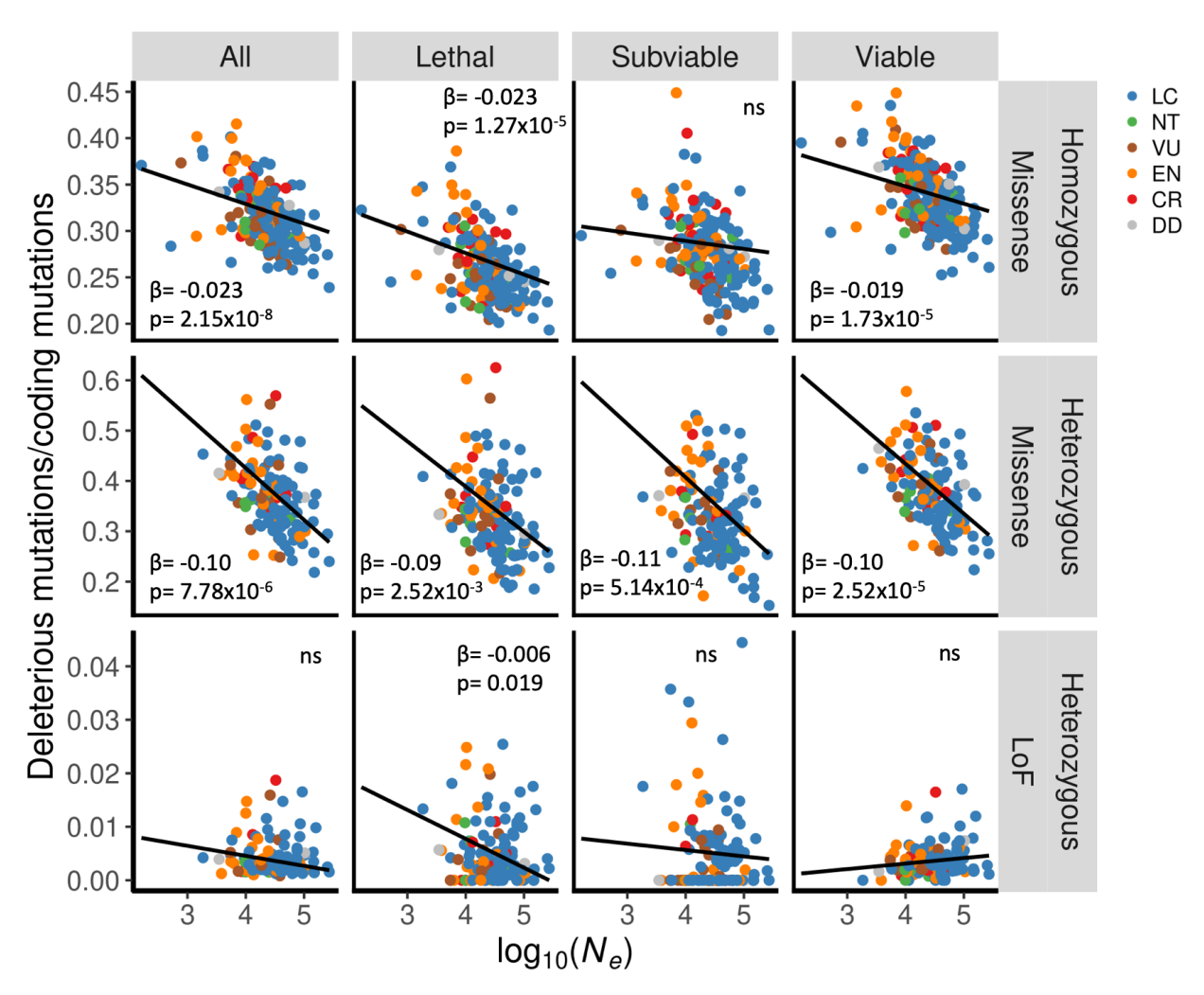


Figure S5. Proportion of heterozygous loss of function (LoF), heterozygous missense, and homozygous missense mutations in protein-coding genes classified as lethal, subviable or viable in knockout mice as a function of harmonic mean  $N_e$  across species. For most IMPC categories, proportions of heterozygous and homozygous missense alleles were negatively correlated with harmonic mean of  $N_e$ , but heterozygous LoF alleles were generally not. P-values and coefficients were estimated using phylogenetic correction in phylolm.

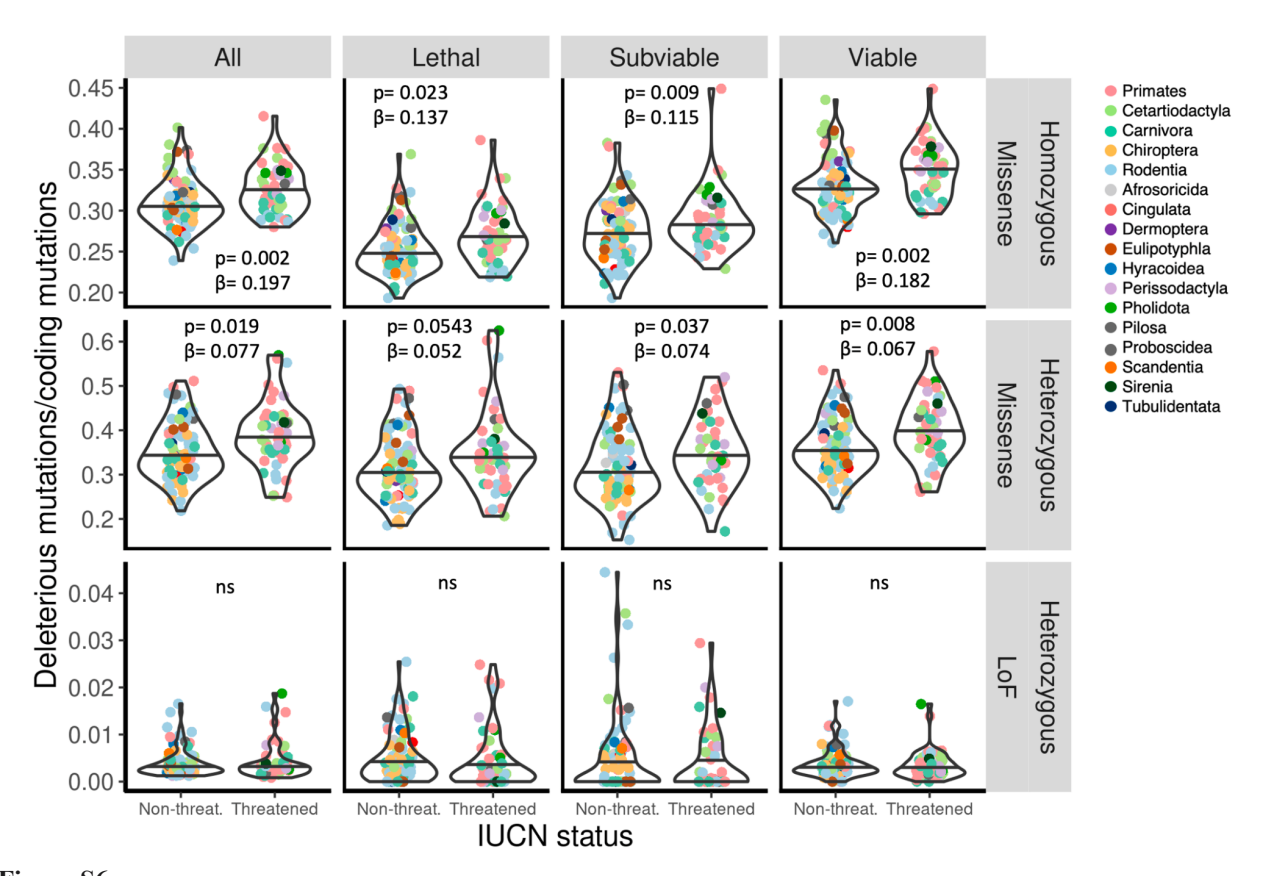
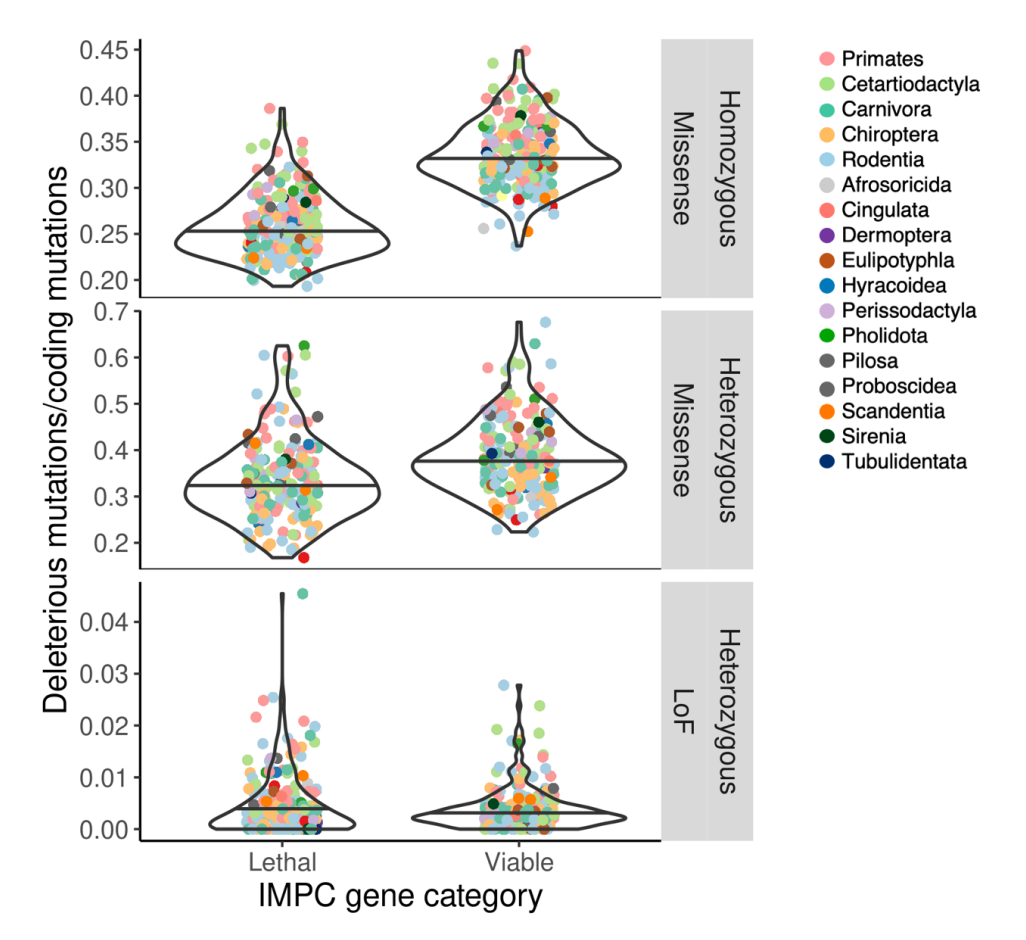


Figure S6. Proportion of heterozygous LoF, heterozygous missense, and homozygous missense mutations in protein-coding genes classified as lethal, subviable or viable in knockout mice for non-threatened and threatened species. For most IMPC categories, species with proportionally more heterozygous and homozygous missense alleles were more likely to be threatened. P-values shown were estimated using phylogenetic correction in phyloglm.  $\beta$  coefficients indicate the change in odds of being threatened with a 1% increase in deleterious mutations. Phylogenetically corrected means did not significantly differ (all p>0.15).



**Figure S7. Proportionally fewer missense mutations in genes associated with lethal phenotypes.** Missense mutations were less frequent in genes classified as IMPC lethal relative to genes classified as IMPC viable (ANOVA, p<2e-16 and p=4.42e-9 for homozygous and heterozygous mutations, respectively). The difference between the two categories for heterozygous LoF alleles was not significant (p=0.19).

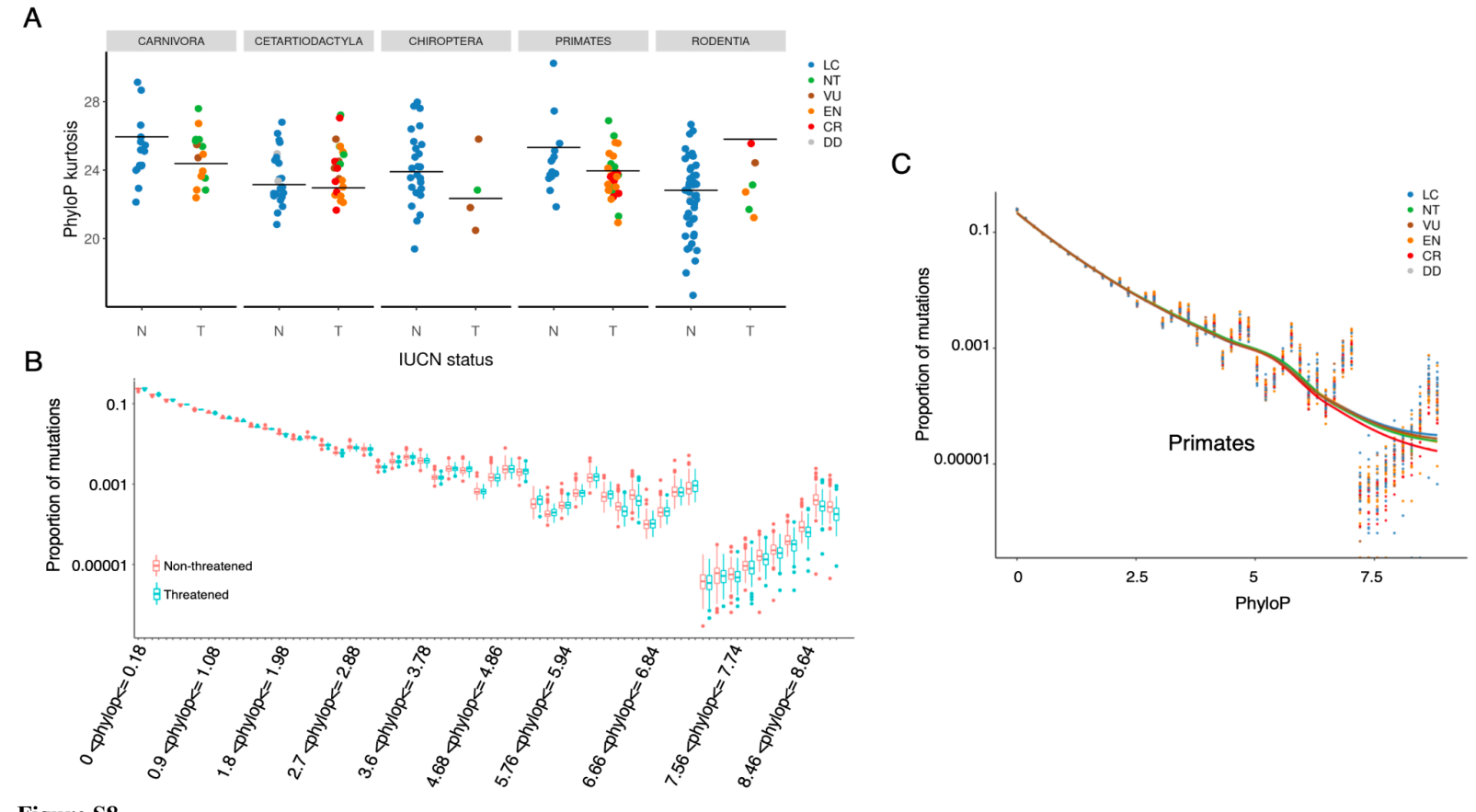
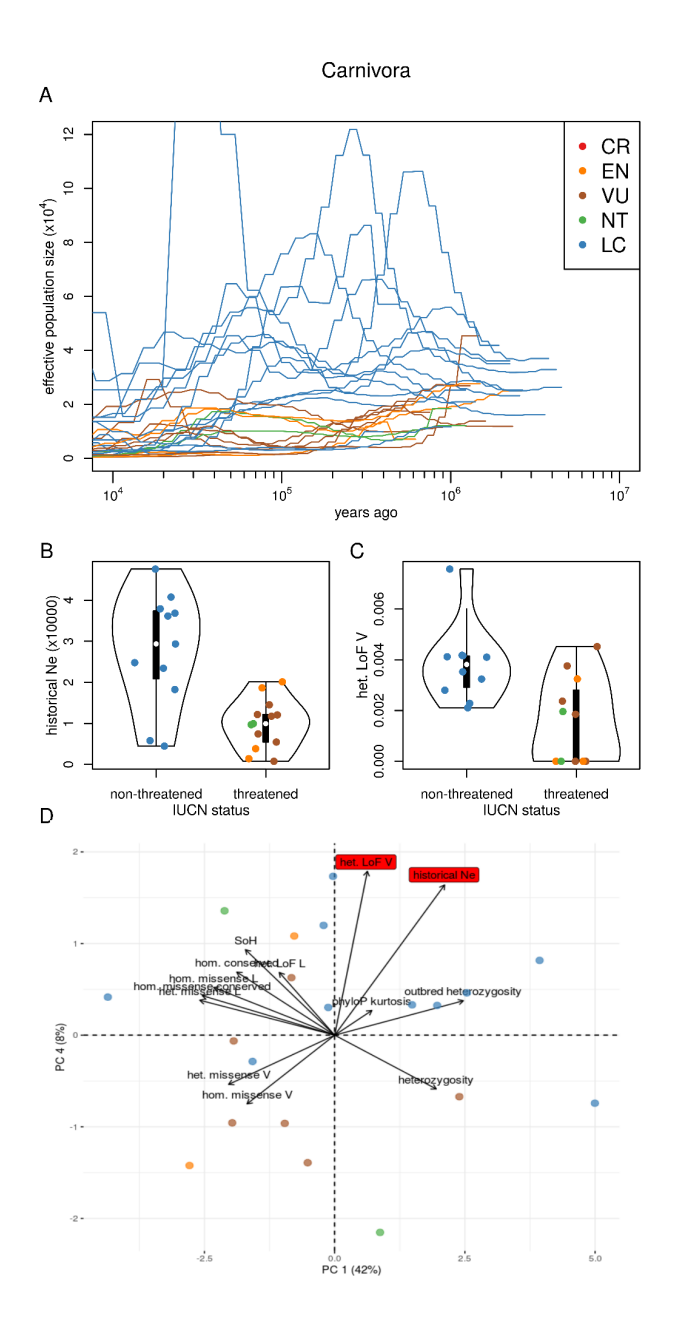
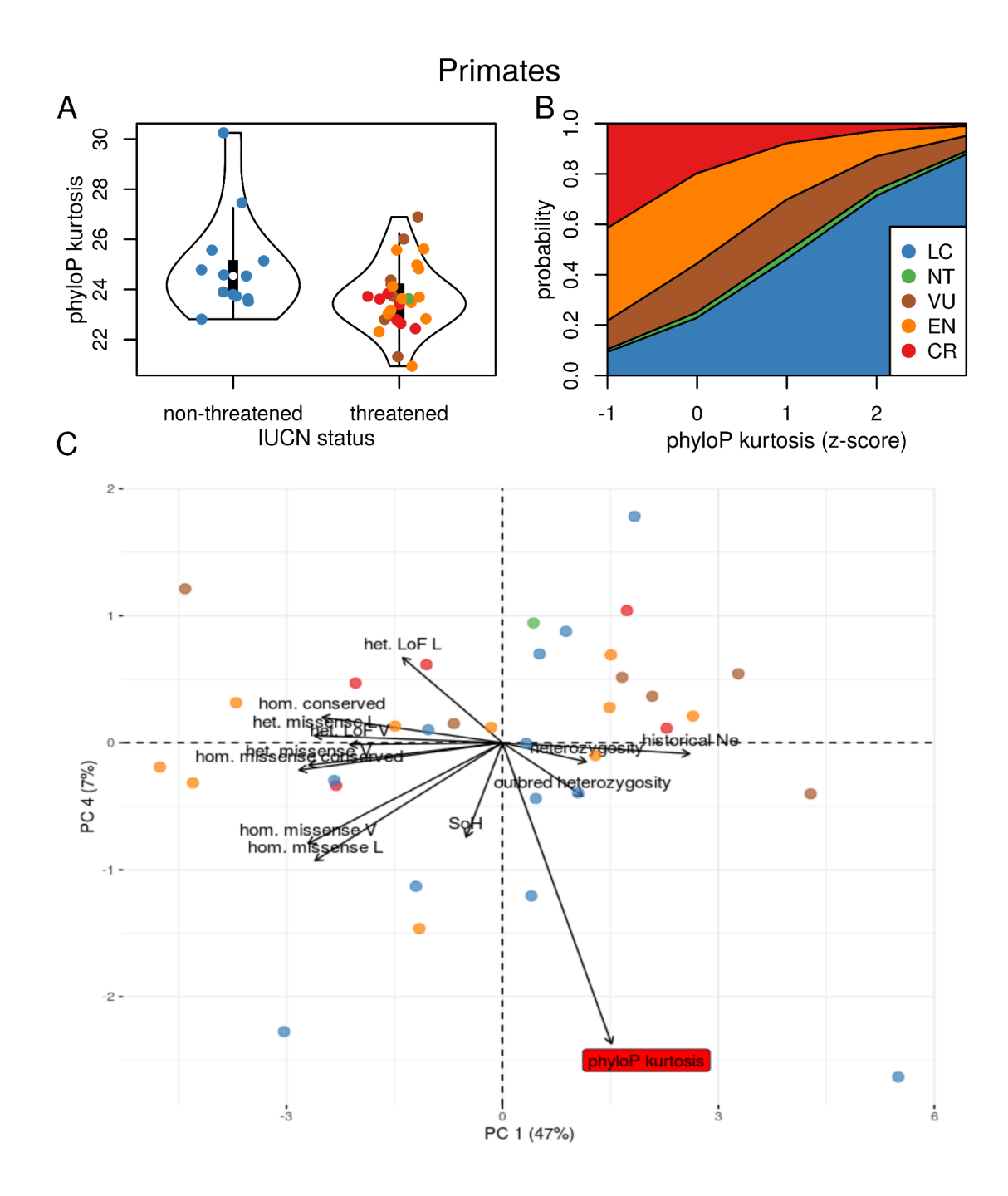


Figure S8.

Genome-wide conservation scores suggest fewer substitutions at highly conserved sites in threatened species. A) Kurtosis of the phyloP distribution across substitutions (larger numbers reflect fatter right tails) was significantly lower in threatened species across all taxa (p=0.004), and within Primates (p=0.003) and Carnivora (p=0.019). Horizontal lines show coefficients of means after phylogenetic correction in phylolm. B) Proportion of genome-wide substitutions in phyloP bins for threatened and non-threatened species across species. (C) Proportion of genome-wide substitutions in phyloP bins for threatened and non-threatened species, showing fewer substitutions in higher phyloP bins in threatened compared to non-threatened species within Primates. Lines show smoothed means for IUCN categories.



**Figure S9. Predictive metrics for Carnivora** A) Plots of  $N_e$  through time estimated from PSMC and used to calculate historical  $N_e$ . B) Historical  $N_e$  is significantly lower in threatened species (ordinal regression, p=0.0055). C) The proportion of heterozygous variants that were loss of function in genes categorized as viable (het. LOF V) is significantly lower in threatened species (ordinal regression, p=0.0064). D) PCA space of the most significant PCs (PC1, p=0.075; PC4, p=0.040) of genomic predictor variables in PC regression models. Vectors indicate variable loading with the two most significant variables from ordinal regression models shown in red. Dots represent species and show their scores in PCA space. Colors in all panels represent the IUCN category of the species. SoH=runs of homozygosity.



**Figure S10. Predictive metrics for Primates** A) PhyloP kurtosis is significantly lower in threatened species (phylolm, p=0.003). B) Probability of IUCN categories for phyloP kurtosis score in the ordinal regression model (p=0.01). C) PCA space of genomic predictor variables showing PC1 (p=0.62) and the most significant predictor in the PC regression model PC4 (p=0.063). Vectors indicate variable loading, with PhyloP kurtosis (shown in red) as the major contributor to PC4. Dots represent species and show their scores in PCA space. Colors in all panels represent the IUCN category of the species. SoH=runs of homozygosity.

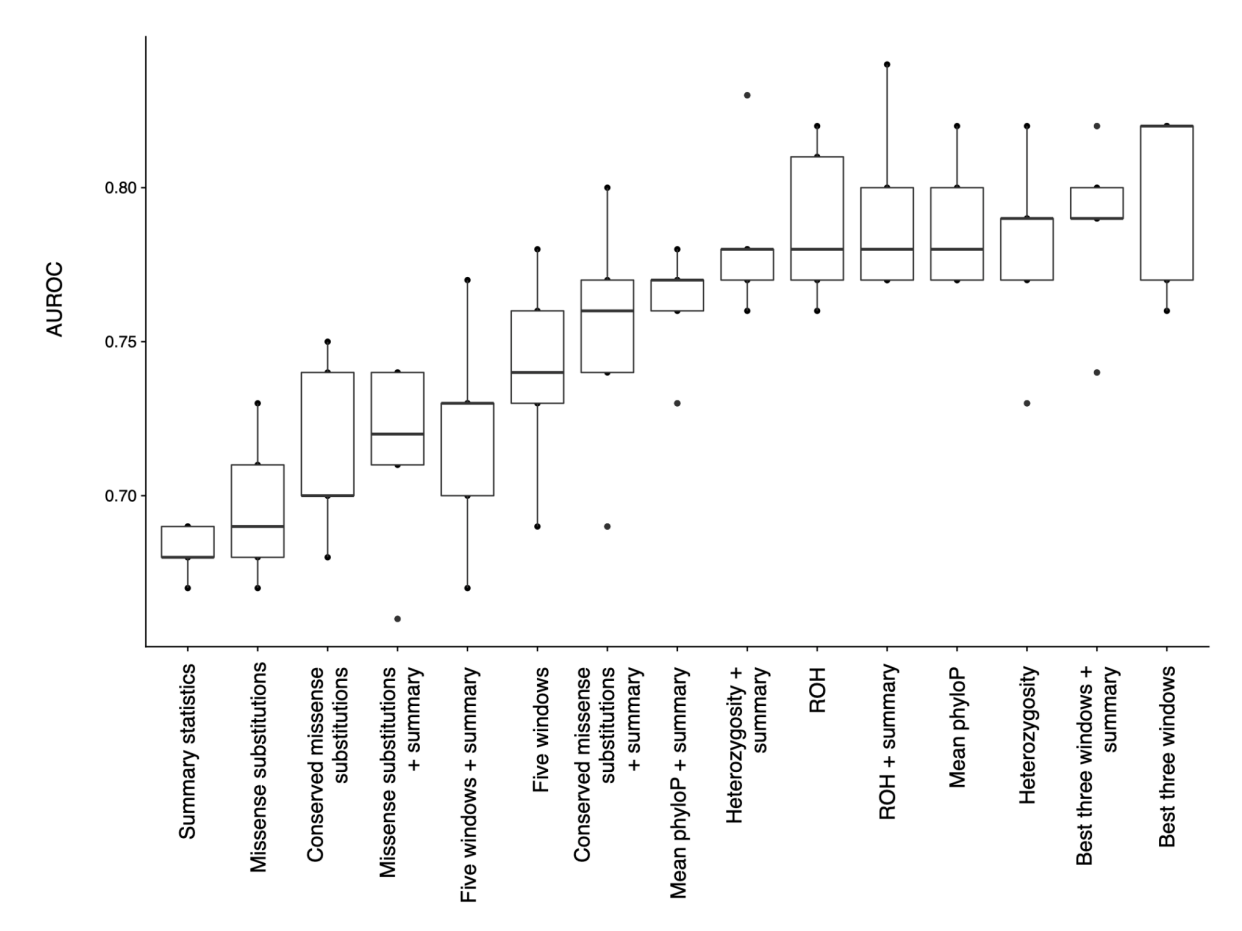


**Figure S11.**Performance measurements (AUROC) across five training-test replicates of "individual" models that included window-based metrics and/or genome-wide summary statistics (table S5; see table S4 for data descriptions).

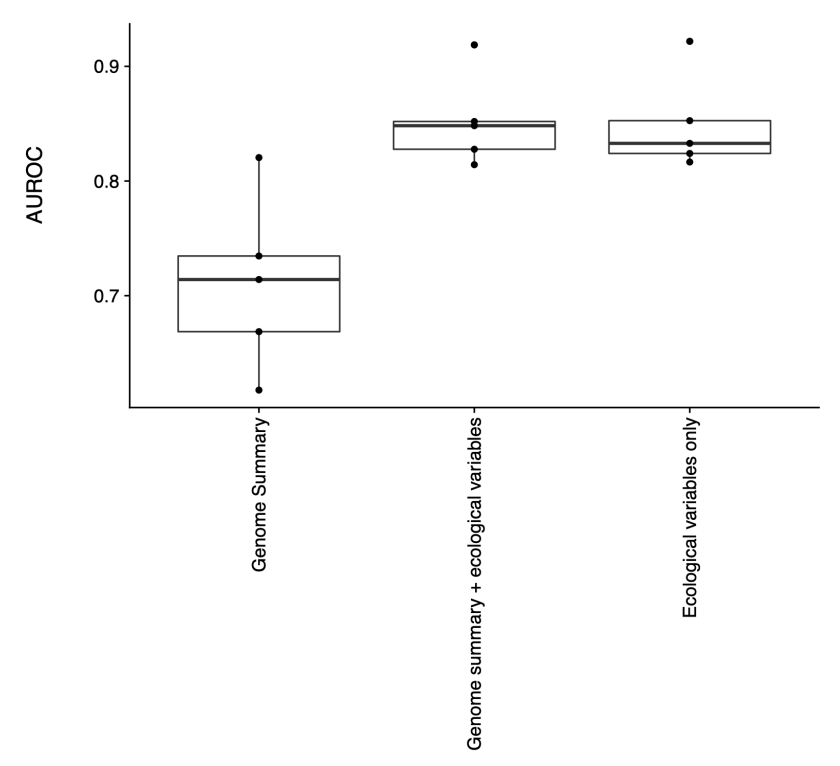


**Figure S12.**Performance measurements (AUROC) across five training-test replicates of "composite" models that included genome-wide summary statistics, ecological variables, or both (table S6; see table S4 for descriptions).

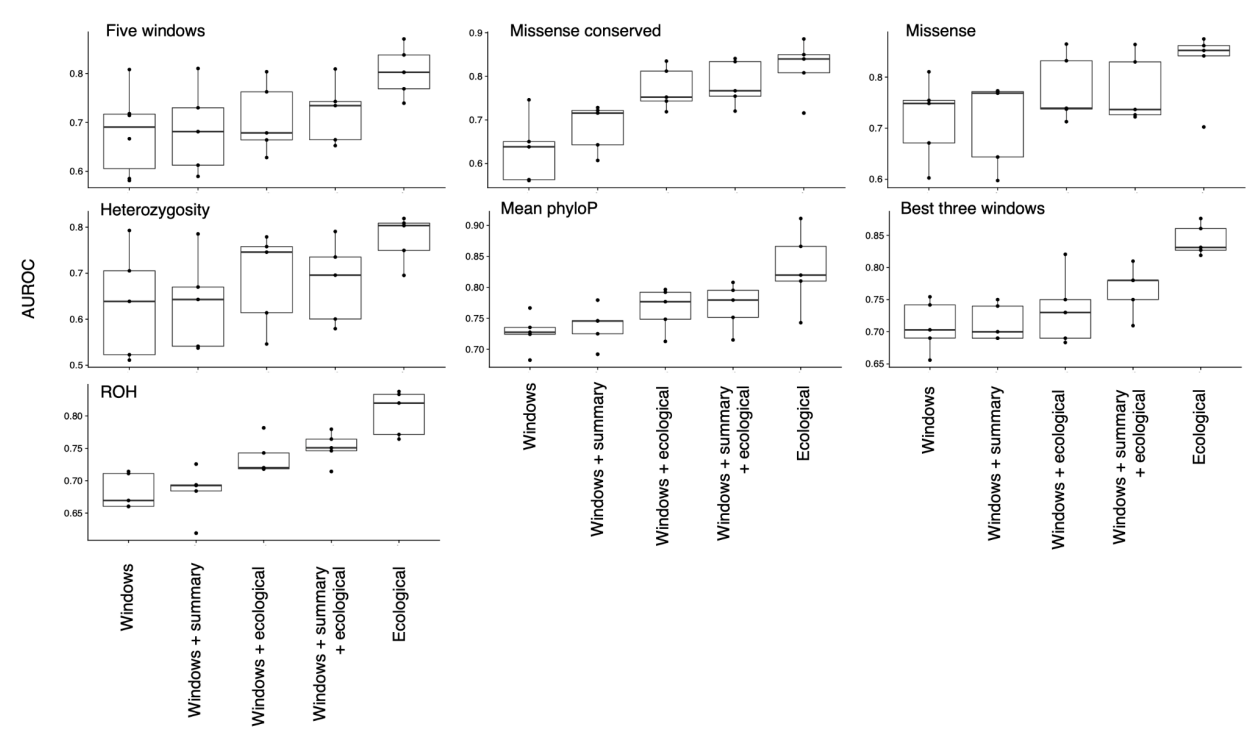


Figure S13.

Performance measurements (AUROC) across five training-test replicates of "composite" models that included genomic window-based metrics, genome-wide summary statistics, ecological variables, or combinations of these data types (table S6; see table S4 for descriptions).

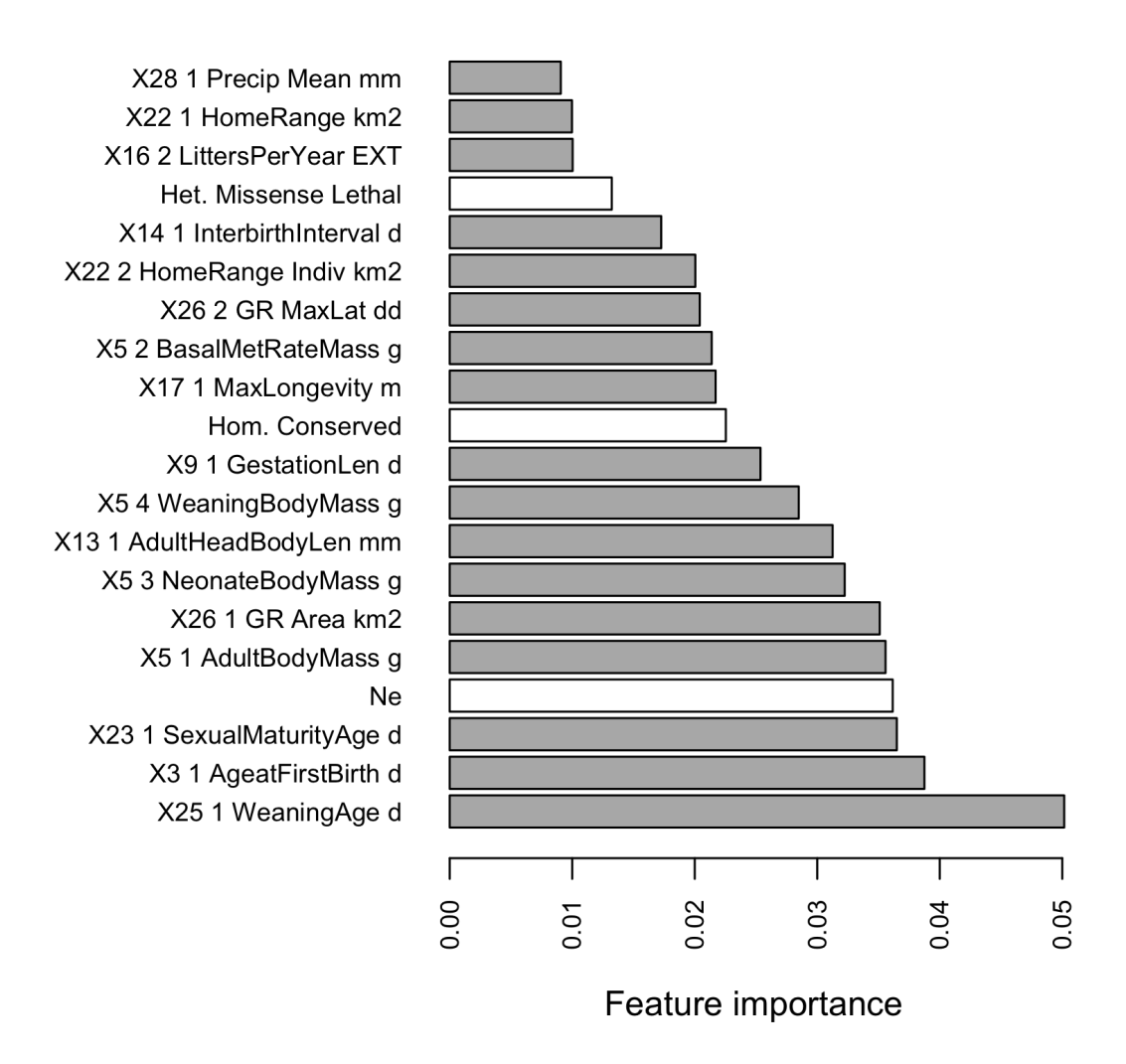


Figure S14.

Top 20 most important features in random forest models to predict conservation status. Most important features from the model including 13 genomic summary variables and 40 ecological variables across (AUROC=0.85). Feature importance was averaged across five test-training replicates. Genomic features are highlighted in white and ecological features from PanTHERIA are in dark gray.

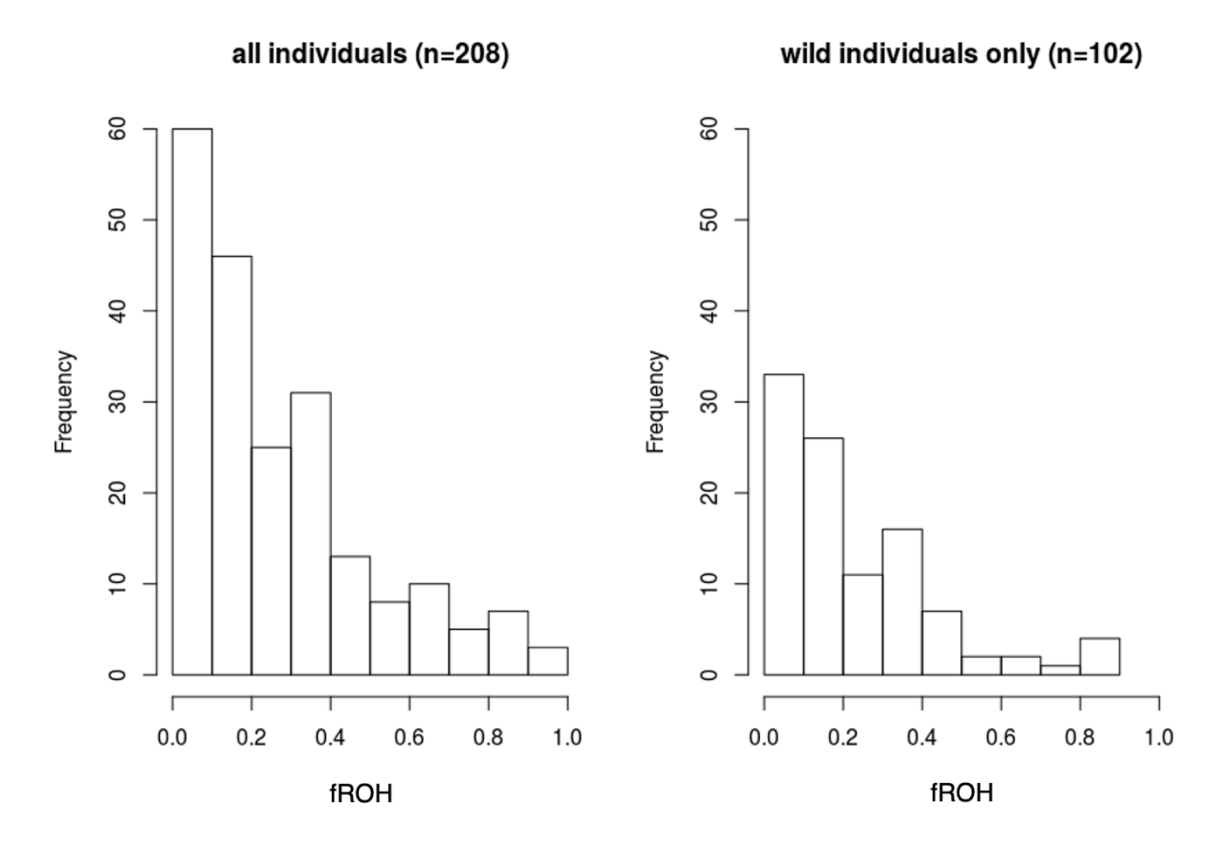


Figure S15.

Distribution of fRoH values for A) all species with fRoH estimates and B) species represented by a wild caught individual only.

**Table S1**. Data for the 241 Zoonomia species analyzed, including species name, taxonomic order, diet classification, wild or captive status of the sequenced sample, IUCN Red List category, NCBI accession numbers, genome contiguity statistic (contig N50), generation time, census size (Nc), and values for 13 genomic summary statistics used in analyses.

**Table S2**. Details and results for variables used in statistical regression models, including the transformation used to increase normality of the distribution and number of samples with an estimate. Model results indicate if the variable was dropped from the final model (and the reason it was dropped) or the p-values and untransformed coefficients for the final model. Bold values indicate the variable was significant in the model at the p=0.05 threshold.

variable name	variable description	transfor m	sampl e size	logistic regression	ordinal regression	Carnivora ordinal regression	Cetartiodactyla ordinal regression	Primate ordinal regression
historical $N_e$	harmonic mean of temporal estimates of $N_e$ from PSMC	log	210	p=3.8e-05, coefficient=-1.42	p=0.009, coefficient=-0.85	p=0.29, coefficient=-1.17	dropped (p=0.40)	dropped (p=0.14)
heterozygosity	genome-wide heterozygosity	none	209	dropped (correlated)	dropped (p=0.18)	dropped (p=0.22)	dropped (p=0.25)	dropped (p=0.32)
outbred heterozygosity	mode of heterozygosity in non- RoH regions	log	209	p=0.25, coefficient=-0.33	dropped (p=0.17)	p=0.68, coefficient=0.52	dropped (p=0.33)	dropped (p=0.69)
fRoH	percentage of the genome in RoH	square root	208	p=0.028, coefficient=-0.63	dropped (p=0.97)	dropped (p=0.83)	p=0.084, coefficient=0.88	dropped (p=0.56)
hom.	proportion of homozygous substitutions with phylop>2.27	log	241	p=0.19, coefficient=-0.31	p=0.99, coefficient=- 0.0055	dropped (p=0.31)	dropped (p=0.27)	dropped (p=0.80)
phyloP kurtosis	tailedness of phylop distribution across substitutions	none	241	dropped (p=0.33)	dropped (p=0.33)	dropped (p=0.47)	dropped (p=0.70)	p=0.023, coefficient=-1.06
hom. missense conserved	proportion of hom. missense that are at sites with phylop>2.27	none	239	dropped (correlated)	dropped (correlated)	dropped (p=0.30)	dropped (p=0.47)	dropped (p=0.38)
het. missense L	in lethal genes, the proportion of heterozygous coding variants that are missense	log	190	dropped (p=0.12)	dropped (correlated)	p=0.18, coefficient=2.23	dropped (p=0.76)	dropped (p=0.98)
het. missense	in viable genes, the proportion of heterozygous coding variants that are missense	log	196	dropped (p=0.16)	p=0.40, coefficient=-0.23	p=0.99, coefficient=0.008	dropped (p=0.28)	dropped (p=0.59)
het. LoF L	in lethal genes, the proportion of heterozygous coding variants that are LoF	log (+0.01)	190	p=0.41, coefficient=-0.15	dropped (p=0.56)	dropped (p=0.81)	p=0.60, coefficient=-0.29	dropped (p=0.55)
het. LoF V		log (+0.001)	196	dropped (p=0.62)	dropped (p=0.77)	p=0.067, coefficient=-1.15	dropped (p=0.32)	dropped (p=0.14)

	that are LoF							
hom. missense L	in lethal genes, the proportion of homozygous coding variants that are missense	log	239	dropped (correlated)	dropped (correlated)	dropped (p=0.65)	dropped (p=0.37)	dropped (p=0.53)
hom. missense V	in viable genes, the proportion of homozygous coding variants that are missense	none	239	p=0.38, coefficient=0.25	p=0.59, coefficient=-0.17	dropped (p=0.55)	dropped (p=0.26)	dropped (p=0.28)
order	taxonomic order	NA	241	NA	p=0.023, 0.045, 0.41, 0.93; coefficients=- 2.12, -1.67, 0.62, 0.058	NA	NA	NA
diet	diet type (herbivore, omnivore, carnivore)	NA	241		p=0.0037, 0.86; coefficient <sub>h</sub> =1.88 , coefficient <sub>o</sub> =0.11	dropped (rank-deficient)	p=0.15, <b>0.034</b> ; coefficient <sub>h</sub> =1.59 , coefficient <sub>o</sub> =4.07	dropped (rank-deficient)
wild	sample from wild or captive population	NA	225		p=0.96, coefficient=-0.20		p=0.93, coefficient=0.099	dropped (p=0.30)

**Table S3.** Loadings for genomics summary statistics of the first five principal components (PCs; accounting for >80% of total variance) used in models to predict threatened status of species across all orders. P-values are reported for PCs that significantly predicted threatened status. Summary statistics are described in table S2.

	PC1 (p=0.0038)	PC2	PC3 (p=5.6e-4)	PC4	PC5
hom. conserved	0.215	0.305	-0.302	0.403	-0.080
phyloP kurtosis	-0.122	-0.282	0.317	-0.483	0.171
historical N <sub>e</sub>	-0.306	0.091	-0.384	0.191	0.125
heterozygosity	-0.242	0.419	-0.118	-0.244	-0.056
outbred heterozygosity	-0.229	0.416	-0.004	-0.273	0.023
fRoH	0.124	-0.455	-0.082	0.322	-0.027
hom. missense conserved	0.386	0.283	0.096	0.104	0.039
het. missense L	0.347	-0.167	-0.258	-0.24	-0.066
het. missense V	0.375	-0.148	-0.112	-0.216	0.048
het. LoF L	0.111	-0.044	-0.431	-0.392	-0.644
het. LoF V	0.107	-0.025	-0.517	-0.221	0.713
hom. missense L	0.384	0.264	0.177	-0.062	0.047
hom. missense V	0.371	0.248	0.26	-0.089	0.103

**Table S4.** Genomic and ecological variables used in machine learning models to predict IUCN status in mammalian species. Genomic window-based variables were estimated within 50KB homologous windows lifted over to the human genome. Genomic summary variables are genome-wide summary statistics. Ecological variables were obtained from the PanTHERIA database.

	Genomic window-based variables	Description							
1	Heterozygosity	Mean heterozygosity in homologous 50KB windows							
2	RoH	Mean RoH in homologous 50KB windows							
3	Mean phyloP	Mean phyloP across substitutions in homologous 50KB windows							
4	Missense conserved substitutions	Proportion of homozygous missense substitutions in homologous 50KB windows that are at evolutionarily conserved sites (phyloP>2.27)							
5	Missense substitutions	Proportion of homozygous coding substitutions in homologous 50KB windows that are missense							
	Genomic summary variables								
1	Historical N <sub>e</sub>	Harmonic mean of historical effective population size							
2	Heterozygosity	Mean genome-wide heterozygosity							
3	Heterozygosity (non-RoH)	Mean heterozygosity outside of RoH							
4	fRoH	Proportion of the genome in RoH							
5	Conserved homozygous	Proportion of homozygous that are at evolutionarily conserved sites (phyloP>2.27)							
6	PhyloP kurtosis	Kurtosis of phyloP across homozygous							
7	Missense homozygous at conserved sites	Proportion of missense homozygous that are at evolutionarily conserved sites (phyloP>2.27)							
8	Heterozygous missense lethal	Proportion of heterozygous coding variants in IMPC lethal genes that are missense							
9	Heterozygous missense viable	Proportion of heterozygous coding variants in IMPC viable genes that are missense							
10	Heterozygous LoF lethal	Proportion of heterozygous coding variants in IMPC lethal genes that are LoF							
11	Heterozygous LoF viable	Proportion of heterozygous coding variants in IMPC viable genes that are LoF							
12	Homozygous missense lethal	Proportion of homozygous coding variants in IMPC lethal genes that are missense							
13	Homozygous missense viable	Proportion of homozygous coding variants in IMPC viable genes that are missense							
	Ecological variables								
1	X5 1 Adult Body Mass g	Mass of adult (or age unspecified) live or freshly-killed specimens (excluding pregnant females) using captive, wild, provisioned, or unspecified populations; male.							

		female, or sex unspecified individuals; primary, secondary, or extrapolated sources;
		all measures of central tendency; in all localities
2	X13 1 Adult Head BodyLen mm	Total length from tip of nose to anus or base of tail of adult (or age unspecified) live, freshly-killed, or museum specimens using captive, wild, provisioned, or unspecified populations; male, female, or sex unspecified individuals; primary, secondary, or extrapolated sources; all measures of central tendency; in all localities
3	X2 1 Age at Eye Opening d	Age at which both eyes are fully open after birth using captive, wild, provisioned, or unspecified populations; male, female, or sex unspecified individuals; primary, secondary, or extrapolated sources; all measures of central tendency; in all localities
4	X3 1 Age at First Birth d	Age at which females give birth to their first litter (eutherians), or their young attach to teats (metatherians) or hatch out (monotremes), using non-captive, wild, provisioned, or unspecified populations; primary, secondary, or extrapolated sources; all measures of central tendency; in all localities
5	X18 1 Basal Met Rate mL O2 hr	Basal metabolic rate of adult (or age unspecified) individual(s) using captive, wild, provisioned, or unspecified populations; male, female, or sex unspecified individuals; primary, secondary, or extrapolated sources; all measures of central tendency; in all localities. Metabolic rate was measured when individual(s) were experiencing neither heat nor cold stress (i.e. are in their thermoneutral zone); are resting and calm; and are post—absorptive (are not digesting or absorbing a meal) and data were only accepted where there was also a measure of body mass for the same individual(s)
6	X5 2 Basal Met Rate Mass g	Mass of individual(s) from which the basal metabolic rate was taken
7	X6 1 Diet Breadth	Number of dietary categories eaten by each species measured using any qualitative or quantitative dietary measure, over any period of time, using any assessment method, for non-captive or non-provisioned populations; adult or age unspecified individuals, male, female, or sex unspecified individuals; primary, secondary, or extrapolated sources; all measures of central tendency; in all localities. Categories were defined as vertebrate, invertebrate, fruit, flowers/nectar/pollen, leaves/branches/bark, seeds, grass and roots/tubers
8	X9 1 Gestation Len d	Length of time of non-inactive fetal growth, using captive, wild, provisioned, or unspecified populations; male, female, or sex unspecified individuals; primary, secondary, or extrapolated sources; all measures of central tendency; in all localities. Gestation was measured between specified start and end points as follows: Start points – conception, fertilization, first observed copulation, fertilization, implantation, laying, palpably pregnant, removal of pouch young, capture (except marsupials) or unspecified. End points – birth, hatching or unspecified
9	X12 1 Habitat Breadth	Number of habitat layers used by each species measured using any qualitative or quantitative time measure, for non-captive populations; adult or age unspecified individuals, male, female, or sex unspecified individuals; primary, secondary, or extrapolated sources; all measures of central tendency; in all localities. Categories were defined as above ground dwelling, aquatic, fossorial and ground dwelling
10	X22 1 Home Range km2	Size of the area within which everyday activities of individuals or groups (of any type) are typically restricted, estimated by either direct observation, radio telemetry, trapping or unspecified methods over any duration of time, using non-captive populations; male, female, or sex unspecified individuals; primary, secondary, or extrapolated sources; all measures of central tendency; in all localities
11	X22 2 Home Range Indiv km2	Size of the area within which everyday activities of individuals are typically restricted, estimated by either direct observation, radio telemetry, trapping or unspecified methods over any duration of time, using non-captive populations; male, female, or sex unspecified individuals; primary, secondary, or extrapolated sources; all measures of central tendency; in all localities
12	X14 1 Inter birth Interval d	The length of time between successive births of the same female(s) after a successful or unspecified litter using non-captive, wild, provisioned, or unspecified populations; primary, secondary, or extrapolated sources; all measures of central tendency; in all

		localities
13	X15 1 Litter Size	Number of offspring born per litter per female, either counted before birth, at birth or after birth, using captive, wild, provisioned, or unspecified populations; male, female, or sex unspecified individuals; primary, secondary, or extrapolated sources; all measures of central tendency; in all localities
14	X16 1 Litters Per Year	Number of litters per female per year using non-captive, wild, provisioned, or unspecified populations; male, female, or sex unspecified individuals; primary, secondary, or extrapolated sources; all measures of central tendency; in all localities
15	X17 1 Max Longevity m	Maximum adult age measured either through direct observation, capture-recapture estimates, projected from physical wear or unspecified, using captive, wild, provisioned, or unspecified populations; male, female, or sex unspecified individuals; primary, secondary, or extrapolated sources; in all localities
16	X5 3 Neonate Body Mass g	Mass of live or freshly-killed specimens of infants at either a near term embryonic stage, birth, immediately after birth or up to an age of seven days after birth, using captive, wild, provisioned, or unspecified populations; male, female, or sex unspecified individuals; primary, secondary, or extrapolated sources; all measures of central tendency; in all localities
17	X21 1 Population Density n km2	Number of individuals per square kilometer, estimated with either direct, indirect or unspecified counts, measured in any area size within a human, ecological or unspecified boundary, over any duration of time, using non-captive, non-provisioned populations; male, female, or sex unspecified individuals; primary, secondary, or extrapolated sources; all measures of central tendency; in all localities
18	X10 1 Population Grp Size	Number of individuals, adults or definition unspecified in a group that spends the majority of their time in a 24 hour cycle together, measured over any duration of time, using non-captive populations; male, female, or sex unspecified individuals; primary, secondary, or extrapolated sources; all measures of central tendency; in all localities
19	X23 1 Sexual Maturity Age d	Age when individuals are first physically capable of reproducing, defined as either physically sexually mature, age at first mating or unspecified (males and females), age at first estrus or age at first pregnancy (females only), age at spermatogenesis or age at testes descent (males only), using captive, wild, provisioned, or unspecified populations; male, female, or sex unspecified individuals, primary, secondary, or extrapolated sources; all measures of central tendency; in all localities
20	X10 2 Social Grp Size	Number of individuals, adults or definition unspecified in a group that spends the majority of their time in a 24 hour cycle together where there is some indication that these individuals form a social cohesive unit, measured over any duration of time, using non-captive populations; male, female, or sex unspecified individuals; primary, secondary, or extrapolated sources; all measures of central tendency; in all localities
21	X24 1 Teat Number	Total number of teats present, using captive, wild, provisioned, or unspecified populations; male, female, or sex unspecified individuals; primary, secondary, or extrapolated sources; all measures of central tendency; in all localities
22	X25 1 Weaning Age d	Age when primary nutritional dependency on the mother ends and independent foraging begins to make a major contribution to the offspring's energy requirements, measured as either weaning/lactation length, nutritionally independent, first solid food, last observed nursing, age at first flight (bats only), age at pouch exit or length of teat Attachment (marsupials only) or unspecified definition, using captive, wild, provisioned, or unspecified populations; male, female, or sex unspecified individuals; primary, secondary, or extrapolated sources; all measures of central tendency; in all localities
23	X5 4 Weaning Body Mass g	Mass of live or freshly-killed specimens of weanlings, using captive, wild, provisioned, or unspecified populations; male, female, or sex unspecified individuals; primary, secondary, or extrapolated sources; all measures of central tendency; in all localities

24	X16 2 Litters Per Year EXT	Species medians of the consolidated values
25	X26 1 GR Area km2	Total extent of a species range with a global equal-area projection
26	X26 2 GR Max Lat dd	Maximum latitudinal extent of each species range calculated using a global geographic projection (decimal degrees)
27	X26 3 GR Min Lat dd	Minimum latitudinal extent of each species range calculated using a global geographic projection (decimal degrees)
28	X26 4 GR Mid Range Lat dd	Median latitudinal extent of each species range calculated using a global geographic projection (decimal degrees)
29	X26 5 GR Max Long dd	Maximum longitudinal extent of each species range calculated using a global geographic projection (decimal degrees)
30	X26 6 GR Min Long dd	Minimum longitudinal extent of each species range calculated using a global geographic projection (decimal degrees)
31	X26 7 GR Mid Range Long dd	Median longitudinal extent of each species range calculated using a global geographic projection (decimal degrees)
32	X27 1 Hu Pop Den Min n km2	Minimum human population density (persons per km²) using the Gridded Population of the World (GPW) (CIESIN and CIAT 2005) for 1995
33	X27 2 Hu Pop Den Mean n km2	Mean human population density (persons per km²) using the Gridded Population of the World (GPW) (CIESIN and CIAT 2005) for 1995
34	X27 3 Hu Pop Den 5p n km2	5th percentile human population density (persons per km²) using the Gridded Population of the World (GPW) (CIESIN and CIAT 2005) for 1995
35	X27 4 Hu Pop Den Change	Mean rate of increase in human population density using the Gridded Population of the World (GPW) (CIESIN and CIAT 2005) for 1990 and 1995 as: (1995–1990)/1990
36	X28 1 Precip Mean mm	Mean monthly precipitation (mm) calculated using data from ftp://ftp.ngdc.noaa.gov/Solid_Earth/Ecosystems/GEDII_a/datasets/a03/lc.htm
37	X28 2 Temp Mean 01 deg C	Mean monthly temperature (0.1°C) calculated using data from ftp://ftp.ngdc.noaa.gov/Solid_Earth/Ecosystems/GEDII_a/datasets/a03/lc.htm
38	X30 1 AET Mean mm	Mean monthly AET (Actual Evapotranspiration Rate) from 1920 to 1980 (mm) calculated using the Global Resource Information Database of UNEP and is available from http://www.grid.unep.ch/data/grid/gnv183.php)
39	X30 2 PET Mean mm	Mean monthly PET (Potential Evapotranspiration Rate) from 1920 to 1980 (mm) calculated using the Global Resource Information Database of UNEP and is available from http://www.grid.unep.ch/data/grid/gnv183.php)

**Table S5.** Machine learning models to predict conservation status from genomic summary statistics, genomic metrics in homologous 50KB windows, and ecological variables across mammal species. Performance was measured by the median AUROC across five training-test replicates. The first AUROC value is for models where missing data was imputed by the median of the lowest taxonomic level, the second value in parentheses is for models with missing data imputed across all species. Data types included in the models were grouped as window-based metrics (Genomic windows), 13 genome-wide summary statistics (Genomic summary), and 39 ecological variables (Ecological).

				Data types	
Model	AUROC	N	Ecological	Genomic summary	Genomic windows
Ecological variables	0.88 (0.88)	212	x		
Genomic summary statistics + ecological variables	0.86 (0.86)	210	X	x	
Windows-based mean phyloP + genomic summary statistics	0.77 (0.8)	236		X	X
Windows-based mean phyloP	0.78 (0.77)	236			x
Windows-based mean phyloP + ecological variables	0.73 (0.75)	208	х		X
Windows-based missense substitutions + ecological variables	0.78 (0.74)	208	x		x
All five genomic windows-based metrics + genomic summary statistics	0.73 (0.74)	195		X	X
Windows-based missense substitutions + genomic summary statistics + ecological variables	0.78 (0.74)	208	X	X	X
All five genomic windows-based metrics	0.74 (0.73)	195			X
Windows-based missense substitutions	0.69 (0.73)	236			X
Three best genomic windows-based metrics + ecological variables	0.82 (0.73)	173	X		X
Windows-based mean phyloP + genomic summary statistics + ecological variables	0.75 (0.73)	208	x	x	x
Windows-based conserved missense substitutions + ecological variables	0.82 (0.72)	208	X		x

				Data types	
Model	AUROC	N	Ecological	Genomic summary	Genomic windows
Three best genomic windows-based metrics + genomic summary statistics + ecological variables	0.78 (0.72)	173	X	х	X
All five genomic windows-based metrics + ecological variables	0.79 (0.71)	172	X		X
All five genomic windows-based metrics + genomic summary statistics + ecological variables	0.77 (0.71)	172	x	X	X
Three best genomic windows-based metrics	0.82 (0.7)	196			X
Windows-based RoH + ecological variables	0.81 (0.7)	174	X		X
Windows-based conserved missense substitutions + genomic summary statistics	0.76 (0.7)	236		X	X
Three best genomic windows-based metrics + genomic summary statistics	0.79 (0.69)	196		x	X
Windows-based missense substitutions + genomic summary statistics	0.72 (0.69)	236		X	X
Windows-based conserved missense substitutions + genomic summary statistics + ecological variables	0.81 (0.69)	208	x	x	x
Windows-based conserved missense substitutions	0.7 (0.67)	236			X
Windows-based RoH + genomic summary statistics + ecological variables	0.83 (0.66)	174	x	x	X
Genomic summary statistics	0.68 (0.65)	236		x	
Windows-based RoH + genomic summary statistics	0.78 (0.63)	197		x	X
Windows-based heterozygosity + ecological variables	0.68 (0.61)	174	X		x
Windows-based heterozygosity + genomic summary statistics + ecological variables	0.7 (0.61)	174	X	x	X

				Data types	
Model	AUROC	N	Ecological	Genomic summary	Genomic windows
Windows-based RoH	0.78 (0.59)	197			X
Windows-based heterozygosity + genomic summary statistics	0.78 (0.53)	197		x	x
Windows-based heterozygosity	0.79 (0.52)	197			x

**Table S6.** Performance (median AUROC across five training-test replicates) of machine learning models to predict conservation status across the same set of species, comparing models with genomic variables only, ecological variables only, and combining both ecological and genomic variables.

Genomic variable type	Genomic only	Ecological only	Ecological + Genomic	# species
Genome-wide summary statistics	0.71	0.83	0.85	210
Window-based Missense substitutions	0.75	0.85	0.74	209
Window-based Mean phyloP of substitutions	0.73	0.82	0.78	209
Three best window-based genomic metrics	0.70	0.83	0.73	174
All five window-based genomic metrics	0.69	0.80	0.68	173
Window-based RoH	0.67	0.82	0.72	175
Window-based Heterozygosity	0.64	0.80	0.75	175
Window-based conserved missense substitutions	0.64	0.84	0.75	209